Journal of
Medicinal Chemistry

Article

Structure-activity relationship in pyrazolo[4,3-c]pyridines, first inhibitors of PEX14-PEX5 Protein-Protein Interaction (PPI) with trypanocidal activity

Maciej Dawidowski, Vishal C. Kalel, Valeria Napolitano, Roberto Fino, Kenji Schorpp, Leonidas Emmanouilidis, Dominik Lenhart, Michael Ostertag, Marcel Kaiser, Marta Kolonko, Bettina Tippler, Wolfgang Schliebs, Grzegorz Dubin, Pascal Mäser, Igor Tetko, Kamyar Hadian, Oliver Plettenburg, Ralf Erdmann, Michael Sattler, and Grzegorz M Popowicz

J. Med. Chem., **Just Accepted Manuscript** • DOI: 10.1021/acs.jmedchem.9b01876 • Publication Date (Web): 20 Dec 2019

Just Accepted

is published by the American Chemical Society. 1155 Sixteenth Street N.W., Washington, DC 20036

	Mäser, Pascal; Swiss Tropical and Public Health Institute; University of Basel Tetko, Igor; Institute of Structural Biology, Helmholtz Zentrum München Hadian, Kamyar; Helmholtz Zentrum Munchen Deutsches Forschungszentrum fur Umwelt und Gesundheit, Assay Development and Screening Platform Plettenburg, Oliver; Helmholtz Zentrum Munchen Deutsches Forschungszentrum fur Umwelt und Gesundheit, Institute of Medicinal Chemistry; Institute of Organic Chemistry, Leibniz Universität Hannover Erdmann, Ralf; Institute of Biochemistry and Pathobiochemistry, Department of Systems Biochemistry, Faculty of Medicine, Ruhr-University Bochum Sattler, Michael; Institute of Structural Biology, Helmholtz Zentrum München; Center for Integrated Protein Science Munich at Chair of Biomolecular NMR, Department Chemie, Technische Universität München Popowicz, Grzegorz; Helmholtz Zentrum München, Institute of Structural Biology; Center for Integrated Protein Science Munich at Chair of Biomolecular NMR, Department Chemie, Technische Universität München

Structure-activity relationship in pyrazolo[4,3-*c*]pyridines, first inhibitors of PEX14-PEX5 Protein-Protein Interaction (PPI) with trypanocidal activity

Maciej Dawidowski[1,2,3], Vishal C. Kalel[4], Valeria Napolitano[5,6], Roberto Fino[1,2], Kenji Schorpp[7], Leonidas Emmanouilidis[1,2]†, Dominik Lenhart[1,2,8], Michael Ostertag[1,2], Marcel Kaiser[9,10], Marta Kolonko[1,11], Bettina Tippler[4], Wolfgang Schliebs[4], Grzegorz Dubin[6], Pascal Mäser[9,10], Igor V. Tetko[1], Kamyar Hadian[7], Oliver Plettenburg[8,12], Ralf Erdmann[4], Michael Sattler[1,2*], Grzegorz M. Popowicz[1,2*]*

[1]Institute of Structural Biology, Helmholtz Zentrum München, Ingolstädter Landstrasse 1, 85764 Neuherberg, Germany.

[2]Center for Integrated Protein Science Munich at Chair of Biomolecular NMR, Department Chemie, Technische Universität München, Lichtenbergstrasse 4, 85747 Garching, Germany.

[3]Department of Drug Technology and Pharmaceutical Biotechnology Medical University of Warsaw, Banacha 1, 02-097 Warszawa, Poland

[4]Institute of Biochemistry and Pathobiochemistry, Department of Systems Biochemistry, Faculty of Medicine, Ruhr-University Bochum, 44780 Bochum, Germany.

[5]Faculty of Biochemistry, Biophysics and Biotechnology, Jagiellonian University, Gronostajowa 7, Krakow, 30-387, Poland

[6]Małopolska Center of Biotechnology, Jagiellonian University in Kraków, Gronostajowa 7, Kraków, 30-387, Poland

[7]Assay Development and Screening Platform, Institute of Molecular Toxicology and Pharmacology, Helmholtz Zentrum München, Ingolstädter Landstrasse 1, 85764 Neuherberg, Germany.

[8]Institute of Medicinal Chemistry, Helmholtz Zentrum München, Ingolstädter Landstr. 1, Neuherberg, 85764, Germany

[9]Swiss Tropical and Public Health Institute, Socinstrasse 57, 4051 Basel, Switzerland.

[10]University of Basel, 4001 Basel, Switzerland.

[11]Department of Biochemistry, Faculty of Chemistry, Wrocław University of Science and Technology, Wybrzeże Wyspiańskiego 27, 50-370, Wrocław, Poland.

[12]Institute of Organic Chemistry, Leibniz Universität Hannover, Schneiderberg 1b, Hannover, 30167, Germany

ABSTRACT

Trypanosoma protists are pathogens leading to a spectrum of devastating infectious diseases. The range of available chemotherapeutics against *Trypanosoma* is limited and the existing therapies are partially ineffective and cause serious adverse effects. Formation of the PEX14-PEX5 complex is essential for protein import into the parasites' glycosomes. This transport is critical for parasite metabolism and failure leads to mislocalization of glycosomal enzymes, with fatal consequences for the parasite. Hence, inhibiting the PEX14-PEX5 protein-protein interaction (PPI) is an attractive way to affect multiple metabolic pathways. Herein, we have used structure-guided computational screening and optimization to develop the first line of

compounds that inhibit PEX14-PEX5 protein-protein interaction. The optimization was driven by several X-ray structures, NMR binding data and molecular dynamics simulations. Importantly, the developed compounds show significant cellular activity against *Trypanosoma*, including the human pathogen *T. brucei gambiense* and *T. cruzi* parasites.

INTRODUCTION

Human African trypanosomiasis (HAT, sleeping sickness) and Chagas disease (American trypanosomiasis) are among most devastating and deadliest parasitic diseases. They occur predominantly in sub-Saharian Africa and Latin America, respectively, but Chagas disease has spread globally due to international human migration. Both qualify as neglected tropical diseases (NTDs) threatening millions of people in poor communities.[1-4] The impact of *Trypanosoma* protists on livestock is also threatening the well-being of multiple communities.[5]

HAT is caused by two protozoans: *Trypanosoma brucei gambiense* and *Trypanosoma brucei rhodesiense* (accounting for 98% and 2% of HAT cases, respectively), transmitted by the bite of an infected tsetse fly. The disease consists of two phases: the haemolymphatic stage (stage I) with trypanosomes being present in the blood and lymphatic system and the meningoencephalitic stage (stage II), when parasites have spread to the central nervous system (CNS). Without appropriate diagnosis and treatment the disease can be fatal.[3, 6] No effective vaccine has so far been been developed because the parasites employ several immune evasion strategies such as antigenic variation. Therefore, chemotherapy is the only therapeutic option currently available (Figure 1).[7, 8] Suramin and pentamidine are used in stage I of HAT, while melarsoprol, eflornithine and nifurtimox-eflornithine combination therapy (NECT) are used in stage II of the disease. Unfortunately, these drugs have severe side effects and require continuous parenteral administration, which is not optimal, given that the patients live in rural African areas with very limited health resources.[6, 9] There is a better treatment option, since

recently a first all-oral drug fexinidazole completed clinical trials in humans and was approved for HAT treatment.[10-13] The efficacy of this monotherapy is comparable to intravenous NECT and the possibility of oral administration makes it easier to use in rural African realities. Nevertheless, cross-resistance with nifurtimox is likely to develop due to the same mechanism of action and no convenient polytherapy is available to overcome this issue.[12, 14-16] Another drug candidate, the benzoxaborole derivative SCYX-7158 (acoziborole) is currently in advanced phase of clinical trials.[12, 17] In spite of these promising developments, the Drugs for Neglected Diseases initiative (DNDi) still requires new candidates for stage-2 HAT treatment.[15]

The situation is more dramatic for Chagas disease, caused by *Trypanosoma cruzi*. The parasite is spread by triatomine bugs ('kissing bugs'), by blood transfusions, congenitally, and even orally, by contaminated food.[18] It is considered to be the parasitic disease with the greatest socioeconomic impact in Latin America and one of the leading causes of myocarditis. There are two stages of the disease. In the acute phase, the symptoms vary between the individuals and in most cases they decline spontaneously after 1-2 months. In the chronic phase, the patients may develop potentially fatal cardiac and digestive pathologies. Currently, there are two drugs for Chagas disease, benznidazole and nifurtimox (Figure 1). However, both have serious side effects and are ineffective in the chronic phase of the disease.[4, 19]

Undeniably, there is an urgent need for novel drugs against *Trypanosoma* infections, especially for Chagas disease, with high clinical efficiency, favorable pharmacological profiles and ease of use. In an ideal setting, the pipeline would comprise several new agents that are suitable for combination therapy, which, in turn, would allow for better efficacy and minimal risk of resistance development.[2, 16] This can be achieved *inter alia* by finding promising targets and pathways essential for parasite survival. In the past, various molecular targets have been

proposed and successfully validated.[16, 20, 21] It is intriguing that, although the trypanosomatids share similarities in genetic sequence and biochemical pathways,[22, 23] so far most drug discovery campaigns aimed either at *T. brucei* or *T. cruzi*, with fewer seeking for new, broad-spectrum agents which would affect both species.[24-27]

Glycosomes are peroxisome-related organelles unique to kinetoplastids, including *Trypanosoma* spp. These organelles contain the enzymes required for glycolysis and for other intermediary metabolic pathways.[28] Hence, glycosomes are essential for parasite survival and they have long been considered attractive targets for development of new drugs against trypanosomatids.[20, 29, 30]

As glycosomes lack DNA, glycosomal matrix proteins encoded in the nuclear genome have to be post-translationally transported from the cytosol to the organelle. Cargo proteins are imported by a cascade of interactions of specialized transport proteins, called peroxins (PEX#). The PEX14-PEX5 protein-protein interaction (PPI) plays a key role in this process. The PEX5 import receptor is capable of binding short peroxisomal targeting sequences (PTS) of the cargo. Next, the PEX5-cargo complex binds PEX14, which is localized at the glycosomal membrane and is required for cargo translocation into the matrix of the organelle.[30, 31] Many of the glycosomal enzymes have been proposed and validated as potential drug targets.[20] However, targeting the glycosomal transport system should be a more attractive drug target because it provides the opportunity to interfere with the function of many critical metabolic processes at once. Furthermore, mislocalization to the cytosol provides the glycosomal kinases access to the cytosolic ATP pool. Enzymes such as *T. brucei* hexokinase function at such a high rate that they deplete ATP faster than it can be replenished by substrate-level phosphorylation, which will be fatal to the trypanosomes.[32]

A series of RNAi studies has previously shown the importance of PEX14 function for glucose metabolism in *Trypanosoma*.[32-34] Recently, we reported a proof-of-concept study for targeting the PEX14-PEX5 PPI in *T. brucei* and *T. cruzi* parasites by small molecules.[35] Using a structure-based drug discovery (SBDD) approach we developed a subset of prototypic pyrazolo[4,3-*c*]pyridine derivatives – the first inhibitors of this PPI and the first compounds that disrupt glycosomal import of matrix proteins and kill *T. brucei* and *T. cruzi in vitro* in nanomolar concentrations. Here, we present the details on the medicinal chemistry program that led to this group of active molecules along with the in-depth structure–activity relationship (SAR) study.

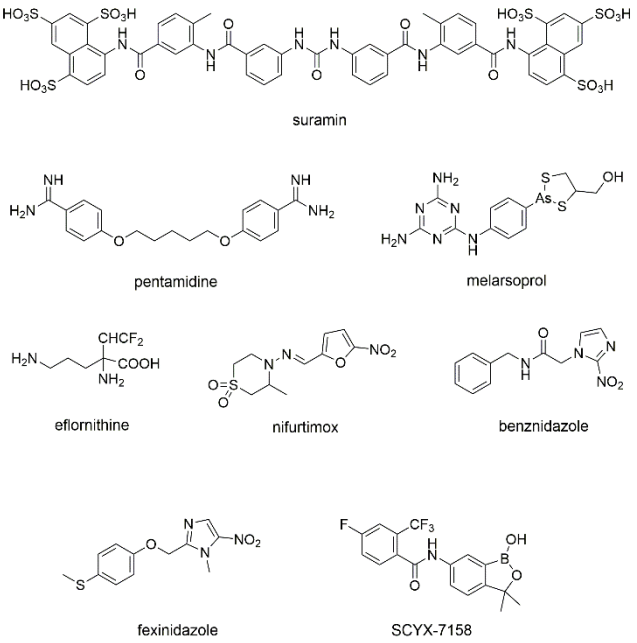

Figure 1. Structures of drugs used for the treatment of *Trypanosoma*-related diseases and clinical candidates.

RESULTS AND DISCUSSION

Structural basis for PEX14-PEX5 PPI targeting. During the initial phase of the project, the structural basis for the PEX14-PEX5 PPI interaction was known (Figure 2)[36-38]. The *N*-terminal part of PEX5 contains several diaromatic WXXX(F/Y) motifs that address the respective hydrophobic Trp and Phe/Tyr pockets on the surface of the *N*-terminal helical

domain (NTD) of PEX14. These two relatively shallow cavities are separated by two π-stacked phenyl rings of PEX14 (Phe17 and Phe34, the explanation of residue numbering among different species is given in Table S1) that protrude to the solvent. In addition to the hydrophobic and aromatic binding of Trp and Phe/Tyr of WXXX(F/Y) motifs in PEX5 with their respective hotspots on the PEX14 surface, the positively charged Lys38 and Arg22 side chains of PEX14 plausibly facilitate the protein-protein complex formation by cation-π interactions. Other hydrophilic residues that might be of an importance for *Tb*PEX14 ligand design are Asn13, Glu16 and Asp20. These three residues are different in *T. cruzi* and human sequences, thus they might account for the ligands' cross-species selectivity (Figure 2, *right*).

The PEX14-PEX5 protein-protein interface poses several challenges for medicinal chemistry that are typical for the PPI target class[39]. First, it is hydrophobic in nature, with only few water exposed polar amino acid side chains in the spatial vicinity. Furthermore, the interface is relatively flat, with only two shallow cavities in the highly solvent-exposed surface. The Phe hotspot appeared as particularly difficult to address, being a 'shelf'[40-42] rather than a classical PPI pocket.

We created a pharmacophore model that mimicked the native binding of the PEX5 WXXX(F/Y) motif to *Tb*PEX14. Two pharmacophoric elements were set as hydrophobic, aromatic rings addressing the respective Trp and Phe pockets. Further, we anticipated that the presence of 'protruding' Phe17 and Phe34 side-chains can be an exploitable feature for ligand design and we defined the third pharmacophore as another connecting aromatic ring that would allow for additional π-stacking. The *in silico* screening cascade using a *Tb*PEX14 homology model prepared from the NMR structure of *Hs*PEX14 NTD (PDB 2W84)[36] identified several compounds with convincing docking poses. We tested these hits for binding to ^{15}N-labelled *Tb*PEX14 NTD using the ^{1}H-^{15}N HSQC NMR chemical shift perturbations (CSP) assay. A

pyrazolo[4,3-*c*]pyridine derivative **1** was the most potent hit, with K_D of 163 μM in the NMR CSP analysis and was resynthesized. The compound disrupted the interaction of the PEX5-derived peptide (ALSEN**W**AQE**F**LA) with both *Tb*PEX14 and *Tc*PEX14, having EC_{50} of 265 μM and 539 μM, respectively, in the AlphaScreen[43] assays (Figure 3 and Table 1). Furthermore, **1** is characterized by a proper drug-likeness profile and was chemically tractable, rendering this compound an attractive starting point for medicinal chemistry optimization.

The docking results suggested that the phenyl residue of **1** addressed the Trp pocket on the *Tb*PEX14 surface, while the indole moiety filled the Phe hotspot (Figure 4, *top*). Such placement of aromatic residues is in fact a mirror image of the native binding mode of PEX5 WXXX(F/Y) fragments to PEX14. However, we have previously shown that the Trp pocket of PEX14 can effectively accommodate Phe residue of F/YXXXF motif in its PPI with another peroxin, PEX19.[36] Another hallmark of the docking-derived binding pose of **1** to PEX14 is that the pyrazolo[4,3-*c*]pyridine central scaffold of the hit compound lays over the Phe17 and Phe34 residues, forming the favorable π-π interactions. We have also identified lower-scored poses, in which the projection of the aromatic phenyl and indole residues of **1** in *Tb*PEX14 cavities was reversed, i.e. directly mimicking the native placement of the aromatic rings in the PEX14-PEX5 PPI (Figure 4, *bottom*). Although this inverted binding pose seemed less plausible due to the number of possible unfavorable interactions with the hydrophilic residues present in the vicinity of the hotspots, it could not be completely disregarded because the overall shape of the PEX14-PEX5 PPI interface is highly symmetrical.

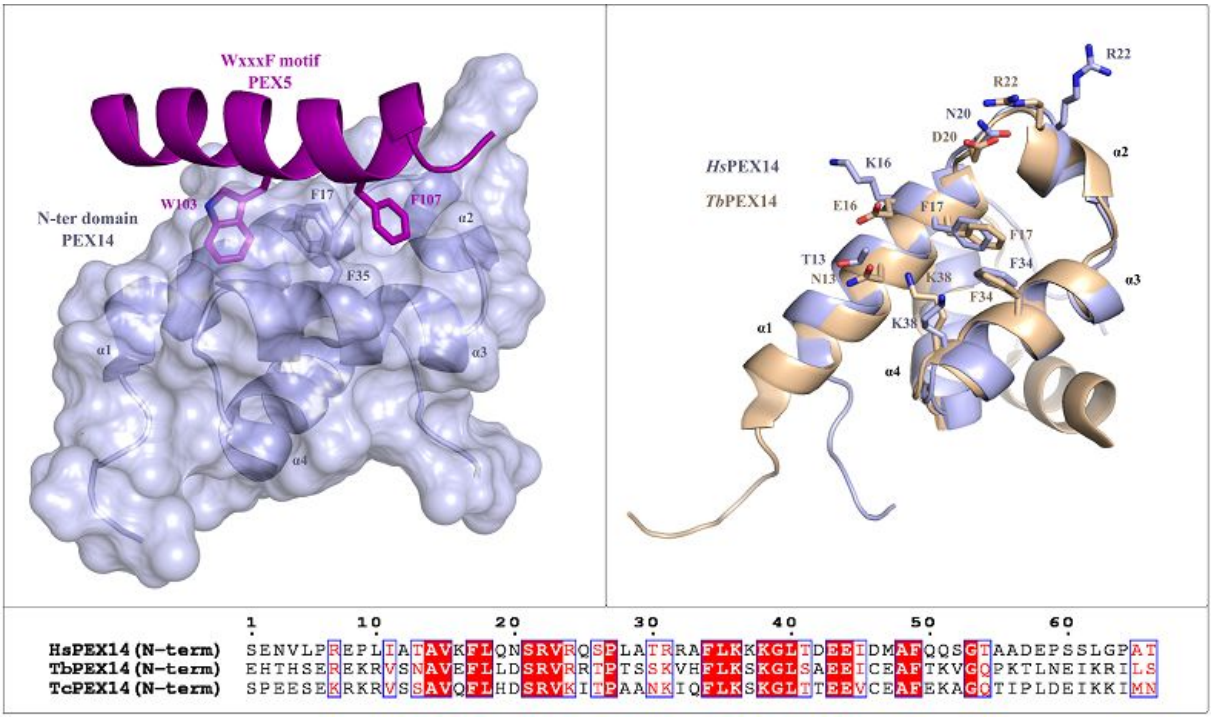

Figure 2. Structural basis for PEX14-PEX5 PPI interface targeting. *Left*: Solution NMR structure of the *Hs*PEX14 NTD in complex with the di-aromatic WXXXF pentapeptide motif of PEX5 (PDB code: 2W84[36]). PEX14 is shown in light blue, whereas PEX5 is shown in magenta. Two hydrophobic cavities on PEX14 surface accommodating Trp103 and Phe107 residues of PEX5 WXXXF are separated by two π-stacked phenylalanine side chains (Phe17 and Phe34). *Right*: Superposition of the solution NMR structures of *Hs*PEX14 (light blue, PDB code: 2W84) and *Tb*PEX14 (gold, PDB code: 5MMC[35]) NTDs. The polar residues (represented as sticks) surrounding the binding pocket are significantly different in both species. *Bottom:* Sequence alignment of *Hs*PEX14, *Tb*PEX14 and *Tc*PEX14.

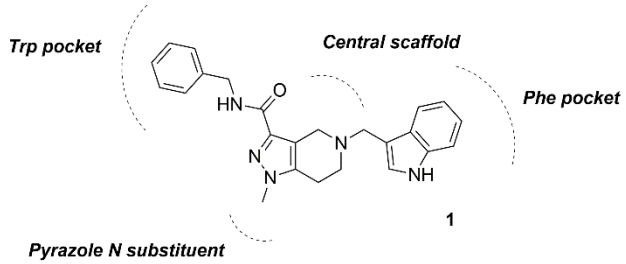

*Tb*PEX14, Kd ~ 50 μM
*Tb*PEX14-PEX5, EC_{50} = 265 μM
*Tc*PEX14-PEX5, EC_{50} = 539 μM

cLogP = 2.8
MW = 399
nON = 6
nOHNH = 2

Figure 3. Structure, properties and proposed derivatization sites of the pyrazolo[4,3-*c*]pyridine *in silico* hit **1**.

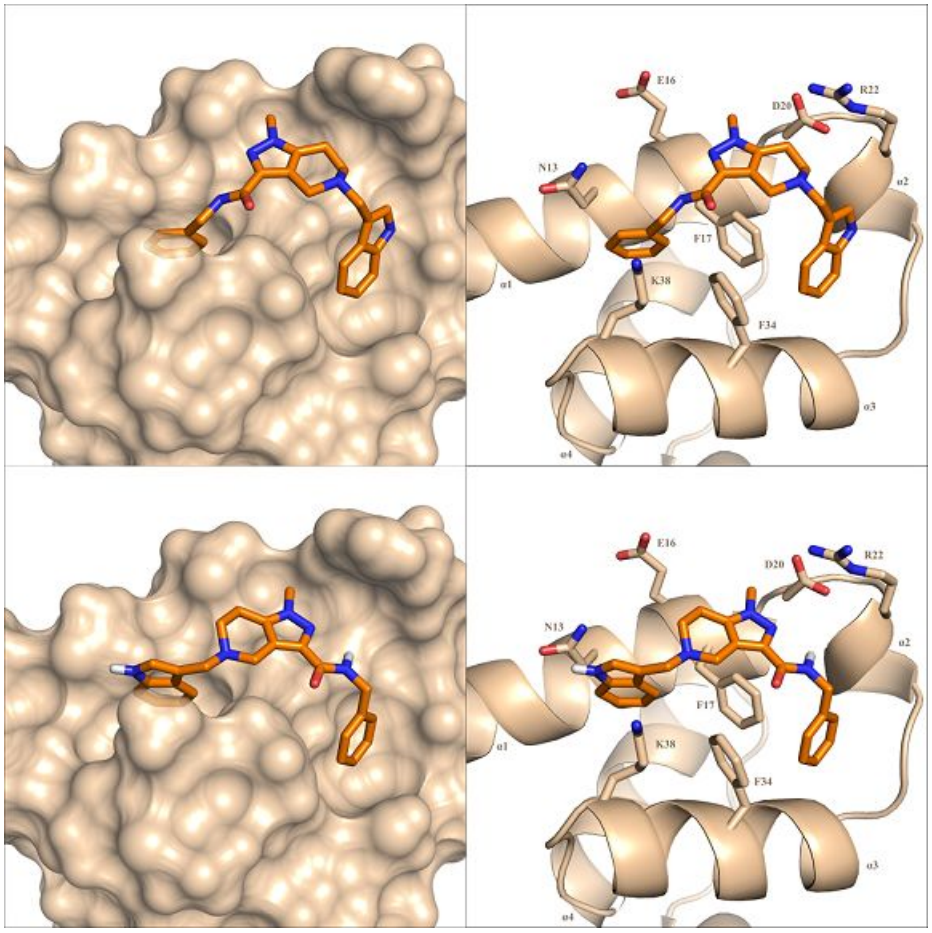

Figure 4. Docking poses of **1** to *Tb*PEX14-PEX5 PPI interface. *Top*: Phenyl residue of **1** occupies the Trp pocket while the indole is positioned in the Phe pocket on the PEX14 surface. *Bottom*: The 'reversed' binding mode of **1** to *Tb*PEX14-PEX5 PPI interface. Surface (*left*) and cartoon (*right*) representation of *Tb*PEX14 (gold).

Initial optimization trials. For optimization purposes we divided the initial hit **1** into four regions: 1) the pyrazole *N* substituent, 2) the residue addressing Trp pocket, 3) the residue addressing Phe pocket and 4) the central scaffold (Figure 3).

According to the preferred docking pose of **1**, the methyl group on pyrazole *N*-1 atom points to the solvent-exposed region of the interface, suggesting that substituents of different size should be tolerable at this position. Despite the proximity of Asn13 (Ser13 in *Tc*PEX14 and Thr13 in *Hs*PEX14) and Glu16 (Gln16 in *Tc*PEX14 and Lys16 in *Hs*PEX14), we expected that modifications addressing this region of the interface may affect the ligand's physicochemical properties (e.g. solubility) rather than significantly influence the affinity to the target. We have found that the binding to PEX14 depends on the position of the substituent in the pyrazole ring.

Contrary to the active hit **1**, the *N*-2 regioisomer **2** showed modest inhibitory activity in the AlphaScreen assay (Table 1) and did not bind *Tb*PEX14 in a ^{1}H-^{15}N HSQC NMR experiment. This was inconsistent with the anticipated binding mode of **1** to *Tb*PEX14, since the distance to the proximal Asn13 and Glu16 should allow the methyl group to be tolerated at the *N*-2 position of the pyrazole. Compound **3** lacking substituents at the *N*-1 atom of the pyrazole had a slightly decreased ability to disrupt PEX5 interaction with both *T. brucei* and *T. cruzi* PEX14, and it was inactive against the human protein. Likewise, the hydroxyethyl derivative **4** showed no superior activity compared to **1**. Carboxylate derivatives **5-7** proved inactive. In conclusion, the initial SAR of the solvent-exposed region could not be fully rationalized on the basis of molecular docking. We have chosen the hydroxyethyl residue in this position due to the superior solubility of the compounds and sought further structural modifications that would yield more potent compounds suitable for co-crystallization trials with *Tb*PEX14.

Since the binding of the PEX5 WXXX(F/Y) motifs to PEX14 is hydrophobic and aromatic in nature, we assumed that optimizing the residues addressing the Trp and Phe hotspots would likely improve ligand affinity. Structural data show that the Trp pocket is quite shallow (Figures 2 and 4). As a result, the orientation of the indole ring in the native PEX14-PEX5 PPI is vertical with respect to the surface of the interface, and the imidazole component of the fused system slightly points out from the hotspot cavity, being surrounded by Lys38 and Asn13 (Ser13 in *Tc*PEX14 and Thr13 in *Hs*PEX14). On the other hand, this pocket has an elongated shape and the docking pose of **1** suggested that there is space that could be filled by a residue larger than the unsubstituted phenyl. Hence, we first modified the substitution pattern on the phenyl ring (Table 1). We synthesized derivatives **8**-**12** having various small lipophilic substituents in meta- and para- position, none of which showed superior activity or species selectivity, when compared to **1**. In contrast to the flat SAR of the substituted phenyls, derivatives **13** and **14** bearing naphthalene moiety, were more effective in disrupting the *Tb*PEX14-PEX5 PPI, with

AlphaScreen-derived EC_{50} values 5 and 8-fold lower than the respective parent compounds **1** and **4**. We have also observed the increased ability of these derivatives to interrupt the *Tc* and *Hs*PEX14-PEX5 complex formation.

As already mentioned, the Phe hotspot on the PE14-PEX5 PPI interface appeared more difficult to target than the Trp pocket because this cavity is shallow and more exposed to solvent. The docking pose of **1** in *Tb*PEX14 showed that this region of the interface is well-filled by the indole moiety of the inhibitor. In fact, replacement of the bicyclic aromatic system of **1** with smaller phenyls yielded only very weak compounds **15-18** (Table 1). Interestingly, inhibitor **19** bearing a bulky naphthalene was inactive, while its 4-methoxy derivative **20**, proved 10-fold more potent in disrupting the *Tb*PEX14-PEX5 PPI than **4**.

Secondary optimization – Phe pocket. The above SAR was in large parts difficult to rationalize without additional structural data. Fortunately, at this stage of the project we were able to obtain a high-resolution X-ray structure of *Tb*PEX14 bound to **13** (PDB code: 5L87[35], Figure 5) that guided further optimization. Overall, the crystallographic data were consistent with the binding mode of **1** to *Tb*PEX14 as predicted by docking. According to the *Tb*PEX14-**13** complex structure, the double aromatic naphthalene system effectively filled the Trp hotspot. However, unlike the vertically oriented Trp side chain in the native PEX5 WXXX(F/Y)-PEX14 PPI, the orientation of the naphthyl group in the Trp pocket is horizontal. A very important feature of the X-ray structure that could not have been predicted on the basis of docking is the presence of one structural water that mediated binding of **13** to the *Tb*PEX14 Asn13 side chain. This has a pronounced influence on the ligand binding mode. Most of all, the ligand is shifted towards Asn13 and Glu16 residues with respect to its orientation speculated on the basis of docking. As a consequence, the indole residue of **13** is shifted out towards the upper rim of the Phe pocket rather than being deeply inserted into this cavity as we

postulated previously. Thus, the filling of the hotspot by the indole can be considered shallow and suboptimal. On the other hand, the aromatic residue of **13** is closer to the Arg22 side chain of PEX14, which, in turn, can stabilize the ligand-protein complex by forming cation-π interactions. The presence of the above-mentioned thermodynamically stable water molecule may also explain the loss of affinity of **2**, in which the methyl group attached to the *N*-2 pyrazole nitrogen atom interferes with the solvation shell of the protein-ligand complex.

Driven by the obtained high-resolution structural information we decided to systematically exploit the SAR of the Phe hotspot, while keeping the Trp pocket occupied by the naphthyl (Table 2). The overall optimization strategy was thus focused on preserving the orientation of the aromatic portion of the substituents addressing the Phe hotspot close to its rim, while simultaneously extending the ligand deeper towards its bottom. First, we synthesized compounds **21-24** bearing various small substituents in the *N*-1 position of the indole system, of which only the methyl and ethyl derivatives **21** and **22**, respectively, showed potency comparable to **14** in the AlphaScreen assay. On the other hand, compounds **23** and **24**, with larger, more polar pendant residues, were slightly less active in disrupting the PEX14-PEX5 PPI. As seen in the *Tb*PEX14-**13** complex structure, the Phe pocket of the interface is filled tightly by the indole residue of the ligand. Hence, there is no possibility of rotation along the *N*-CH_2 bond that links the indole residue to the central scaffold, which would be required to accommodate large indole *N*-1 substituents. Furthermore, as observed in the *Tb*PEX14-**13** complex structure, the ligand binds to the interface in its low-energy conformation. Hence, a considerable entropic penalty would have to be paid for the *N*-1 substituted ligand adaptation to the hotspot.

While indole *N*-1 substituents are in a steric conflict with the amino acid side chain forming the Phe pocket and there is no possibility to compensate this by the adjustment of ligand's

orientation, the analysis of the *Tb*PEX14-**13** complex structure showed that there is enough space in the hotspot to accommodate substituents in the C-7 position. Therefore, in the next optimization round we synthesized compounds **25**-**27** having small residues attached to this carbon atom (Table 2). Gratifyingly, these proved superior to **14** in disrupting the *Tb*PEX14-PEX5 complex formation, each being 2 times more potent than the parent compound in the AlphaScreen assay. As of *Tc* and *Hs*PEX14-PEX5 PPI inhibition, the results varied. Compound **25** had a comparable activity to the parent **14**, while its *N*-1 methyl derivative **26** was 2-times more active. On the other hand, **27** bearing a methyl ester function on C-7 of indole was 2-fold less potent in inhibiting the *T. cruzi* protein. We have also synthesized **28**, in which indole was attached to the central scaffold through C-2 carbon atom, allowing for a deeper insertion of the aromatic residue into the pocket (Table 2). As a result, **28** was more active than its C-3 regioisomer **14** and roughly equipotent to the isomeric methoxy indole derivative **26**.

The different activities of the undecorated indole derivative **14** and **26** resulting from the unequally deep occupation of the Phe pocket recalled the observations made previously for naphthalenes **19** and **20** during the initial optimization trials. With the aim to improve binding of the ligands and to further investigate SAR in the Phe pocket, we solved the crystal structure of the methoxynaphthalene derivative **20** in complex with *Tb*PEX14 (PDB code: 5L8A[35], Figure 6). Overall, the binding mode of **20** to *Tb*PEX14-PEX5 PPI interface closely resembled the one observed for **13** in the *Tb*PEX14-**13** complex. Thus, the phenyl ring of the inhibitor was buried in the Trp pocket, while the naphthalene system filled the upper part of the Phe hotspot, with the methoxy residue reaching the bottom part of the cavity. Importantly, the orientation of the pyrazolo[4,3-*c*]pyridine central scaffold in **13** and **20** was identical, which was a clear indication that a more potent PEX14-PEX5 PPI inhibitor can be obtained by merging those two ligands. Indeed, the hybrid molecule **29** showed a superior activity in the AlphaScreen *Tb*PEX14-PEX5 PPI inhibition assay, when compared to both parent compounds

(Table 2). The methoxy group present at the C-4 atom of the naphthalene in **29** was crucial for the high-affinity interaction with *Tb*PEX14, since derivatives **30** and **31** lacking this residue proved significantly less active. Next, we synthesized **32**, in which one of the fused benzenes of the naphthalene system was saturated. The compound was 3-times less potent than the parent **29**, most likely due to its inability to form cation-π and π-π interactions with the Arg22 and Phe17 residues, respectively. Next, we investigated compounds **33-35** having small substituents other than methoxy at C-4 carbon of the naphthalene. Switching to a larger methylthiol group in **33** resulted in a 3-times stronger inhibition of the *Tc*PEX14-PEX5 complex formation when compared to **29**. Sulfoxide **34**, an expected metabolite of **33**, was significantly less potent. The dimethylamino derivative **35** was as active as the parent compound **29** in inhibiting the *Tb*PEX14-PEX5 PPI, and significantly more potent against *Tc* and *Hs*PEX14.

Finally, we synthesized a series of phenyl derivatives **36-45** having small lipophilic substituents in para- or (and) meta- positions (Table 2). By this, we wanted to verify whether a single aromatic system can outcompete, or at least be as active as, the bulkier and highly lipophilic indoles and naphthalenes. By changing the substitution patterns on the phenyl, we have observed that a gain of potency can be achieved by expanding the ligand towards the bottom of the pocket, similar to what had been observed for the bicyclic aromatic systems in **14** and **21-35**. Several phenyl derivatives were equipotent to **14** in disrupting the *Tb*PEX14-PEX5 complex formation, however, none of them could outcompete the more potent **25-28** nor the C-4 substituted naphthalenes **29** and **33-35**.

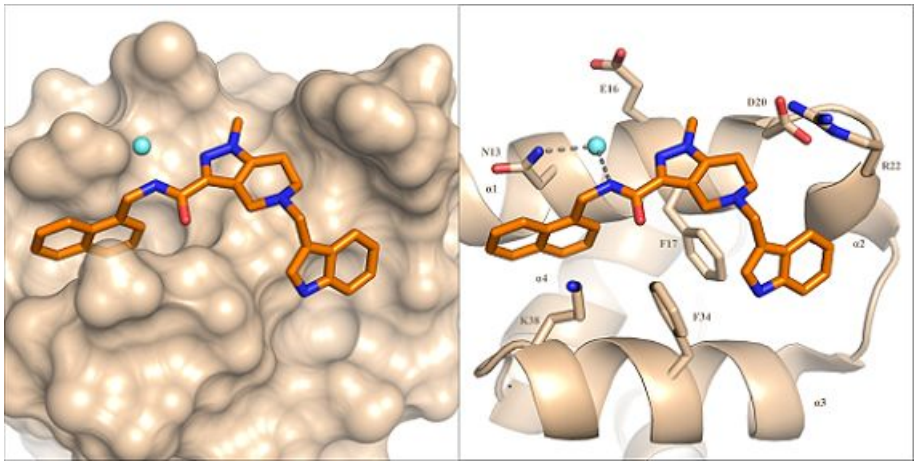

Figure 5. Crystal structure of *Tb*PEX14 in complex with **13** (PDB code: 5L87[35]). *Left*: surface representation of *Tb*PEX14 (gold). A highly conserved water molecule is represented as a sphere. *Right*: cartoon representation of *Tb*PEX14; relevant residues are shown as sticks. A water-mediated hydrogen bond between PEX14 N13 side chain and the amide nitrogen of **13** is presented (gray dashed line).

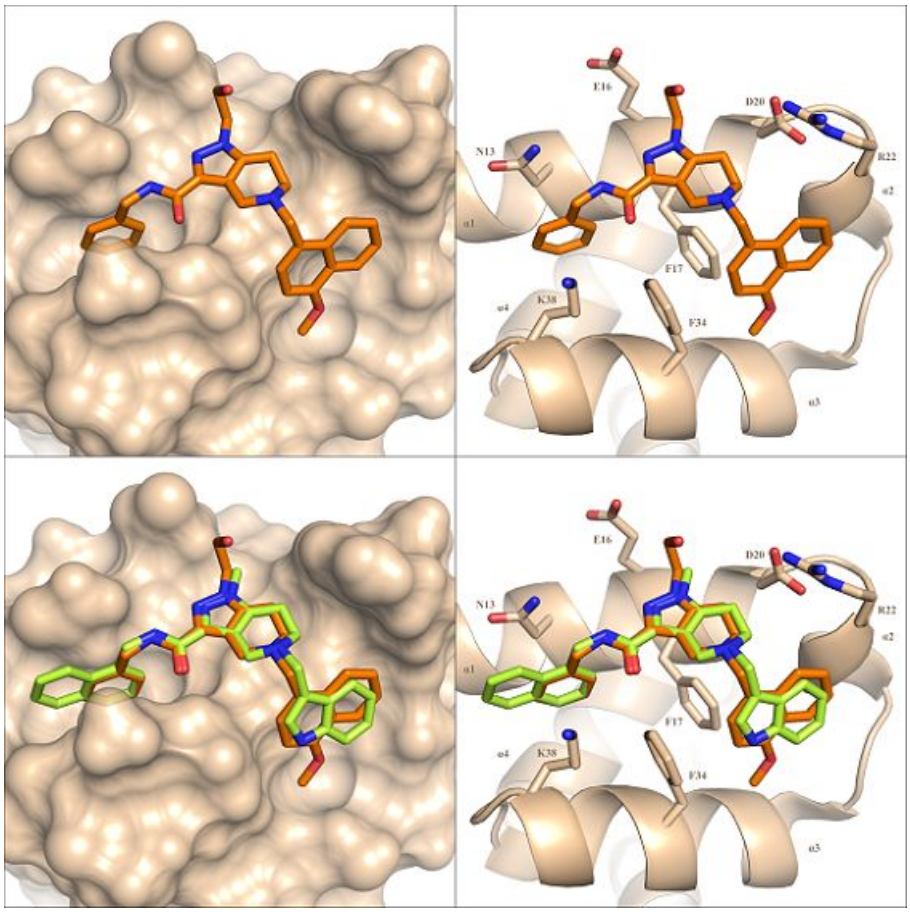

Figure 6. *Top:* Crystal structure of TbPEX14 in complex with **20** (PDB code: 5L8A[35]). *Bottom*: overlay of the binding poses of **13** (purple) and **20** (green). Surface (*left*) and cartoon (*right*) representation of *Tb*PEX14 (gold).

Secondary optimization – around Trp pocket. To further expand the SAR information in PEX14-PEX5 PPI targeting we turned our attention to the region of the interface near the entrance to the Trp hotspot. The crystallographic structures of *Tb*PEX14 in complex with **13** and **20** show that the amide moiety that projects the aromatic residue of the ligand into the Trp pocket is in a low-energy conformation, i.e. coplanar with the pyrazole ring. Hence, we posed the question whether an entropic gain from freezing this favorable conformation can be achieved and we synthesized **46** and **47**, tricyclic derivatives of **29** (Table 3). Both compounds were less potent than the parent inhibitor in the AlphaScreen assay. As previously mentioned, the *Tb*PEX14-**13** complex structure shows an important interaction of the amide NH proton with Asn13 of the protein, mediated through a water molecule. Hence, it is possible that the gain in entropy in **46** and **47** from freezing the molecules in their low-energy conformations cannot compensate the loss in binding affinity caused by the inability of forming the mentioned important connection through water. Intriguingly, this structural change proved deleterious for the ability of the inhibitors to bind *Tc* and *Hs*PEX14 but did not abolish its interaction with the *T. brucei* protein. As a result, **46** and **47** are highly selective in inhibiting the latter PPI. To further explore the importance of the amide linkage in this region of the ligand, we synthesized **48**, a derivative of **29** in which carbonyl oxygen was removed (Table 3). The obtained inhibitor projecting the naphthalene into Trp pocket through alkylamino linker was significantly weaker in inhibiting the PEX14-PEX5 PPI than the parent molecule. We attributed this to the repulsive interactions with Lys38, weaker hydrogen bond accepting properties of the amine and to the increased conformational freedom of the linker when compared to the amide. With the aim to explore the possible polar interactions with Asn13 and Lys38 surrounding the entrance to the Trp pocket, we synthesized sulfonamide **49** (Table 3). The compound failed to inhibit the *Tb*PEX14-PEX5 PPI, likely due to the inability of the relatively narrow Trp pocket to accommodate the sulfonamide moiety.

Secondary optimization – amines in *N*-1 pyrazolo substituent. Our initial optimization trials showed that the substitution pattern at *N*-1 of pyrazole does not significantly alter binding of the ligands to the PEX14-PEX5 PPI interface. However, a closer inspection of the *Tb*PEX14-**20** complex structure revealed that the pendant hydroxyalkyl chain can adopt a conformation in which the hydroxyl lies in a spatial proximity of the carboxylic amino acid residues, Glu16, Asp20 in the solvent-exposed region. Therefore, we posed a question if a switch to an amine can lead to a further improvement in the binding affinity originating from additional electrostatic contacts. Indeed, a simple –OH to $–NH_2$ transition resulted in primary amine **50** which was 6-fold more active in disrupting the *Tb*PEX14-PEX5 PPI and 5-fold more potent against *Tc*PEX14, respectively, than the parent **29** (Table 4). Encouraged by this result, we pursued a series of derivatives **51-61** with various alkylamine residues at the *N*-1 pyrazolo position. Secondary and tertiary amines were tolerated. An important observation was that binding to PEX14 correlates positively with the basicity of the substituents (e.g. **50** *vs* **58**, **54** *vs* **57**, **55** *vs* **56, 59** *vs* **60**) rather than with their hydrogen bond donor or acceptor capabilities (e.g. **50** *vs* **58**).

We solved high-resolution crystal structures of **50** and **61** in complex with the *Tb*PEX14 *N*-terminal domain (PDB codes: 5N8V[35] and 6SPT, Figures 7 and 8, respectively). The *Tb*PEX14-**50** complex structure provides a snapshot of the pendant amino group interacting with Glu16 (Figure 7). However, this interaction is not seen in the *Tb*PEX14-**61** complex structure (Figure 8), which reflects the flexibility of the hydroxyalkyl chain. As X-ray crystallography may not always precisely reveal the flexible ligand-protein interactions due to the crystal symmetry-related contacts, we analyzed the binding of the amino groups in **50** and **61** and hydroxyl of **29** with the carboxylic residues of Glu16 and Asp20 of *Tb*PEX14 by performing molecular dynamics (MD) simulations (Figure 9 and Figure S2 – see *Supporting Information*). The computations clearly show the high occurrence of interactions of the amino groups with both

residues. In contrast, the MD simulation did not show significant interaction of the pendant hydroxyethyl group of derivative **29**. Here, the occurrence of the interaction during the MD run is much lower.

The negatively charged Glu16 residue is present in the *Tb*PEX14 amino acid sequence, but not in *Tc*PEX14 (Gln16) or *Hs*PEX14 (Lys16). Furthermore, in the *Hs*PEX14 sequence Asp20 is replaced by the neutral Asn20. In this context, it is intriguing that the ligands bearing positive charge (i.e. amines **50**-**55**, **59** and **61**) show enhanced inhibitory activity in the latter two PPIs. On the other hand, it has been shown that the binding affinity and thermodynamics in solvent-exposed protein cavities, such as those present on PEX14 surface, is not only affected by the direct interactions of ligand atoms with protein residues, but can also depend significantly on the alterations of the water envelope around the ligand-protein complex.[44] Indeed, both *Tb*PEX14-**50** and *Tb*PEX14-**61** complex X-ray structures document the involvement of the flexible alkylamines in the water network around the ligand. Similar engagement can be expected in *Tc* and *Hs*PEX14, which might explain the enhancement in inhibitory activity of the ligands against the PPIs of those proteins with PEX5.

Overall, the sum of the effects described above provided a significant improvement of the activity of the ligands against all three tested PEX14 proteins. This enhancement was most pronounced in the case of *Tb*PEX14-PEX5 PPI, which resulted in the higher selectivity of compounds towards this PPI.

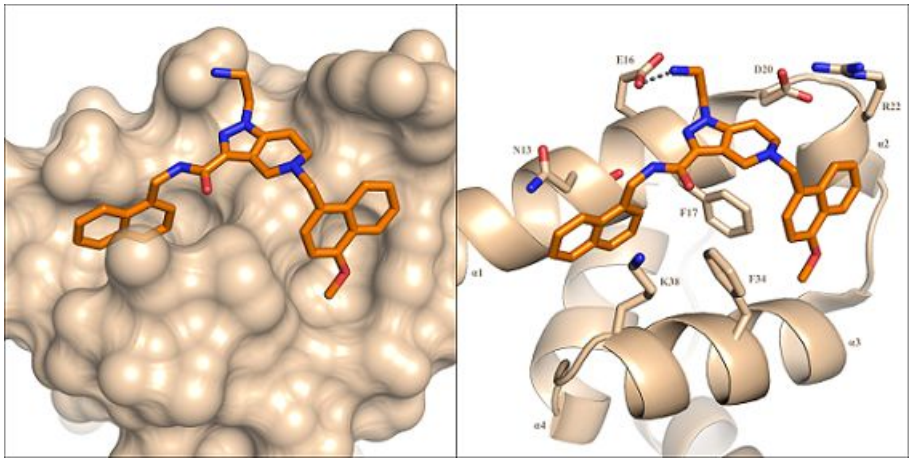

Figure 7. High resolution crystal structure of *N*-terminal domain of *Tb*PEX14 in complex with compound **50** (PDB code: 5N8V[35]). Surface (*left*) and cartoon (*right*) representation of *Tb*PEX14 (gold).

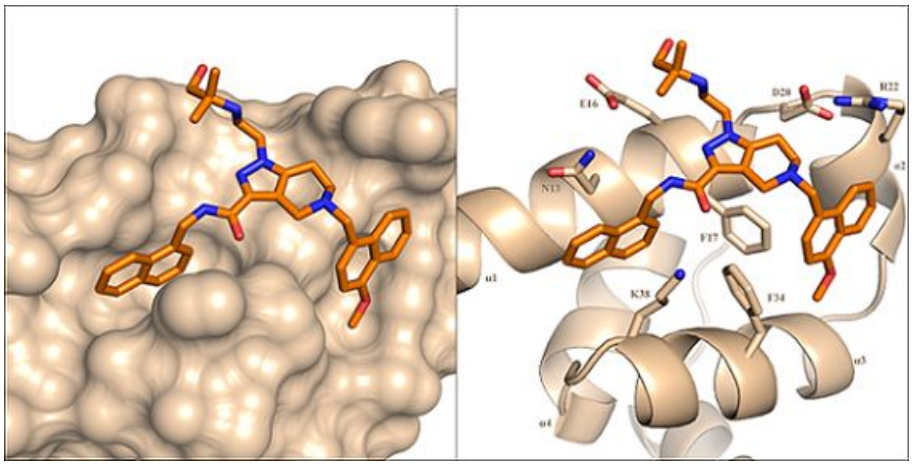

Figure 8. High resolution crystal structure of *N*-terminal domain of *Tb*PEX14 in complex with compound **61** (1.2 Å, PDB code: 6SPT). Surface (*left*) and cartoon (*right*) representation of *Tb*PEX14 (gold).

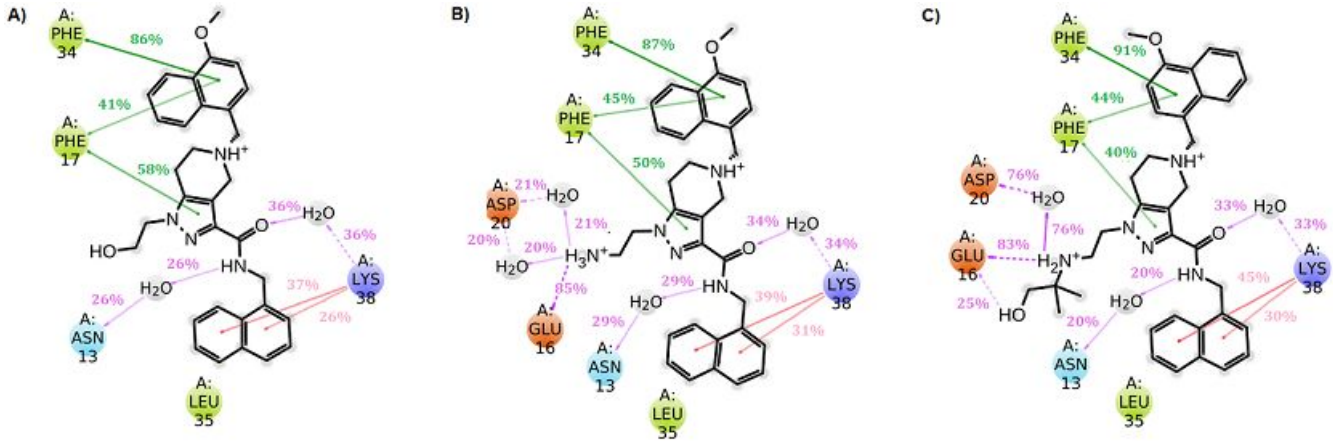

Figure 9. Ligand interaction diagrams of the final molecular dynamics simulations snapshots. The MDs were performed for *Tb*PEX14-**29** (A), *Tb*PEX14-**50** (B) and *Tb*PEX14-**61** (C) complexes. Blue lines represent H-bonding interactions, red cation-π and green π –π interactions. Introduction of alkylamine residues at *N*-1 pyrazolo position leads to formation of direct and water-mediated interaction pattern significantly improving compound affinity.

Secondary optimization – central scaffold. Finally, we decided to obtain some SAR information of the central bicyclic scaffold. Quaternization of the tertiary amine in **29** resulted in a permanently charged derivative **62**, which did not show superior binding to PEX14 (Table 5). Decreasing the size of the aliphatic ring of **29** by one methylene unit produced the pyrrolo[3,4-*c*]pyrazole **63**, which was 2-fold more active than the parent compound in inhibiting the *Tb*PEX14-PEX5 PPI, and 3-fold more potent against *Tc*PEX14 and *Hs*PEX14. The amino derivative of alcohol **63**, compound **64**, showed the expected enhancement in PEX14 binding, with respect to its 6-membered ring homologue **50**. Finally, the amino alcohol **65** was the most potent PEX14 binder, representing a first inhibitor of *Tb*PEX14-PEX5 PPI with submicromolar EC_{50} value in the AlphaScreen assay.

Cellular activity of the PEX14-PEX5 PPI inhibitors. The synthesized compounds were evaluated for their trypanocidal effect against *T. brucei brucei* bloodstream form (Lister 427, MITat 1.2) in the resazurin-based cell survival assay. *T. b. brucei* is the causative agent of animal trypanosomiasis and was used as a model organism for the primary screening of trypanocidal activities of the inhibitors. The obtained EC_{50} values are presented in Tables 1-5. Besides several outliers, the trypanocidal activity of the tested derivatives correlates well with the results of the AlphaScreen-based *Tb*PEX14-PEX5 PPI inhibition assay. We have also observed a remarkable enhancement of the antiparasitic activity in compounds bearing an aminoalkyl chain attached to the *N*-1 position of the pyrazole, resulting in submicromolar EC_{50} values in the resazurin-based assay (Tables 4 and 5). We attribute this to the greater inhibitory

potency of those compounds against the *Tb*PEX14-PEX5 PPI. Compounds **50**-**52** were most active from the series, having EC_{50} values below 100 nM (Table 4).

Additionally, the investigated PEX14-PEX5 PPI inhibitors were assayed for their cytotoxicity in the human-derived HepG2 cell line (Tables 1-5). In general, the cytotoxicity of some of the compounds followed their inhibitory activity against *Hs*PEX14-PEX5 PPI. This was most pronounced for many of the indole derivatives (eg. **2**-**8**, **14**, **21**-**28**). On the other hand, some other active *Hs*PEX14 ligands did not follow this trend (eg. naphthalenes **20**, **29**, **35**). Overall, the selectivity index for trypanocidal activity against *T. b. brucei* improved along with increased efficacy of compounds in disrupting PEX14-PEX5 PPI. This was most pronounced in the alkylamine derivatives (Tables 4 and 5), many of which displayed favorable selectivity profiles (eg. **50**, **51**, **53**, **54**, **61**, **64**, **65**).

The PEX14-PEX5 PPI inhibitors showing high trypanocidal efficacy against *T. b. brucei* were further evaluated activity against *T. b. rhodesiense* STIB900, a human pathogen derived from an African (United Republic of Tanzania) patient (Table 6). In general, the results followed the SAR pattern observed in the primary *T. b. brucei* screening. The *T. b. rhodesiense* STIB900 strain was even more susceptible to the PEX14-PEX5 PPI inhibitors, which resulted in more preferable selectivity indices. The high activity of the compounds against the human pathogen may have practical implications and merit further development of the PEX14-PEX5 PPI inhibitors as potential treatments against HAT.

Unlike *T. brucei*, *T. cruzi* parasites do not use glycolysis as the main energy source for the cell. However, they still use glycosomes to compartmentalize other essential metabolic processes. Hence, we wanted to check whether impairing the function of the organelle by PEX14-PEX5 PPI inhibition is also lethal to *T. cruzi*. When assayed for their trypanocidal activity against the amastigote forms of the *T. cruzi* Tulahuen strain C2C4 grown in rat L-6 myoblasts (Table 6),

the tested PEX14-PEX5 PPI inhibitors demonstrated varied efficiency. The IC_{50} values were higher than those obtained for *T. brucei* and thus the selectivity indices determined with uninfected L-6 cells were narrower. The aminoalkyl derivatives **50**, **61** and **64** displayed highest potency, showing sub-micromolar trypanocidal activities and fair therapeutic indices. A general observation was that the correlation between the ability to break the PEX14-PEX5 PPI and trypanocidal efficacy is less clear in *T. cruzi* than in *T. brucei*. Presumably, this reflects the characteristics of the assay, in which the *T. cruzi* parasites are located within myoblasts and therefore the compounds have to pass multiple cellular membranes and environments to reach the target.

Table 1. Initial optimization of **1**.

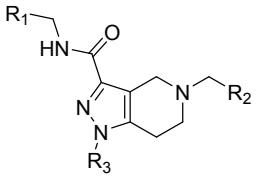

#	R_1	R_2	R_3	*Tb*PEX14 EC_{50} [µM][a]	*Tc*PEX14 EC_{50} [µM][a]	*Hs*PEX14 EC_{50} [µM][a]	*T. brucei* EC_{50} [µM][b]	*HepG2* EC_{50} [µM][b]	SI[c]
1		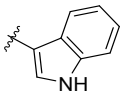		265±37	539±75	223±30	18.5 (15.2-22.6)	>50	>2.7
2[d]		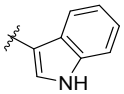		>1000	>1000	>1000	18.6 (13.7-25.2)	>50	>2.7
3		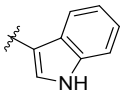		441±47	768±150	>1000	5.16 (3.02-7.30)	29.4 (20.8-41.6)	>5.7
4		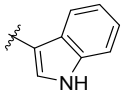	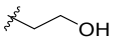	421±19	828±127	>1000	21.0 (17.8-24.7)	>50	>2.4
5		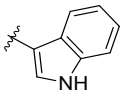	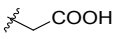	>1000	>1000	>1000	>50	>50	nd

6		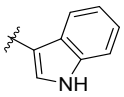	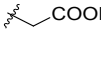	550±144	>1000	>1000	16.7 (13.6-20.5)	>50	>3.0
7		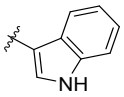		>1000	>1000	>1000	3.05 (2.83-3.27)	29.7 (22.5-36.9)	>9.7
8	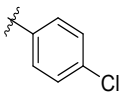	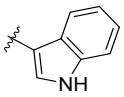		740±167	384±69	555±120	5.74 (4.57-7.22)	>20	>3.5
9	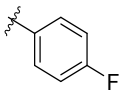	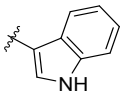		559±33	505±42	509±35	11.5 (6.75-19.7)	nd	nd
10	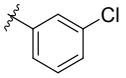	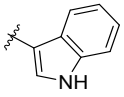		381±60	632±83	218±15	5.19 (3.04-7.34)	nd	nd
11	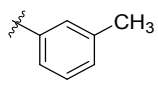	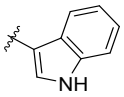		233±25	422±29	244±21	11.8 (3.9-35.7)	34.8 (31.3-38.7)	2.9
12	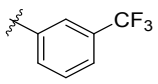	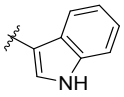		879±140	625±94	427±54	4.25 (3.84-4.71)	nd	nd
13	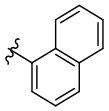	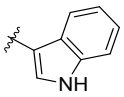		51.3±2.1	99.5±25.7	51.1±4.1	2.96 (2.84-3.08)	14.4 (12.8-16.8)	4.9
14	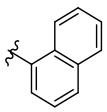	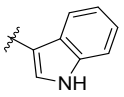		53.7±4.8	68.0±4.3	57.9±3.3	4.50 (3.87-5.23)	7.87 (7.28-8.44)	2.7
15				>1000	>1000	>1000	2.15 (1.42-3.26)	>50	>23.2
16		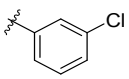		>1000	nd	nd	nd	nd	nd
17		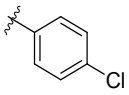		>1000	nd	nd	nd	nd	nd
18		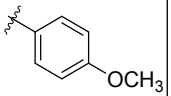		627±76	>1000	>1000	1.74 (0.82-3.60)	>50	>28.7

19		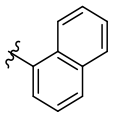	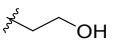	>1000	nd	nd	nd	nd	nd
20		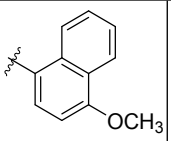	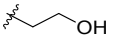	46.3±0.40	704±449	135±15	9.33 (8.43-10.3)	34.9 (28.3-41.5)	>3.6

[a] EC_{50} values were calculated as a Hill curve fit to 12 point titration. SD represents fitting error. nd = not determined. [b]EC_{50} values are shown as mean (n=4). Values in parentheses are 95% confidence intervals. [c]Selectivity index is calculated as *HepG2* EC_{50} [μM]/*T. brucei* EC_{50} [μM]. [d]*N*-2 regioisomer of **1**.

Table 2. Secondary optimization of the residue addressing the Phe pocket.

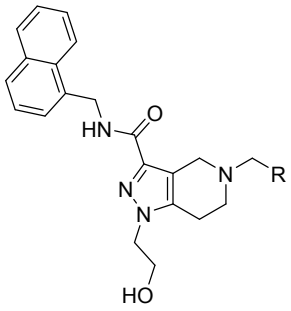

#	R	*Tb*PEX14 EC_{50} [µM][a]	*Tc*PEX14 EC_{50} [µM][a]	*Hs*PEX14 EC_{50} [µM][a]	*T. brucei* EC_{50} [µM][b]	*HepG2* EC_{50} [µM][b]	SI[c]
14	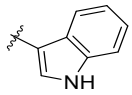	53.7±4.8	68.0±4.3	57.9±3.3	4.50 (3.87-5.23)	7.87 (7.28-8.44)	1.7
21	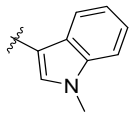	40.2±2.1	73.2±4.6	43.9	2.62 (2.42-2.85)	8.60 (7.25-10.14)	3.3
22	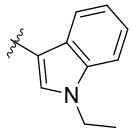	49.4±4.8	68.5±3.5	63.4	2.86 (2.18-3.76)	nd	nd
23	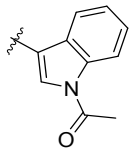	86.7±10.1	166±15	141	5.70 (2.82-11.70)	22.7 (18.0-27.4)	4.0
24	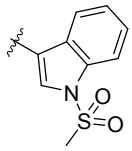	80.9±19.5	118±12	176	6.09 (5.66-6.56)	13.3 (9.9-17.5)	2.2
25	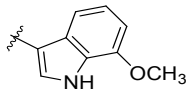	24.4±0.1	65.1±11.1	51.9±2.0	4.38 (4.08-4.70)	13.8 (11.9-15.6)	3.2
26	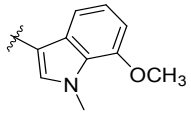	25.4±1.6	37.3±2.0	23.9±1.9	3.36 (2.90-3.90)	7.34 (6.26-8.42)	2.2
27	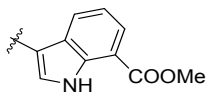	28.9±1.5	102±38	59.5±3.8	5.46 (4.59-6.22)	12.9 (13.2-16.6)	2.7

28	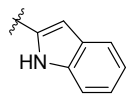	20.3±2.6	43.6±4.4	35.5±1.6	5.41 (4.29-6.84)	9.39 (8.64-10.21)	1.7
29	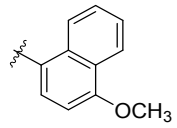	14.8±1.9	104±40	39.7±5.0	3.56 (3.29-3.85)	>50	>14.0
30	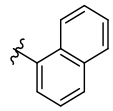	454±143	>1000	>1000	7.95 (6.74-9.38)	9.11 (8.93-9.24)	1.5
31	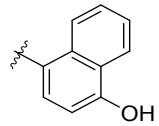	565±369	>1000	>1000	>20	>50	nd
32	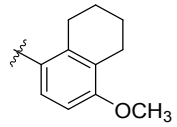	38.3±1.7	142±49	60.8±4.7	nd	nd	nd
33	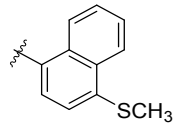	19.0±4.4	38.0±11.8	32.4±14.8	3.92 (2.78-5.51)	nd	nd
34	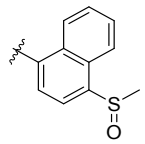	122±27	168±11.1	437±137	8.40 (7.53-9.36)	29.2 (25.9-32.5)	3.5
35	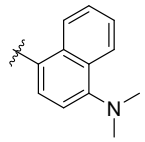	16.2±5.9	21.0±2.2	16.4±2.3	5.70 (4.81-6.76)	>50	>8.8
36		200±25	>1000	503±55	13.1 (11.3-14.9)	38.2 (30.6-47.1)	2.9
37	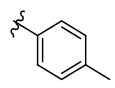	75.1±2.9	387±178	181±19	7.26 (6.07-8.45)	nd	nd
38	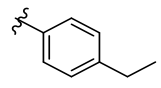	55.7	nd	nd	7.62 (6.68-8.72)	nd	nd
39	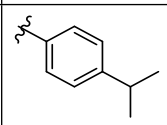	56.2±5.6	126±51	149±30	3.29 (3.16-3.44)	nd	nd

40	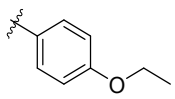	51.7±4.5	369±201	113	6.22 (5.90-6.52)	nd	nd
41	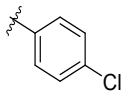	53.2±7.0	229±44	86.1±8.6	3.98 (3.83-4.14)	14.1 (12.3-16.1)	3.5
42	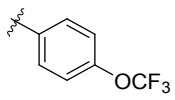	95.0±14.8	280±54	116±15	5.64 (5.08-6.21)	nd	nd
43	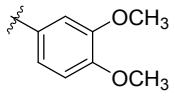	50.9±4.8	287±64	138±13	10.4 (8.3-12.9)	40.8 (34.7-46.9)	3.9
44	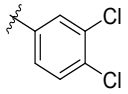	44.7±5.4	354±173	95.5±9.8	4.29 (3.36-5.22)	nd	nd
45	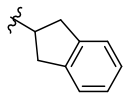	137±63	259±160	422±342	nd	13.8 (12.3-15.4)	nd

[a]EC_{50} values were calculated as a Hill curve fit to 12 point titration. SD represents fitting error. nd = not determined. [b]EC_{50} values are shown as mean (n=4). Values in parentheses are 95% confidence intervals. [c]Selectivity index is calculated as *HepG2* EC_{50} [µM]/*T. brucei* EC_{50} [µM].

Table 3. Secondary optimization around the Trp pocket.

#	R	***Tb*PEX14 EC_{50} [µM][a]**	***Tc*PEX14 EC_{50} [µM][a]**	***Hs*PEX14 EC_{50} [µM][a]**	***T. brucei* EC_{50} [µM][b]**	***HepG2* EC_{50} [µM][b]**	**SI[c]**
46	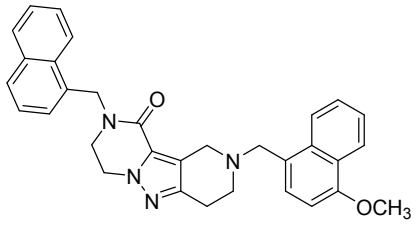	49.2±19.5	463±203	>1000	6.42 (5.61-7.20)	>50	>7.8
47	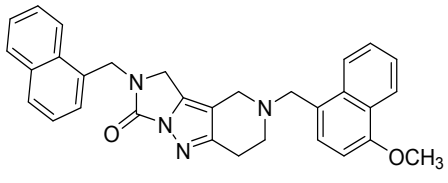	103±17	448±408	>1000	5.61 (5.13-6.11)	>50	>8.9

48	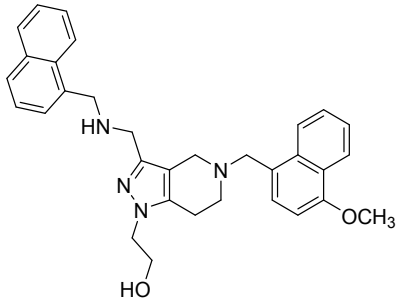	174±17	176±9	nd	nd	29.6 (24.4-36.2)	nd
49	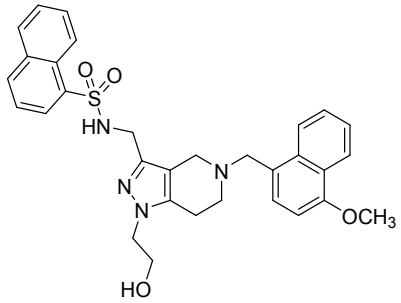	>1000	208±33	>1000	5.94 (3.63-9.73)	16.4 (13.6-19.7)	2.8

[a]EC_{50} values were calculated as a Hill curve fit to 12 point titration. SD represents fitting error. nd = not determined. [b]EC_{50} values are shown as mean (n=4). Values in parentheses are 95% confidence intervals. [c]Selectivity index is calculated as *HepG2* EC_{50} [µM]/*T. brucei* EC_{50} [µM].

Table 4. Secondary optimization of the pyrrole *N*-substituent: amines.

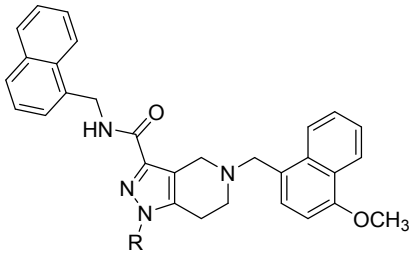

#	R	*Tb*PEX14 EC_{50} [µM][a]	*Tc*PEX14 EC_{50} [µM][a]	*Hs*PEX14 EC_{50} [µM][a]	*T. brucei* EC_{50} [µM][b]	*HepG2* EC_{50} [µM][b]	SI[c]
29	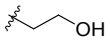	14.8±1.9	104±40	39.7±5.0	3.56 (3.29-3.85)	>50	>14.0
50	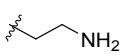	3.94±0.40	22.1±2.3	19.3±2.3	0.081 (0.075-0.087)	3.74 (3.04-4.44)	46.1
51	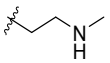	1.86±0.09	31.9±1.7	9.31±1.07	0.099 (0.095-0.103)	7.36 (6.33-8.39)	74.3
52	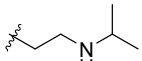	1.80±0.10	25.3±1.44	7.89±1.14	0.070 (0.051-0.096)	nd	nd

53		1.92±0.19	19.9±1.5	9.55±0.93	0.292 (0.275-0.310)	>50	>100
54	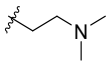	3.2±0.48	21.5±1.7	8.69±0.84	0.236 (0.223-0.248)	8.84 (6.53-10.75)	37.5
55	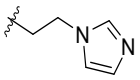	2.9±0.2	10.7±1.3	7.25±0.56	2.46 (2.22-2.79)	7.54 (5.30-10.35)	3.1
56	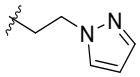	34.4±11.2	247±113	94.5±21.4	3.60 (3.23-4.20)	nd	nd
57	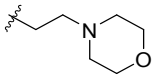	88.1±13.1	162±43	166±35	3.58 (3.19-4.02)	42.0 (32.9-59.9)	11.7
58	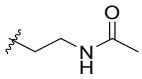	17.9±1.17	70.8±7.6	33.5±5.0	5.73 (4.90-6.70)	4.92 (3.60-6.25)	<1
59	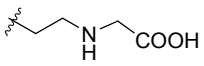	4.05±0.60	41.9±3.2	nd	4.74 (4.14-5.38)	nd	nd
60	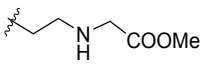	57.6±6.5	333±34	nd	4.68 (4.36-5.03)	nd	nd
61	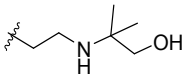	7.78±1.6	27.5±3.4	9.31±1.07	0.503 (0.486-0.531)	6.50 (6.06-7.16)	12.9

[a]EC_{50} values were calculated as a Hill curve fit to 12 point titration. SD represents fitting error. nd = not determined. [b]EC_{50} values are shown as mean (n=4). Values in parentheses are 95% confidence intervals. [c]Selectivity index is calculated as *HepG2* EC_{50} [µM]/*T. brucei* EC_{50} [µM].

Table 5. Secondary optimization – central scaffold.

#	Compound structure	***Tb*PEX14 EC_{50} [µM][a]**	***Tc*PEX14 EC_{50} [µM][a]**	***Hs*PEX14 EC_{50} [µM][a]**	***T. brucei* IC_{50} [µM][b]**	***HepG2* IC_{50} [µM][b]**	**SI[c]**
29	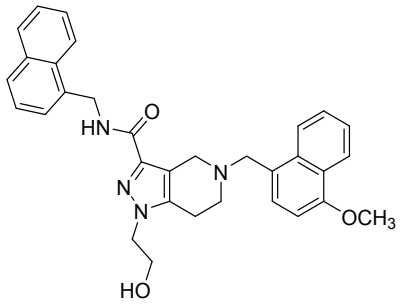	14.8±1.9	104±40	39.7±5.0	3.56 (3.29-3.85)	>50	>14.0

62	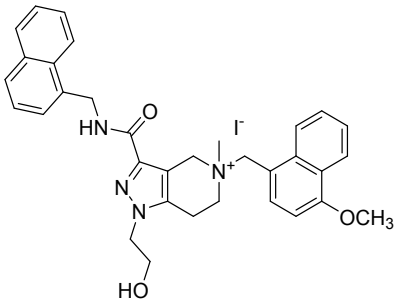	17.8±1.8	54.4±3.9	34.0±3.9	10.1 (8.5-13.4)	>50	>5.0
63	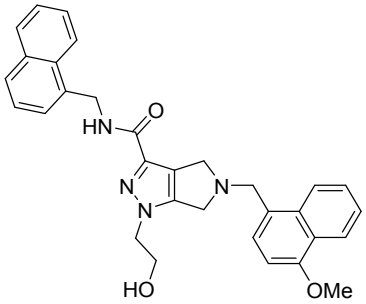	8.17±0.69	30.0±1.8	15.3±0.5	6.01 (4.65-7.77)	nd	nd
50	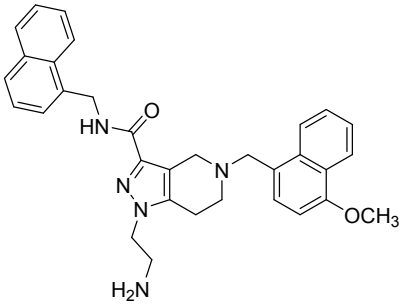	3.94±0.40	22.1±2.3	19.3±2.3	0.081 (0.075-0.087)	3.74 (3.02-4.44)	46.2
64	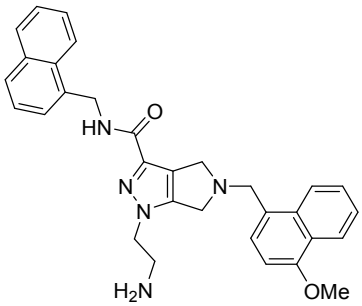	1.22±0.22	15.8±1.2	4.38±0.71	0.225 (0.207-0.244)	3.67 (3.52-3.82)	16.3
65	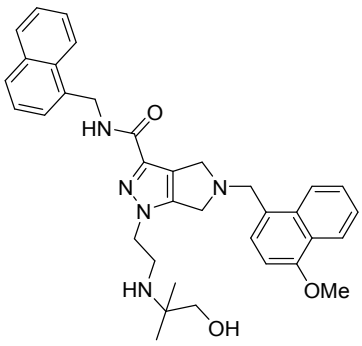	0.67±0.15	11.7±0.4	3.48±0.11	0.549 (0.513-0.587)	3.82 (3.60-4.04)	7.0

[a]EC_{50} values were calculated as a Hill curve fit to 12 point titration. SD represents fitting error. nd = not determined. [b]EC_{50} values are shown as mean (n=4). Values in parentheses are

95% confidence intervals. [c]Selectivity index is calculated as *HepG2* EC_{50} [µM]/*T. brucei* EC_{50} [µM].

Table 6. *In vitro* trypanocidal activity of compounds against *T. brucei rhodesiense STIB900* and *T. cruzi.*

#	*T. b. rhodesiense* IC_{50} [µM][a]	*T. cruzi* IC_{50} [µM][a]	*L6* IC_{50} [µM][a]	SI[b]
1	1.52±0.67	9.16±0.87	16.8±0.2	1.8
2	6.00±0.06	16.8±0.9	34.5±3.9	2.1
4	6.38±0.40	21.5±0.2	43.2±3.2	2.0
14	2.14±0.18	5.22±0.01	5.93±0.16	1.1
29	4.42±0.16	3.83±1.94	12.7±2.6	3.3
33	5.54±0.28	4.35±0.09	17.6±0.70	4.0
50	0.012±0.004	0.320±0.074	1.80±0.06	5.6
52	0.009±0.001	3.16±1.36	1.66±0.01	>1
58	1.98±0.57	7.22±1.30	5.84±0.70	>1
61	0.029±0.001	2.20±0.28	1.82±0.10	>1
63	1.89±0.28	1.52±0.32	9.19±0.42	6.0
64	0.075±0.008	0.627±0.290	1.96±0.04	3.1
65	0.179±0.048	2.28±0.12	1.96±0.10	>1

[a]EC_{50} values are shown as mean±deviation from the mean (n=2). [c]Selectivity index is calculated as *L6* EC_{50} [µM]/*T. cruzi* EC_{50} [µM].

Chemistry. The synthetic pathway used to access the *in silico* hit **1** and its C-2 regioisomer **2** is shown in Scheme 1. The key pyrazolo[4,3-*c*]pyridine **66** was obtained by adopting a literature method[45] to a *one-pot* process, without isolating the intermediate mixed-Claisen condensation product. The subsequent *N*-methylation of the pyrazole ring of **66** resulted in two chromatographically separable regioisomers **67** and **68**, in a 60:40 proportion. The 1,5,7-Triazabicyclo[4.4.0]dec-5-ene (TBD)-catalyzed aminolysis[46] of the respective esters **67** and **68**, followed by Boc-deprotection and reductive amination steps, gave the corresponding regioisomeric compounds **1** and **2**.

Scheme 1. Synthetic route to the *in silico* hit **1** and its C-2 regioisomer **2**[a]

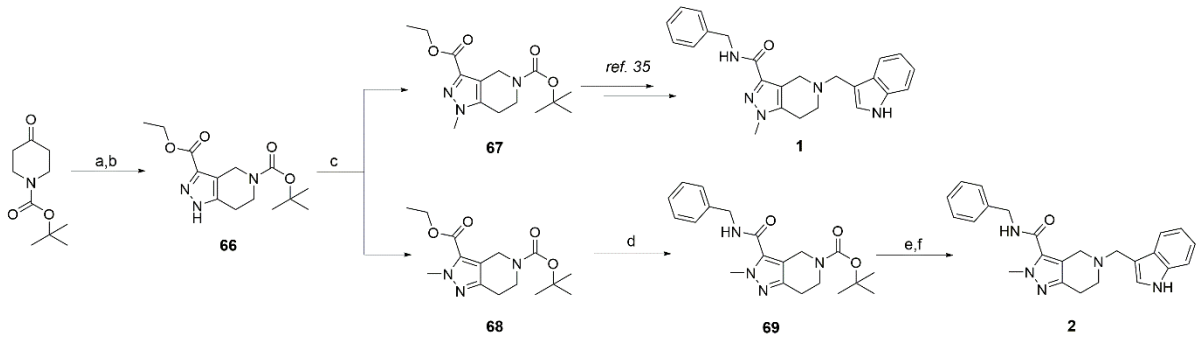

[a]Reagents and Conditions: (a) LHMDS, THF, -78 °C, then $(COOEt)_2$, THF, -78 °C to rt; (b) hydrazine hydrate, THF, EtOH, AcOH, reflux; (c) Cs_2CO_3, DMF, rt, then MeI, DMF, rt; (d) benzylamine, TBD, THF, 60 °C; (e) 4 M HCl, 1,4-dioxane, rt; (f) TEA, THF, rt, then AcOH, indole-3-carboxaldehyde, $NaBH(OAc)_3$, THF, rt.

Highlighted in Scheme 2 are the synthetic routes employed for initial optimization trials. Compound **66** was used as a common intermediate to synthesize the derivatives having various substituents in the *N*-1 position of the pyrazolo[4,3-*c*]pyridine system. Aminolysis of **66** resulted in **70**, which was subjected to Boc-deprotection and reductive amination steps to give the *N*-1 unsubstituted derivative **3**. Conversion of **70** to **71** and **72** by *N*-alkylation and *N*-acylation reactions, respectively, followed by the deprotection/reductive amination sequence, resulted in corresponding derivatives **6** and **7**. Ester **6** was saponified to give the carboxylate **5**.

Attempts to obtain the hydroxyethyl derivatives **73** and **74** by the direct *N*-alkylation of **66** with 2-bromoethanol resulted in low conversions and afforded complex mixtures that were difficult to purify. Hence, we turned to a more practical route employing one pot mixed-Claisen condensation and pyrazole formation that gave the mixture of regioisomers **73** and **74** in a 75:25 proportion. These regioisomers were readily separable by recrystallization and chromatography. Deprotection and reductive amination of intermediate **73** afforded compound **75** that served as a starting material for subsequent aminolyses, leading to derivatives **4** and **8-12** bearing various phenyl substituents. Finally, reaction of ester **73** with benzylamine gave intermediate **76** that was used in the subsequent Boc-deprotection and reductive amination steps that led to derivatives **15-19** with different aromatic substituents addressing the Phe pocket of PEX14.

Scheme 2. Synthetic routes employed for the initial optimization trials (Table 1)[a]

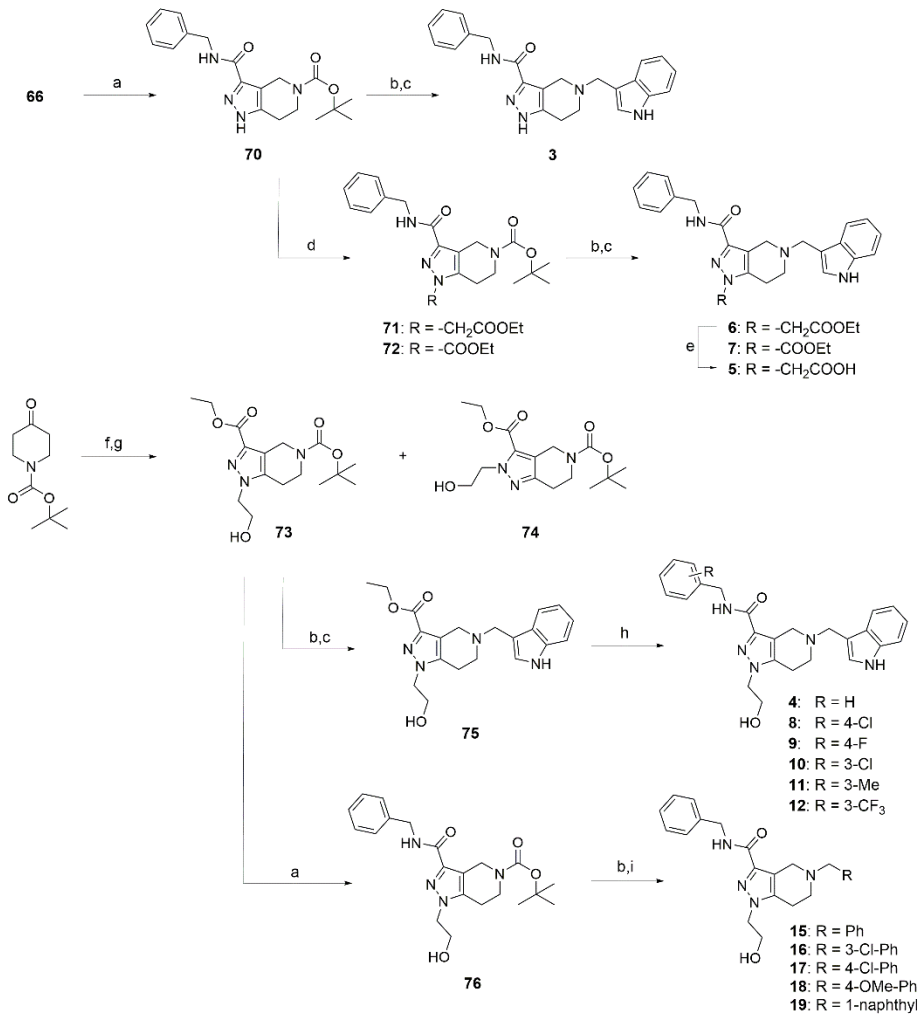

[a]Reagents and conditions: (a) benzylamine, TBD, THF, 60 °C; (b) 4 M HCl, 1,4-dioxane, rt; (c) TEA, THF, rt, then AcOH, indole-3-carboxaldehyde, $NaBH(OAc)_3$, THF, rt; (d) Cs_2CO_3, DMF, rt, then ethyl 2-bromoacetate, DMF, rt (for **71**) or ethyl chloroformate, DIPEA, 0 °C to rt (for **72**); (e) KOH, $EtOH/H_2O$, rt, then NH_4Cl, $EtOH/H_2O$, rt; (f) LHMDS, THF, -78 °C, then $(COOEt)_2$, THF, -78 °C to rt; (g) 2-hydrazinoethanol, THF, EtOH, AcOH, reflux; (h) amine, TBD, THF, 60 °C; (i) TEA, THF, rt, then AcOH, aldehyde, $NaBH(OAc)_3$, THF, rt.

The synthetic route used for the secondary optimization trials of the residue addressing the Phe pocket is shown in Scheme 3. Briefly, ester **73** was converted to amide **77** by the previously described method.[35] Intermediate **77** was then Boc-deprotected and the resulting amine salt **78** was used to generate the desired derivatives **14**, **21**-**28**, and **30**-**45** either by reductive aminations or by the $ZnCl_2$-mediated Mannich reaction.[47]

Scheme 3. Synthetic routes employed for the optimization of the residue addressing the Phe pocket (Table 2)[a]

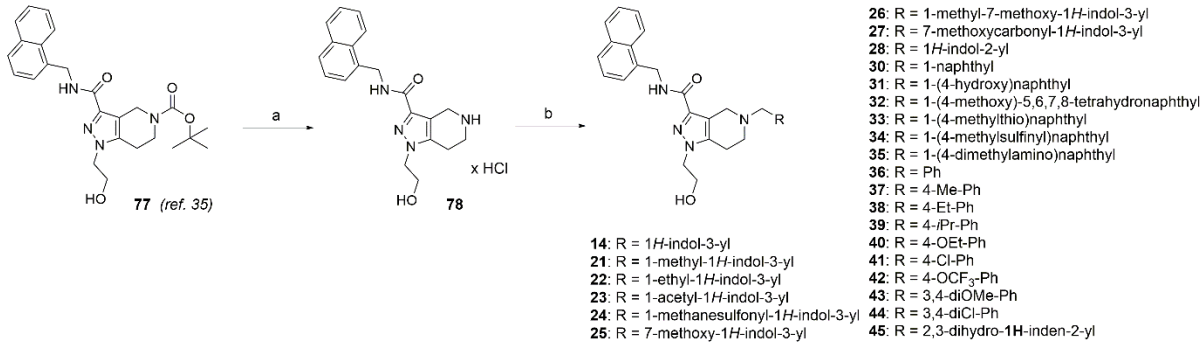

[a]Reagents and Conditions: (a) 4 M HCl, 1,4-dioxane, rt; (b) TEA, THF, rt, then AcOH, aldehyde, $NaBH(OAc)_3$, THF, rt (for **14**, **21**-**26**, **28** and **30**-**45**) or 7-methoxycarbonyl-*1H*-indole, $HCHO_{aq}$, $ZnCl_2$, EtOH, rt (for **27**).

The synthesis of compounds **46**-**49**, having modifications within the region projecting aromatic residues to the Trp pocket of PEX14, is depicted in Scheme 4. Intermediate **80** was obtained from compound **74** by an aminolysis/Boc-deprotection/reductive amination sequence. The hydroxyl group of **80** was then converted to mesylate and the subsequent treatment with a strong base induced the ring closure leading to compound **46**. To obtain the sterically constrained derivative **47**, intermediate **66** was first converted to compound **82** in a manner similar to synthesis of compound **80** from **74**. The amide **82** was then reduced with $LiAlH_4$ and the resulting amine **83** was treated with 1,1'-Carbonyldiimidazole (CDI) to afford tricyclic compound **47**. Derivatives **48** and **49** were accessed by reductive amination or acylation, respectively, of the common intermediate amine **86** obtained from compound **73** by a sequence comprising of aminolysis/Boc-deprotection/reductive amination/$LiAlH_4$ reduction.

Scheme 4. Synthetic routes employed for the optimization around the Trp pocket (Table 3)[a]

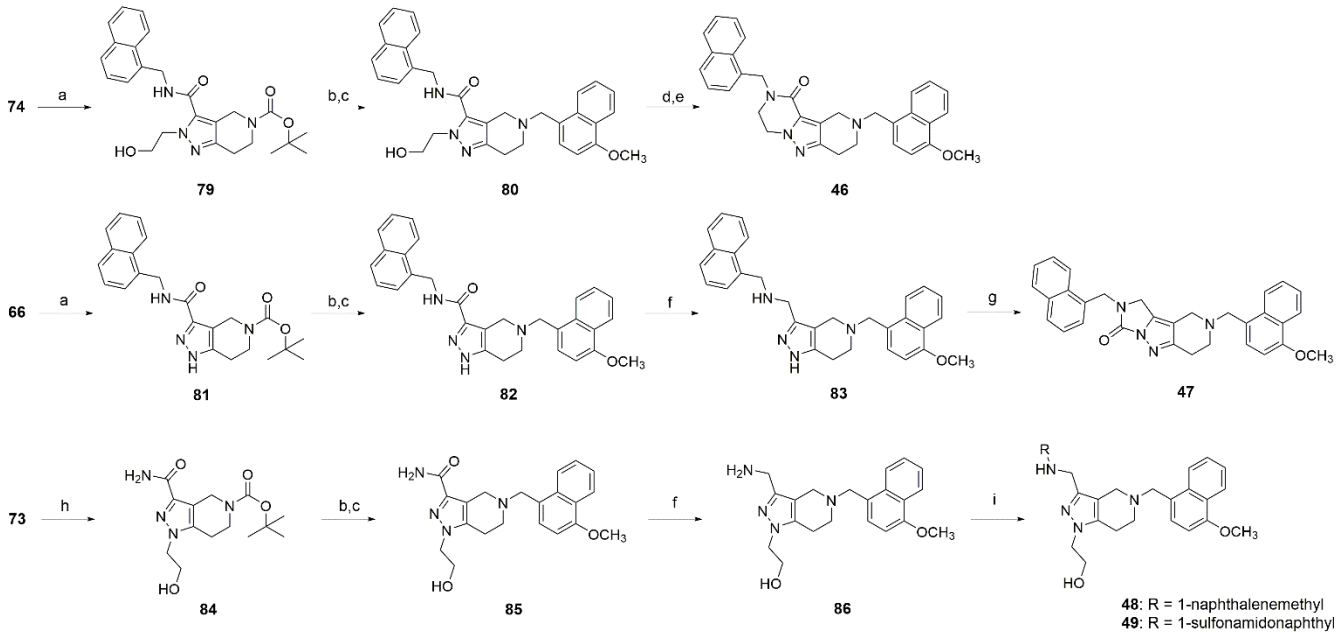

[a]Reagents and Conditions: (a) 1-naphthalenemethylamine, TBD, THF, 60 °C; (b) 4 M HCl, 1,4-dioxane, rt; (c) TEA, THF, rt, then AcOH, 4-methoxy-1-naphthaldehyde, $NaBH(OAc)_3$, THF, rt; (d) MsCl, DIPEA, DMAP, DCM, 0 °C to rt; (e) *t*BuOK, THF, 0 °C to rt; (f) $LiAlH_4$, THF, rt, then reflux; (g) CDI, DCM, rt; (h) NH_{3aq}, EtOH, reflux; (i) TEA, THF, rt, then AcOH, 1-naphthalenecarboxaldehyde, $NaBH(OAc)_3$, THF, rt (for **48**), or 1-naphthalenesulfonyl chloride, TEA, DMAP, DCM, 0 °C to rt (for **49**).

Scheme 5 shows the synthesis of pyrazolo[4,3-*c*]pyridine derivatives bearing various alkylamino substituents on the *N*-1 atom. Compounds **51**, **55**-**57**, and **59** were obtained from the tosylate **87** by the *N*-alkylation reactions of the appropriate aliphatic amines or heterocyclic bases. Glycinate ester **59** was saponified to give the corresponding carboxylic acid **60**. Compounds **52**, **54** and **58** were obtained by reductive amination or acetylation of the primary amine **50**. The azetidine derivative **53** was synthesized from compound **82** by alkylation of the pyrazole nitrogen atom with *tert*-butyl 3-((methylsulfonyl)oxy)azetidine-1-carboxylate, followed by removal of the Boc protecting group.

Scheme 5. Synthetic routes employed for the secondary optimization of the pyrazole *N*-substituent (Table 4)[a]

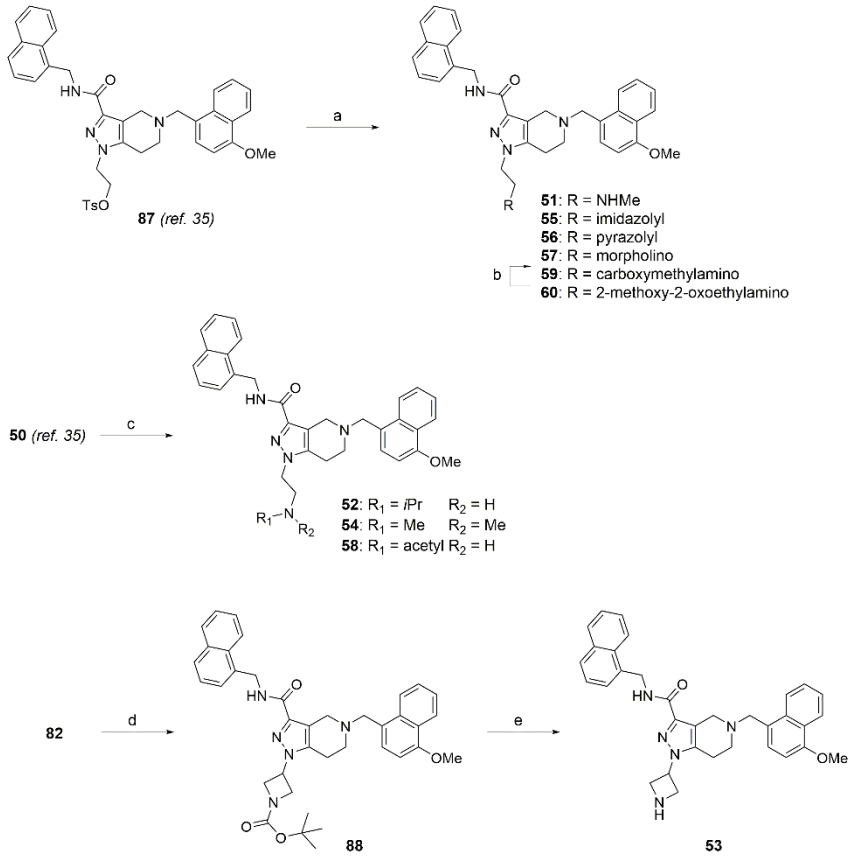

[a]Reagents and Conditions: (a) $MeNH_2$, DCM/EtOH, reflux (for **51**), imidazole, Cs_2CO_3, DMF, 60 °C (for **55**), pyrazole, Cs_2CO_3, DMF, 60 °C (for **56**), morpholine, Cs_2CO_3, DMF, 60 °C (for **57**), methyl glycinate hydrochloride, K_2CO_3, MeCN, reflux (for **59**); (b) NaOH, MeOH/H_2O, rt; (c) acetone, AcOH, $NaBH(OAc)_3$, THF, rt (for **52**), $HCHO_{aq}$, AcOH, $NaBH(OAc)_3$, THF, rt (for **54**) or Ac_2O (neat), 80 °C (for **58**); (d) *tert*-butyl 3-((methylsulfonyl)oxy)azetidine-1-carboxylate, Cs_2CO_3, DMF, 90 °C; (e) 4 M HCl, 1,4-dioxane, rt, then K_2CO_3, rt.

Synthetic routes to compounds with modifications within the central heterobicyclic core are shown in Scheme 6. The quaternary ammonium salt **62** was obtained by treatment of **29** with excess of MeI. To synthesize derivatives with pyrazolo[4,3-*c*]pyrrole heterocycle as the central scaffold we attempted to apply the one-pot procedure used for construction of the homologous (2-hydroxyethyl)-1,4,6,7-tetrahydro-5*H*-pyrazolo[4,3-*c*]pyridines **73** and **74**. This resulted in formation of mixtures containing cyclized regioisomeric products and open-chain hydrazones, as judged by LC-MS analyses. An additional step comprising of prolonged refluxing in acetic acid was required to drive the cyclocondensation process to completion. Acetylation of the

hydroxyl group in products **89** and **90** as well as partial lactonization of the *N*-2 regioisomer **89** to compound **90** was observed at the same time. Acetyl removal with K_2CO_3 in intermediate **89** afforded the free alcohol **92** that gave the final compounds **63**, **64** and **65** in similar synthetic sequences to those used previously for synthesis of derivatives **29**, **50** and **61**.[35]

Scheme 6. Synthetic routes employed for the optimization of the central scaffold (Table 5)[a]

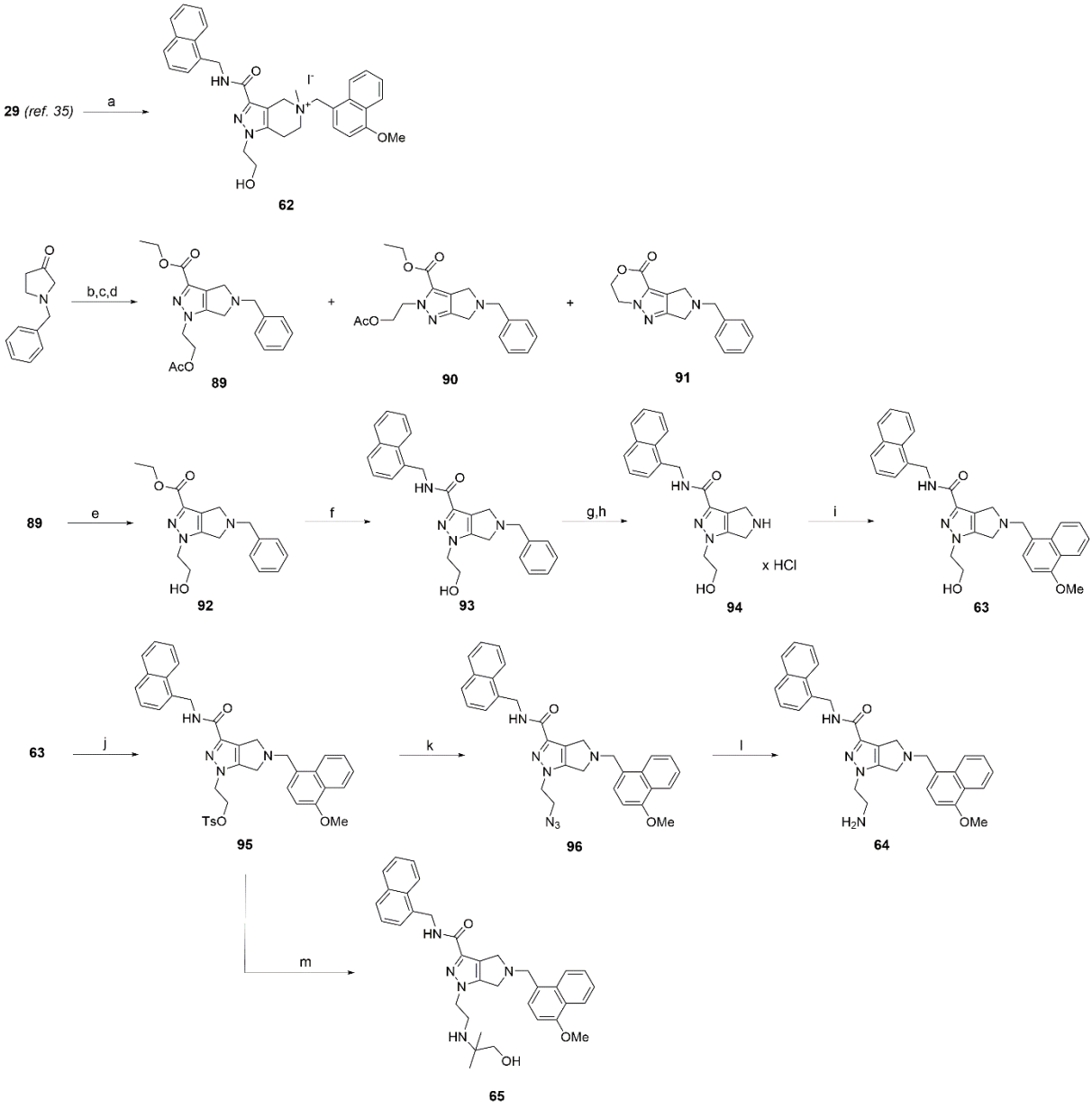

[a]Reagents and Conditions: (a) MeI, $CHCl_3$, rt; (b) LDA, THF, -78 °C, then $(COOEt)_2$, THF, -78 °C to rt; (c) 2-hydroxyethylhydrazine, THF, EtOH, AcOH, reflux; (d) AcOH, reflux; (e) K_2CO_3, EtOH, 60 °C; (f) 1-naphthalenemetylamine, TBD, THF, 60 °C; (g) 1,4-cyclohexadiene, 10% Pd/C, MeOH, reflux; (h) HCl, Et_2O, DCM, 0 °C to rt; (i) 4-methoxy-1-naphthaldehyde, $NaBH(OAc)_3$, AcOH, THF, rt; (j) TsCl, TEA, DMAP, DCM, 0 °C to rt; (k) NaN_3, DMF, 70

°C; (l) PPh_3, THF, rt, then H_2O, THF, 50 °C; (m) 2-amino-2-methyl-1-propanol, K_2CO_3, CH_3CN, reflux.

CONCLUSIONS

Glycosomal enzymes have long been considered attractive molecular targets for combating parasitic diseases, such as HAT and Chagas disease. Targeting the PEX14-PEX5 PPI leads to mislocalization of glycosomal enzymes, which has a dual effect: the absence of the enzymes in the lumen of the glycosome compromises glycosome biogenesis and function, while the presence of the glycosomal kinases in the cytosol dissipates ATP levels. To verify that this is indeed a useful target for molecular intervention, we have used a structure-based drug design approach to develop the first small-molecule agents that inhibit the PEX14-PEX5 PPI. We have performed a systematic optimization of different sites in the initial *in silico* pyrazolo[4,3-*c*]pyridine hit **1** and found compounds that disrupt PEX14-PEX5 PPI, kill *T. brucei* and *T. cruzi* parasites in sub-micromolar concentrations and display fair therapeutic windows between trypanocidal activity and cytotoxicity for the mammalian cells. Hence, the pyrazolo[4,3-*c*]pyridine series of compounds represents an attractive lead series for treatment of HAT and Chagas disease and can also serve as tools for studying biochemical processes related to glycosomes and peroxisomes.

There have been successful medicinal chemistry campaigns that developed new PPI inhibitors as preclinical and clinical candidates. Still, this target class is considered difficult to be targeted by classical small molecules and successful drug development may require involvement of alternative chemical matter that goes far beyond the established criteria of drug-likeness.[39] A good example of such compounds is Venetoclax, a Bcl-2-Bak/Bax PPI inhibitor that displays violations of the classical drug-likeness principles (e.g. large MW, high logD, poor aqueous solubility) but has quite recently been approved for treatment of chronic lymphocytic leukemia (CLL)[48]. The presented PEX14-PEX5 PPI inhibitors display suboptimal pharmacochemical properties[35], since the binding of the ligands to PEX14 hotspots is mostly lipophilicity-driven.

However, we also show that polar interactions with charged amino-acids in the spatial proximity of the PPI hotspots can also be addressed and illustrate this by providing detailed structure activity data. Importantly, our results indicate that addressing specific water-mediated interactions is very important for design of compounds that bind the highly solvent-exposed PEX14 surface, and may be useful to improve the overall physicochemical profile of the obtained inhibitors, which is another subject of our ongoing efforts.

EXPERIMENTAL SECTION

Chemistry. Unless otherwise noted, all reagents were obtained from commercial sources and used without further purification. Technical grade solvents for chromatography and aqueous workup were distilled prior to use. Dry DCM, DMF and THF were purchased from Acros. Manual flash column chromatography (FC) was performed using Merck silica gel 60 (particle size: 0.040-0.063 mm). Automated preparative chromatography was performed on Grace Reveleris Prep purification system using linear gradient elution and Buchi Reveleris Silica 40 μm cartridges for normal phase (SiO_2) and Buchi Reveleris C-18 40 μm cartridges for reverse-phase (RP-C18) separations. Analytical thin layer chromatography (TLC) was performed on Merck silica coated plates (silica gel 60 F 254). Compounds were detected by ultraviolet (UV) irradiation at 254 or 366 nm. The final compounds were ≥95% pure, as determined by HPLC-MS analyses performed on a Dionex UltiMate 3000 HPLC system coupled with a Thermo Finnigan LCQ ultrafleet mass spectrometer, using the following methods: A) Waters X-Bridge C18 (4.6 x 30 mm, 3.5 μm) column; gradient: 5 to 95% of acetonitrile + 0.1% formic acid v/v in water + 0.1% formic acid v/v over 5 min period; flow rate: 1.1 mL/min; UV detection at 214 and 280 nm; B) Thermo Scientific Accucore aQ (2.1 x 50 mm, 2.6 μm) column; gradient: 5 to 95% of acetonitrile + 0.1% formic acid v/v in water + 0.1% formic acid v/v over 5 min period; flow rate: 0.9 mL/min; UV detection at 214 and 280

nm. High-resolution mass spectrometry (HRMS) measurements were performed on a Thermo Finnigan LTQ FT apparatus using an electrospray ionization (ESI) detector. NMR spectra were recorded on a Bruker AV250, Bruker AVHD300, Bruker AV360, Bruker AVHD400 or Bruker AV500C (equipped with a QNP Cryoprobe) spectrometer. NMR peaks are reported as follows: chemical shift (δ) in parts per million (ppm) relative to residual non-deuterated solvent as internal standard ($CHCl_3$: δH = 7.26, δC = 77. 2; DMSO: δH = 2.50, δC = 39.5 ppm), multiplicity (s = singlet, d = doublet, t = triplet, q = quartet, dd = doublet of doublets, dt = doublet of triplets, m = multiplet and bs = broad signal), coupling constant (in Hz) and integration. Compounds **1**, **13**, **20**, **29**, **50**, **61**, **77**, **87** were synthesized as described previously[35].

5-((1*H*-indol-3-yl)methyl)-*N*-benzyl-2-methyl-4,5,6,7-tetrahydro-2*H*-pyrazolo[4,3-*c*]pyridine-3-carboxamide (2). Intermediate **69** (100 mg, 0.27 mmol 1.0 eq.) was dissolved in a 4 M solution of HCl in 1,4-dioxane (0.5 mL). The mixture was stirred for 4 h at rt and concentrated *in vacuo*. The crude solid material was suspended in dry THF (1 mL) and TEA (27 mg, 0.27 mmol, 1.0 eq.) was added. The mixture was stirred for 0.5 h followed by addition of indole-3-carboxaldehyde (39 mg, 0.27 mmol, 1.0 eq.), AcOH (16 mg, 0.27 mmol, 1.0 eq.) and $NaBH(OAc)_3$ (86 mg, 0.40 mmol, 1.5 eq.). After stirring for 12 h, the mixture was quenched with saturated aqueous solution of $NaHCO_3$ (2 mL) and extracted with EtOAc (2x2 mL). The combined organic extracts were washed with water (1 mL), brine (1 mL), dried over anhydrous Na_2SO_4, filtered and concentrated *in vacuo*. The residue was purified by FC (EtOAc/MeOH/TEA 99:1 to 94:5:1) to yield 65 mg (60%) of the title compound **2** as a pale-yellow solid. ^{1}H NMR (500 MHz, $CDCl_3$) δ 8.30 (bs, 1H), 7.69 (d, J = 7.9 Hz, 1H), 7.37 (d, J = 8.2 Hz, 1H), 7.34 - 7.30 (m, 3H), 7.22 (ddd, J = 7.1, 3.1, 1.8 Hz, 2H), 7.13 - 7.07 (m, 2H), 5.79 (t, J = 5.2 Hz, 1H), 4.53 (d, J = 5.7 Hz, 2H), 4.10 (s, 3H), 3.93 (s, 2H), 3.65 (s, 2H), 2.88 (t, J = 5.8 Hz, 2H), 2.79 (t, J = 5.7 Hz, 2H). ^{13}C NMR (126 MHz, $CDCl_3$) δ 160.2,

145.8, 137.7, 136.2, 130.9, 128.8, 127.8, 127.7, 127.6, 123.7, 122.2, 119.7, 119.2, 115.0, 112.3, 111.2, 52.4, 50.1, 49.5, 43.5, 39.1, 23.4. ESI HRMS (m/z): calcd for $C_{24}H_{26}N_5O$ $[M+H]^+$ 400.21319, found 400.21345.

5-((1*H*-Indol-3-yl)methyl)-*N*-benzyl-4,5,6,7-tetrahydro-1*H*-pyrazolo[4,3-*c*]pyridine-3-carboxamide (3). Compound **3** was synthesized employing the procedure described for compound **2**, using intermediate **70** (200 mg, 0.56 mmol, 1.0 eq.), 4 M solution of HCl in 1,4-dioxane (1 mL), TEA (56 mg, 0.56 mmol, 1.0 eq.), indole-3-carboxaldehyde (81 mg, 0.56 mmol, 1.0 eq.), AcOH (34 mg, 0.56 mmol, 1.0 eq.) and $NaBH(OAc)_3$ (119 mg, 0.84 mmol, 1.5 eq.) and dry THF (2 mL). Purification by FC (hexane/EtOAc 1:1 to 0:1, then AcOEt/TEA 99:1) gave 2.15 g (89%) of the title compound **3** as a white solid. ^{1}H NMR (500 MHz, DMSO-d_6) δ 12.86 (bs, 1H), 10.94 (bs, 1H), 8.52 (t, J = 6.5 Hz, 1H), 7.63 (d, J = 7.9 Hz, 1H), 7.35 (d, J = 8.1 Hz, 1H), 7.35 - 7.24 (m, 5H), 7.24 - 7.16 (m, 1H), 7.06 (t, J = 7.5 Hz, 1H), 6.95 (t, J = 7.5 Hz, 1H), 4.35 (d, J = 6.5 Hz, 2H), 3.83 (s, 2H), 3.35 (s, 1H), 2.72 (t, J = 5.6 Hz, 2H), 2.66 (t, J = 5.6 Hz, 2H). ^{13}C NMR (126 MHz, DMSO-d_6) δ 163.0 (bs), 141.5 (bs), 140.5 (bs), 139.0 (bs), 136.9, 128.6, 127.9, 127. 7, 127.0, 124.9, 121.4, 119.6, 118.8, 115.9 (bs), 111.8, 111. 8, 53.1, 49.7, 49.6, 42.1, 22.0 (bs). ESI HRMS (m/z): calcd for $C_{23}H_{24}N_5O$ $[M+H]^+$ 386.19809, found 386.19743.

5-((1*H*-Indol-3-yl)methyl)-*N*-benzyl-1-(2-hydroxyethyl)-4,5,6,7-tetrahydro-1*H*-pyrazolo[4,3-*c*]pyridine-3-carboxamide (4). Compound **4** was synthesized employing the procedure described for compound **69**, using intermediate **75** (120 mg, 0.40 mmol, 1.0 eq.), benzylamine (51 mg, 0.40 mmol, 1.2 eq.) and TBD (15 mg, 0.11 mmol, 0.3 eq.) and dry THF (1 mL). Purification by FC (EtOAc/MeOH/TEA 99:0:1 to 93:6:1) gave 90 mg (64%) of the title compound **4** as a white solid. ^{1}H NMR (500 MHz, DMSO-d_6) δ 10.95 (s, 1H), 8.44 (t, J = 6.0 Hz, 1H), 7.63 (d, J = 7.8 Hz, 1H), 7.36 (d, J = 8.1 Hz, 1H), 7.33 -7.24 (m, 5H), 7.24 –

7.18 (m, 1H), 7.07 (t, *J* = 7.4 Hz, 1H), 6.97 (t, *J* = 7.4 Hz, 1H), 4.91 (t, *J* = 5.5 Hz, 1H), 4.36 (d, *J* = 6.3 Hz, 2H), 4.05 (t, *J* = 5.3 Hz, 2H), 3.84 (bs, 2H), 3.72 (d, *J* = 4.8 Hz, 2H), 3.58 (bs, 2H), 2.73 (bs, 4H). ^{13}C NMR (101 MHz, DMSO-d_6) δ 162.6, 140.50, 140.47, 139.9, 136.3, 128.6, 127.9, 127.8, 127.0, 125.0, 121.4, 119.6, 118.8, 116.5, 111.8, 60.6, 53.0, 52.0, 49.6, 49.5, 42.1, 22.2. ESI HRMS (m/z): calcd. for $C_{25}H_{28}N_5O_2$ $[M+H]^+$ 430.22375, found 430.22358.

2-(5-((1*H*-Indol-3-yl)methyl)-3-(benzylcarbamoyl)-4,5,6,7-tetrahydro-1*H*-pyrazolo[4,3-*c*]pyridin-1-yl)acetic acid (5). Compound **6** (100 mg, 0.21 mmol, 1.0 eq.) was dissolved in EtOH (4mL), followed by addition of aqueous solution of KOH (59 mg, 1.05 mmol, 5.0 eq. in 0.5 mL of water). The solution was stirred for 0.5 h at rt and saturated aqueous solution of NH_4Cl (0.5 mL) was added. The mixture was concentrated *in vacuo* and the residue was refluxed with water (3 mL). The resulting solid was filtered and dried *in vacuo* to give 63 mg (67%) of the title compound **5** as a white solid. ^{1}H NMR (360 MHz, DMSO-d_6) δ 11.16 (bs, 1H), 8.54 (t, *J* = 6.4 Hz, 1H), 7.69 (d, *J* = 7.9 Hz, 1H), 7.39 (d, *J* = 8.2 Hz, 2H), 7.33 - 7.15 (m, 5H), 7.10 (t, *J* = 7.5 Hz, 1H), 7.01 (t, *J* = 7.4 Hz, 1H), 4.75 (s, 2H), 4.33 (d, *J* = 6.4 Hz, 2H), 4.17 (s, 2H), 3.85 (s, 2H), 3.03 (s, 2H), 2.73 (t, *J* = 5.8 Hz, 2H). ^{13}C NMR (91 MHz, DMSO-d_6) δ 169.9, 162.3, 140.4, 140.3, 139.1 (bs), 136.7, 128.6, 128.0, 127.7, 127.0, 126.6 (bs), 121.7, 119.3, 114.7 (bs), 112.0, 108.4 (bs), 52.5 (bs), 51.6 (bs), 48.8 (bs), 48.4 (bs), 42.2, 20.9 (bs). ESI HRMS (m/z): calcd for $C_{25}H_{26}N_5O_3$ $[M+H]^+$ 444.20302, found 444.20284.

Ethyl 2-(5-((1*H*-indol-3-yl)methyl)-3-(benzylcarbamoyl)-4,5,6,7-tetrahydro-1*H*-pyrazolo[4,3-*c*]pyridin-1-yl)acetate (6). Compound **6** was synthesized employing the procedure described for compound **2**, using intermediate **71** (701 mg, 1.59 mmol, 1.0 eq.), 4 M solution of HCl in 1,4-dioxane (5 mL), TEA (161 mg, 1.59 mmol, 1.0 eq.), indole-3-

carboxaldehyde (231 mg, 1.59 mmol, 1.0 eq.), AcOH (95 mg, 1.59 mmol, 1.0 eq.) and $NaBH(OAc)_3$ (506 mg, 2.39 mmol, 1.5 eq.) and dry THF (10 mL). Purification by FC (EtOAc/MeOH/TEA 99:0:1 to 94:5:1) gave 533 mg (71%) of the title compound **6** as a pale-yellow solid. ^{1}H NMR (360 MHz, $CDCl_3$) δ 8.48 (bs, 1H), 7.76 (d, J = 7.8 Hz, 1H), 7.40 - 7.29 (m, 5H), 7.22 - 7.16 (m, 1H), 7.16 - 7.08 (m, 4H), 4.73 (s, 2H), 4.59 (d, J = 6.0 Hz, 2H), 4.22 (q, J = 7.1 Hz, 2H), 3.98 (s, 2H), 3.96 (s, 2H), 2.86 (t, J = 5.7 Hz, 2H), 2.61 (t, J = 5.6 Hz, 2H), 1.27 (t, J = 7.1 Hz, 3H). ^{13}C NMR (91 MHz, CDCl3) δ 167.2, 162.4, 141.4, 140.0, 138.4, 136.4, 128.6, 127.9, 127.9, 127.3, 123.9, 121.9, 119.5, 119.4, 118.1, 112.6, 111.1, 62.0, 52.4, 50.8, 49.6, 48.5, 42.9, 22.1, 14.1. ESI HRMS (m/z): calcd for $C_{27}H_{30}N_5O_3$ [M+H]+ 472.23432, found 472.23447.

Ethyl 5-((1*H*-indol-3-yl)methyl)-3-(benzylcarbamoyl)-4,5,6,7-tetrahydro-1*H*-pyrazolo[4,3-*c*]pyridine-1-carboxylate (7). Compound **7** was synthesized employing the procedure described for compound **2**, using intermediate **72** (545 mg, 1.27 mmol, 1.0 eq.), 4 M solution of HCl in 1,4-dioxane (5 mL), TEA (128 mg, 1.27 mmol, 1.0 eq.), indole-3-carboxaldehyde (184 mg, 1.27 mmol, 1.0 eq.), AcOH (76 mg, 1.27 mmol, 1.0 eq.) and $NaBH(OAc)_3$ (404 mg, 1.91 mmol, 1.5 eq.) and dry THF (10 mL). Purification by FC (EtOAc/MeOH 99:1 to 95:5) gave 510 mg (88%) of the title compound **7** as a white solid. ^{1}H NMR (250 MHz, $CDCl_3$) *δ* 8.41 (bs, 1H), 7.81 - 7.66 (m, 1H), 7.42 - 7.27 (m, 7H), 7.24 - 7.07 (m, 3H), 4.57 (d, *J* = 6.1 Hz, 2H), 4.47 (q, *J* = 7.1 Hz, 2H), 4.05 - 3.86 (m, 4H), 3.02 (t, *J* = 5.8 Hz, 2H), 2.85 (t, *J* = 5.7 Hz, 2H), 1.42 (t, *J* = 7.1 Hz, 3H). ^{13}C NMR (63 MHz, $CDCl_3$) *δ* 161.5, 149.6, 145.2, 143.0, 137.9, 136.3, 128.7, 127.9, 127.8, 127.5, 124.1, 122.0, 120.4, 119.6, 119.4, 111.8, 111.1, 64. 7, 52.2, 49.0, 48.6, 43.0, 25.5, 14.2. ESI HRMS (m/z): calcd for $C_{27}H_{30}N_5O_3$ $[M+H]^+$ 458.21867, found 458.21897.

5-((1*H*-Indol-3-yl)methyl)-*N*-(4-chlorobenzyl)-1-(2-hydroxyethyl)-4,5,6,7-tetrahydro-1*H*-pyrazolo[4,3-*c*]pyridine-3-carboxamide (8). Compound **8** was synthesized employing the procedure described for compound **69**, using intermediate **75** (120 mg, 0.33 mmol, 1.0 eq.), 4-chlorobenzylamine (57 mg, 0.40 mmol, 1.2 eq.) and TBD (15 mg, 0.11 mmol, 0.3 eq.) and dry THF (1 mL). Purification by FC (EtOAc/MeOH/TEA 99:0:1 to 93:6:1) gave 63 mg (41%) of the title compound **8** as a white solid. ^{1}H NMR (360 MHz, DMSO-d_6) δ 10.92 (s, 1H), 8.50 (t, J = 6.3 Hz, 1H), 7.62 (d, J = 7.9 Hz, 1H), 7.39 - 7.30 (m, 3H), 7.30-7.22 (m, 3H), 7.06 (t, J = 7.5 Hz, 1H), 6.95 (t, J = 7.5 Hz, 1H), 4.90 (bs, 1H), 4.32 (d, J = 6.3 Hz, 2H), 4.04 (t, J = 5.4 Hz, 2H), 3.81 (s, 2H), 3.72 (t, J = 5.1 Hz, 2H), 3.55 (s, 2H), 2.71 (bs, 4H). ^{13}C NMR (91 MHz, DMSO-d_6): δ 162.2, 139.9, 139.5, 139.1, 136.4, 131.1, 129.1 (2xC), 128.1 (2xC), 127.4, 124.4, 120.9, 119.1, 118.3, 116.2, 111.3 (2xC), 60.1, 52.5, 51.5, 49.2, 49.1, 41.0, 21.8. ESI HRMS (m/z): calcd. for $C_{25}H_{27}ClN_5O_2$ $[M+H]^+$ 464.18478, found 464.18476.

5-((1*H*-Indol-3-yl)methyl)-*N*-(4-fluorobenzyl)-1-(2-hydroxyethyl)-4,5,6,7-tetrahydro-1*H*-pyrazolo[4,3-*c*]pyridine-3-carboxamide (9). Compound **9** was synthesized employing the procedure described for compound **69**, using intermediate **75** (120 mg, 0.33 mmol, 1.0 eq.), 4-fluorobenzylamine (50 mg, 0.40 mmol, 1.2 eq.) and TBD (15 mg, 0.11 mmol, 0.3 eq.) and dry THF (1 mL). Purification by FC (EtOAc/MeOH/TEA 99:0:1 to 93:6:1) gave 60 mg (41%) of the title compound **9** as a white solid. ^{1}H NMR (500 MHz, $CDCl_3$) δ 10.91 (s, 1H), 8.45 (t, J = 6.2 Hz, 1H), 7.62 (d, J = 7.7 Hz, 1H), 7.35 (d, J = 7.7 Hz, 1H), 7.30 (t, J = 7.1 Hz, 2H), 7.25 (s, 1H), 7.10 (t, J = 8.8 Hz, 2H), 7.05 (t, J = 8.0 Hz, 1H), 6.95 (t, J = 7.5 Hz, 1H),

4.89 (bs, 1H), 4.32 (d, J = 5.6 Hz, 2H), 4.04 (t, J = 5.0 Hz, 2H), 3.82 (s, 2H), 3.71 (d, J = 4.7 Hz, 2H), 3.71 (d, J = 4.7 Hz, 2H), 3.55 (s, 2H), 2.71 (bs, 4H). ^{13}C NMR (91 MHz, $CDCl_3$): δ 162.1, 161.0 (d, $^1J_{CF}$ = 240.0 Hz), 139.0, 139.5, 136.4, 136.2 (d, J_{CF} = 3.0 Hz), 129.3, 129.2, 127.4, 124.4, 120.9, 119.1, 118.3, 116.2, 114.9, 114.7, 111.3 (2xC), 60.1, 52.5, 51.5, 49.2, 49.1, 41.0, 21.8. ESI HRMS (m/z): calcd. for $C_{25}H_{27}FN_5O_2$ $[M+H]^+$ 448.21433, found 448.21425.

5-((1*H*-Indol-3-yl)methyl)-*N*-(3-chlorobenzyl)-1-(2-hydroxyethyl)-4,5,6,7-tetrahydro-1*H*-pyrazolo[4,3-*c*]pyridine-3-carboxamide (10). Compound **10** was synthesized employing the procedure described for compound **69**, using intermediate **75** (120 mg, 0.33 mmol, 1.0 eq.), 3-chlorobenzylamine (57 mg, 0.40 mmol, 1.2 eq.) and TBD (15 mg, 0.11 mmol, 0.3 eq.) and dry THF (1 mL). Purification by FC (EtOAc/MeOH/TEA 99:0:1 to 93:6:1) gave 92 mg (60%) of the title compound **10** as a white solid. ^{1}H NMR (500 MHz, DMSO-d_6) δ 10.91 (s, 1H), 8.53 (t, J = 6.4 Hz, 1H), 7.62 (d, J = 7.8 Hz, 1H), 7.37 - 7.19 (m, 6H), 7.06 (t, J = 7.5 Hz, 1H), 6.95 (t, J = 7.5 Hz, 1H), 4.89 (bs, 1H), 4.34 (d, J = 6.4 Hz, 2H), 4.05 (t, J = 5.5 Hz, 2H), 3.82 (s, 2H), 3.72 (bs, 2H), 3.55 (s, 2H), 2.71 (bs, 4H). ^{13}C NMR (91 MHz, DMSO-d_6): δ 162.2, 142.7, 139.8, 139.6, 136.4, 132.8, 130.1, 127.1, 126.5, 126.0, 124.4, 120.9, 119.1, 118.3, 116.2, 111.3 (2xC), 60.1, 52.5, 51.5, 49.2, 49.1, 41.2, 21.8. ESI HRMS (m/z): calcd. for $C_{25}H_{27}ClN_5O_2$ $[M+H]^+$ 464.18478, found 464.18481.

5-((1*H*-Indol-3-yl)methyl)-*N*-(3-methylbenzyl)-1-(2-hydroxyethyl)-4,5,6,7-tetrahydro-1*H*-pyrazolo[4,3-*c*]pyridine-3-carboxamide (11). Compound **11** was synthesized employing the procedure described for compound **69**, using intermediate **75** (120 mg, 0.33 mmol, 1.0 eq.), 3-methylbenzylamine (48 mg, 0.40 mmol, 1.2 eq.) and TBD (15 mg, 0.11 mmol, 0.3 eq.) and dry THF (1 mL). Purification by FC (EtOAc/MeOH/TEA 99:0:1 to 93:6:1) gave 76 mg (52%) of the title compound **11** as a white solid. ^{1}H NMR (500 MHz,

DMSO-d_6) δ 10.92 (s, 1H), 8.36 (t, J = 6.2 Hz, 1H), 7.62 (d, J = 7.8 Hz, 1H), 7.35 (d, J = 8.1 Hz, 1H), 7.25 (s, 1H), 7.17 (t, J = 7.5 Hz, 1H), 7.10-6.99 (m, 4H), 6.95 (t, J = 7.1 Hz, 1H), 4.88 (t, J = 5.5 Hz, 1H), 4.31 (d, J = 6.3 Hz, 2H), 4.04 (t, J = 5.5 Hz, 2H), 3.83 (bs, 2H), 3.71 (q, J = 5.5 Hz, 2H), 3.50 (bs, 2H), 2.71 (bs, 4H), 2.26 (s, 3H). ^{13}C NMR (91 MHz, $CDCl_3$): δ 162.5, 141.0, 139.7, 138.5, 136.4, 128.7, 128.7, 128.3, 128.0, 125.0, 124.4, 122.1, 119.7, 119.4, 117.4, 111.9, 111.4 (2xC), 61.4, 52.5, 51.2, 49.8, 48.9, 43.0, 22.4, 21.5. ESI HRMS (m/z): calcd. For $C_{26}H_{30}N_5O_2$ $[M+H]^+$ 444.23940, found 444.23924.

5-((1*H*-Indol-3-yl)methyl)-*N*-(3-trifluoroethylbenzyl)-1-(2-hydroxyethyl)-4,5,6,7-tetrahydro-1*H*-pyrazolo[4,3-*c*]pyridine-3-carboxamide (12). Compound **12** was synthesized employing the procedure described for compound **69**, using intermediate **75** (120 mg, 0.33 mmol, 1.0 eq.), 3-methylbenzylamine (70 mg, 0.40 mmol, 1.2 eq.) and TBD (15 mg, 0.11 mmol, 0.3 eq.) and dry THF (1 mL). Purification by FC (EtOAc/MeOH/TEA 99:0:1 to 93:6:1) gave 68 mg (41%) of the title compound **12** as a white solid. ^{1}H NMR (500 MHz, DMSO-d_6) δ 10.91 (s, 1H), 8.61 (t, J = 6.3 Hz, 1H), 7.67 - 7.47 (m, 5H), 7.35 (d, J = 8.1 Hz, 1H), 7.25 (d, 2.0 Hz, 1H), 7.06 (t, J = 7.3 Hz, 1H), 6.95 (t, J = 7.3 Hz, 1H), 4.89 (t, J = 9.2 Hz, 1H), 4.42 (d, J = 6.2 Hz, 2H), 4.05 (t, J = 5.4 Hz, 2H), 3.81 (s, 2H), 3.72 (d, J = 4.9 Hz, 2H), 3.55 (s, 2H), 2.71 (bs, 4H). ^{13}C NMR (91 MHz, DMSO-d_6): δ 162.3, 141.6, 139.8, 139.6, 136.4, 131.5, 129.2, 128.9 (d, J_{CF} = 31.6 Hz), 128.3 (q, J_{CF} = 151 Hz), 127.4, 124.4, 123.8 (d, J_{CF} = 3.8 Hz), 123.3 (d, J_{CF} = 3.3 Hz), 120.9, 119.1, 118.3, 116.2, 111.3 (2xC), 60.1, 52.5, 51.5, 49.2, 49.1, 41.3, 21.8. ESI HRMS (m/z): calcd. for $C_{26}H_{27}F_3N_5O_2$ $[M+H]^+$ 498.21114, found 498.21120.

5-((1*H*-Indol-3-yl)methyl)-1-(2-hydroxyethyl)-*N*-(naphthalen-1-ylmethyl)-4,5,6,7-tetrahydro-1*H*-pyrazolo[4,3-*c*]pyridine-3-carboxamide (14). Compound **78** (120 mg, 0.31

mmol, 1.0 eq.), was suspended in dry THF (5 mL), followed by addition of TEA (31 mg, 0.31 mmol, 1.0 eq.). The mixture was stirred for 0.5 h and indole-3-carboxaldehyde (45 mg, 0.31 mmol, 1.0 eq.), AcOH (19 mg, 0.31 mmol, 1.0 eq.) and $NaBH(OAc)_3$ (100 mg, 0.46 mmol, 1.5 eq.) were added. After stirring for 12 h, the mixture was quenched with saturated aqueous solution of $NaHCO_3$ (5 mL) and extracted with EtOAc (2x5 mL). The combined organic extracts were washed with water (5 mL), brine (5 mL), dried over anhydrous Na_2SO_4, filtered and concentrated *in vacuo*. The residue was purified by automated preparative chromatography (RP-C18, linear gradient from water/MeOH 90:10 to 15:85) to yield 81 mg (54%) of the title compound **14** as a pale-yellow solid. ^{1}H NMR (400 MHz, $CDCl_3$) δ 8.82 (bs, 1H), 8.07 - 8.03 (m, 1H), 7.86 - 7.82 (m, 1H), 7.78 (d, J = 8.1 Hz, 1H), 7.70 (d, J = 7.8 Hz, 1H), 7.50 - 7.44 (m, 2H), 7.44 (dd, J = 6.9 Hz, J = 1.5 Hz, 1H), 7.41 - 7.35 (m, 1H), 7.28 (d, J = 7.9 Hz, 1H), 7.19 (t, J = 5.8 Hz, 1H), 7.16 - 7.07 (m, 2H), 7.03 (d, J = 4.6 Hz, 1H), 5.02 (d, J = 5.6 Hz, 2H), 3.92 (s, 2H), 3.89 (s, 2H), 3.80 (t, J = 4.9 Hz, 2H), 3.68 (t, J = 4.9 Hz, 2H), 2.75 (t, J = 5.9 Hz, 2H), 2.61 (t, J = 5.9 Hz). ^{13}C NMR (101 MHz, $CDCl_3$): δ 162.4, 140.8, 139.8, 136.4, 140.0, 133.8, 131.6, 128.8, 128.6, 128.0, 126.8, 126.7, 126.0, 125.5, 124.3, 123.6, 122.0, 119.6, 119.3, 117.5, 111.6, 111.4, 61.2, 52.4, 51.1, 49.8, 48.7, 41.0, 22.4. ESI HRMS (m/z): calcd. for $C_{29}H_{30}N_5O_2$ $[M+H]^+$ 480.23940, found 480.23940.

***N*,5-Dibenzyl-1-(2-hydroxyethyl)-4,5,6,7-tetrahydro-1*H*-pyrazolo[4,3-*c*]pyridine-3-carboxamide (15).** The crude amine hydrochloride liberated from intermediate **76** (305 mg, 0.91 mmol, 1.0 eq.), was suspended in dry THF (10 mL), followed by addition of TEA (92 mg, 0.91 mmol, 1.0 eq.). The mixture was stirred for 0.5 h and benzaldehyde (96 mg, 0.91 mmol, 1.0 eq.), AcOH (55 mg, 0.91 mmol, 1.0 eq.) and $NaBH(OAc)_3$ (288 mg, 1.36 mmol, 1.5 eq.) were added. After stirring for 12 h, the mixture was quenched with saturated aqueous solution of $NaHCO_3$ (10 mL) and extracted with EtOAc (2x10 mL). The combined organic

extracts were washed with water (5 mL), brine (5 mL), dried over anhydrous Na_2SO_4, filtered and concentrated *in vacuo*. The residue was purified by FC (EtOAc/MeOH/TEA 99:1 to 94:5:1) to yield 184 mg (52%) of the title compound **15** as a pale-yellow solid. ^{1}H NMR (400 MHz, $CDCl_3$) δ 7.43 – 7.30 (m, 8H), 7.30 – 7.23 (m, 2H), 7.20 (t, J = 6.0, 1H), 4.56 (d, J = 6.1 Hz, 1H), 4.01 (t, J = 4.8, 1H), 3.92 – 3.84 (m, 4H), 3.76 (s, 2H), 3,20 (bs, 1H) 2.79 – 2.67 (m, 4H); ^{13}C NMR (101 MHz, $CDCl_3$) δ 162.4, 140.8, 139.5, 138.5, 137.9, 129.2, 128.6, 128.4, 127.8, 127.4, 127.3, 117.2, 61.9, 61.2, 51.1, 49.9, 48.7, 42.8, 22.2; ESI HRMS (m/z): calcd. for $C_{23}H_{27}N_4O_2$ $[M+H]^+$ 391.21285; found 391.21275.

***N*-Benzyl-5-(3-chlorobenzyl)-1-(2-hydroxyethyl)-4,5,6,7-tetrahydro-1*H*-pyrazolo[4,3-*c*]pyridine-3-carboxamide (16).** Compound **16** was synthesized employing the procedure described for compound **15**, using he crude amine hydrochloride liberated from intermediate **76** (105 mg, 0.31 mmol, 1.0 eq.), TEA (31 mg, 0.31 mmol, 1.0 eq.), 3-chlorobenzaldehyde (44 mg, 0.31 mmol, 1.0 eq.), AcOH (19 mg, 0.31 mmol, 1.0 eq.) and $NaBH(OAc)_3$ (98 mg, 0.46 mmol, 1.5 eq.) and dry THF (2 mL). Purification by FC (EtOAc/MeOH/TEA 99:0:1 to 95:4:1) gave 89 mg (68%) of the title compound **16** as a white solid. ^{1}H NMR (500 MHz, $CDCl_3$) δ 7.38 (bs, 1H), 7.32 (d, J = 4.4 Hz, 4H), 7.28 - 7.25 (m, 1H), 7.24 (bs, 3H), 7.11 (t, J = 5.8 Hz, 1H), 4.55 (d, J = 5.8 Hz, 2H), 4.04 (t, J = 5.6 Hz, 2H), 3.93 (t, J = 5.6 Hz, 2H), 3.83 (s, 2H), 3.70 (s, 2H), 2.72 (d, J = 5.0 Hz, 2H), 2.70 (d, J = 5.0 Hz, 2H). ^{13}C NMR (91 MHz, $CDCl_3$): δ 162.5, 141.0, 140.7, 139.6, 138.6, 134.4, 129.8, 129.0, 128.8 (2xC), 128.0 (2xC), 127.5, 127.5, 127.2, 117.4, 61.5, 61.4, 51.1, 50.0, 49.0, 43.0, 22.4. ESI HRMS (m/z): calcd. for $C_{23}H_{26}ClN_4O_2$ $[M+H]^+$ 425.17388, found 425.17420.

***N*-Benzyl-5-(4-chlorobenzyl)-1-(2-hydroxyethyl)-4,5,6,7-tetrahydro-1*H*-pyrazolo[4,3-*c*]pyridine-3-carboxamide (17).** Compound **17** was synthesized employing the procedure described for compound **15**, using he crude amine hydrochloride liberated from intermediate

76 (105 mg, 0.31 mmol, 1.0 eq.), TEA (31 mg, 0.31 mmol, 1.0 eq.), 4-chlorobenzaldehyde (44 mg, 0.31 mmol, 1.0 eq.), AcOH (19 mg, 0.31 mmol, 1.0 eq.) and $NaBH(OAc)_3$ (98 mg, 0.46 mmol, 1.5 eq.) and dry THF (5 mL). Purification by FC (EtOAc/MeOH/TEA 99:0:1 to 95:4:1) gave 110 mg (84%) of the title compound **17** as a white solid. ^{1}H NMR (500 MHz, $CDCl_3$) δ 7.31 (d, J = 4.4 Hz, 4H), 7.29(s, 4H), 7.27 - 7.24 (m, 1H), 7.13 (t, J = 6.1 Hz, 1H), 4.55 (d, J = 6.1 Hz, 2H), 4.02 (t, J = 4.9 Hz, 2H), 3.91 (t, J = 4.9 Hz, 2H), 3.81 (s, 2H), 3.70 (s, 2H), 3.35 (bs, 1H), 2.72 (d, J = 5.2 Hz, 2H), 2.69 (d, J = 5.2 Hz, 2H).^{13}C NMR (91 MHz, $CDCl_3$): δ 162.5, 141.0, 139.6, 138.6, 136.7, 133.1, 130.5 (2xC), 128.8 (2xC), 128.7 (2xC), 128.0 (2xC), 127.5, 117.3, 61.4, 61.2, 51.1, 49.9, 48.9, 43.0, 22.4. ESI HRMS (m/z): calcd. for $C_{23}H_{26}ClN_4O_2$ $[M+H]^+$ 425.17388, found 425.17406.

***N*-Benzyl-5-(4-methoxybenzyl)-1-(2-hydroxyethyl)-4,5,6,7-tetrahydro-1*H*-pyrazolo[4,3-*c*]pyridine-3-carboxamide (18).** Compound **18** was synthesized employing the procedure described for compound **15**, using the crude amine hydrochloride liberated from intermediate **76** (105 mg, 0.31 mmol, 1.0 eq.), TEA (31 mg, 0.31 mmol, 1.0 eq.), 4-methoxybenzaldehyde (42 mg, 0.31 mmol, 1.0 eq.), AcOH (19 mg, 0.31 mmol, 1.0 eq.) and $NaBH(OAc)_3$ (98 mg, 0.46 mmol, 1.5 eq.) and dry THF (5 mL). Purification by FC (EtOAc/MeOH/TEA 99:0:1 to 95:4:1) gave 107 mg (82%) of the title compound **18** as a white solid. ^{1}H NMR (500 MHz, $CDCl_3$) δ 7.31 (d, J = 4.3 Hz, 4H), 7.27 (d, J = 6.7 Hz, 3H), 7.13 (t, J = 5.8 Hz, 1H), 6.85 (d, J = 8.4 Hz, 2H), 4.54 (d, J = 5.8 Hz, 2H), 4.00 (t, J = 4.7 Hz, 2H), 3.89 (t, J = 5.0 Hz, 2H), 3.81 (s, 2H), 3.79 (s, 3H), 3.68 (s, 2H), 3.09 (bs, 1H), 2.71 (d, J = 5.0 Hz, 2H), 2.67 (d, J = 5.0 Hz, 2H).^{13}C NMR (91 MHz, $CDCl_3$): δ 162.5, 159.0, 141.0, 139.7, 138.6, 130.5 (2xC), 130.1, 128.8 (2xC), 127.9 (2xC), 127.5 (2xC), 117.5, 113.9 (2xC), 61.4, 55.4, 51.1, 49.8, 48.7, 42.9, 22.4. ESI HRMS (m/z): calcd. for $C_{24}H_{29}N_4O_3$ $[M+H]^+$ 421.22342, found 421.22375.

***N*-Benzyl-1-(2-hydroxyethyl)-5-(naphthalen-1-ylmethyl)-4,5,6,7-tetrahydro-1*H*-pyrazolo[4,3-*c*]pyridine-3-carboxamide (19).** Compound **19** was synthesized employing the procedure described for compound **15**, using the crude amine hydrochloride liberated from intermediate **76** (52 mg, 0.16 mmol, 1.0 eq.), TEA (16 mg, 0.16 mmol, 1.0 eq.), 1-naphthaldehyde (25 mg, 0.16 mmol, 1.0 eq.), AcOH (9 mg, 0.16 mmol, 1.0 eq.) and $NaBH(OAc)_3$ (51 mg, 0.24 mmol, 1.5 eq.) and dry THF (2 mL). Purification by FC (EtOAc/MeOH/TEA 99:0:1 to 95:4:1) gave 32 mg (45%) of the title compound **19** as a pale-yellow solid. ^{1}H NMR (500 MHz, $CDCl_3$) δ 8.28 (dd, J = 6.7 Hz, 2.7 Hz, 1H), 7.84 (dd, J = 6.3 Hz, 3.1 Hz, 1H), 7.79 (d, J = 8.1 Hz, 1H), 7.49 - 7.46 (m, 3H), 7.42 (dd, J = 8.1 Hz, J = 6.9 Hz, 1H), 7.32 (d, J = 4.4 Hz, 4H), 7.28 - 7.24 (m, 1H), 7.14 (t, J = 6.1 Hz, 1H), 4.56 (d, J = 6.1 Hz, 2H), 4.14 (s, 2H), 4.00 (t, J = 5.6 Hz, 2H), 3.96 (s, 2H), 3.90 (t, J = 5.6 Hz, 2H), 2.78 (t, J = 5.6 Hz, 2H), 2.61 (t, J = 5.6 Hz, 2H), 2.02 (s, 1H).^{13}C NMR (91 MHz, $CDCl_3$): δ 162.5, 141.0, 139.9, 138.6, 134.1, 134.0, 132.8, 128.8 (2xC), 128.5, 128.3, 128.0 (2xC), 127.7, 127.5, 126.0, 125.8, 125.3, 124.8, 117.6, 61.4, 60.1, 51.0, 50.4, 48.8, 43.0, 22.4. ESI HRMS (m/z): calcd. for $C_{27}H_{29}N_4O_2$ $[M+H]^+$ 441.22850, found 441.22828.

1-(2-Hydroxyethyl)-5-((1-methyl-1*H*-indol-3-yl)methyl)-*N*-(naphthalen-1-ylmethyl)-4,5,6,7-tetrahydro-1*H*-pyrazolo[4,3-*c*]pyridine-3-carboxamide (21). Compound **21** was synthesized employing the procedure described for compound **14**, using intermediate **78** (60 mg, 0.16 mmol, 1.0 eq.), TEA (16 mg, 0.16 mmol, 1.0 eq.) 1-methyl-1*H*-indole-3-carbaldehyde (24 mg, 0.16 mmol, 1.0 eq.), AcOH (10 mg, 0.16 mmol, 1.0 eq.), $NaBH(OAc)_3$ (50 mg, 0.23 mmol, 1.5 eq.) and dry THF (2 mL). Purification by automated preparative chromatography (RP-C18, linear gradient from water/MeOH 90:10 to 15:85) gave 60 mg (76%) of the title compound **21** as a pale-yellow solid. ^{1}H NMR (500 MHz, $CDCl_3$) δ 8.07 (d, J = 7.9 Hz, 1H), 7.85 (dd, J = 7.0 Hz, 1.7 Hz, 1H), 7.79 (d, J = 8.1 Hz, 1H), 7.72 (d, J =

7.9 Hz, 1H), 7.55 - 7.47 (m, 2H), 7.46 (d, *J* = 6.8 Hz, 1H), 7.40 (t, *J* = 6.8 Hz, 1H), 7.30 (d, *J* = 8.1 Hz, 1H), 7.23 (t, *J* = 7.6 Hz, 1H), 7.15 - 7.09 (m, 2H), 7.08 (s, 1H), 4.99 (d, *J* = 5.7 Hz, 2H), 3.96 (s, 2H), 3.94 (s, 2H), 3.88 (t, *J* = 5.3 Hz, 2H), 3.78 - 3.73 (m, 5H), 2.79 (t, *J* = 5.6 Hz, 2H), 2.61 (t, *J* = 5.6 Hz, 2H). ^{13}C NMR (75 MHz, $CDCl_3$): δ 162.3, 140.9, 139.7, 137.2, 133.9, 133.8, 131.6, 128.9, 128.8, 128.6, 128.5, 126.8, 126.7, 126.0, 125.5, 123.8, 121.7, 119.6, 119.2, 117.6, 110.7, 109.3, 61.3, 52.4, 51.0, 49.8, 48.8, 41.0, 32.3, 22.4. ESI HRMS (m/z): calcd. for $C_{30}H_{32}N_5O_2$ $[M+H]^+$ 494.25505, found 494.25478.

1-(2-Hydroxyethyl)-5-((1-ethyl-1*H*-indol-3-yl)methyl)-*N*-(naphthalen-1-ylmethyl)-4,5,6,7-tetrahydro-1*H*-pyrazolo[4,3-*c*]pyridine-3-carboxamide (22). Compound **22** was synthesized employing the procedure described for compound **14**, using intermediate **78** (60 mg, 0.16 mmol, 1.0 eq.), TEA (16 mg, 0.16 mmol, 1.0 eq.) 1-ethyl-1*H*-indole-3-carbaldehyde (26 mg, 0.16 mmol, 1.0 eq.), AcOH (10 mg, 0.16 mmol, 1.0 eq.), $NaBH(OAc)_3$ (50 mg, 0.23 mmol, 1.5 eq.) and dry THF (2 mL). Purification by automated preparative chromatography (RP-C18, linear gradient from water/MeOH 90:10 to 15:85) gave 25 mg (31%) of the title compound **22** as a pale-yellow solid. ^{1}H NMR (400 MHz, $CDCl_3$) δ 8.07 (dd, *J* = 8.0 Hz, 1.3 Hz, 1H), 7.85 (dd, *J* = 7.2 Hz, 2.2 Hz, 1H), 7.79 (d, *J* = 8.0 Hz, 1H), 7.71 (d, *J* = 8.0 Hz, 1H), 7.55 - 7.43 (m, 4H), 7.41 (d, *J* = 8.0 Hz, 1H), 7.34 (d, *J* = 8.2 Hz, 1H), 7.24 - 7.18 (m, 2H), 7.15 - 7.10 (m, 2H), 4.99 (d, *J* = 5.7 Hz, 2H), 4.15 (q, *J* = 7.3 Hz, 2H), 4.04 (s, 2H), 4.02 (s, 2H), 3.90 (t, *J* = 4.4 Hz, 2H), 3.78 (t, *J* = 5.4 Hz, 3H), 2.86 (t, *J* = 5.7 Hz, 2H), 2.69 (t, *J* = 5.7 Hz, 2H), 1.46 (t, *J* = 7.3 Hz, 3H). ^{13}C NMR (101 MHz, $CDCl_3$): δ 162.2, 141.0, 139.4, 136.2, 134.0, 133.8, 131.6, 128.8, 128.7, 128.6, 127.7, 126.8, 126.7, 126.0, 125.5, 123.8, 121.7, 119.5, 116.6, 109.6, 109.3, 61.3, 53.6, 52.1, 51.4, 49.4, 48.4, 41.1, 22.0, 15.6. ESI HRMS (m/z): calcd. for $C_{31}H_{34}N_5O_2$ $[M+H]^+$ 508.27070, found 508.27076.

1-(2-Hydroxyethyl)-5-((1-acetyl-1*H*-indol-3-yl)methyl)-*N*-(naphthalen-1-ylmethyl)-4,5,6,7-tetrahydro-1*H*-pyrazolo[4,3-*c*]pyridine-3-carboxamide (23). Compound **23** was synthesized employing the procedure described for compound **14**, using intermediate **78** (60 mg, 0.16 mmol, 1.0 eq.), TEA (16 mg, 0.16 mmol, 1.0 eq.) 1-acetyl-1*H*-indole-3-carbaldehyde (29 mg, 0.16 mmol, 1.0 eq.), AcOH (10 mg, 0.16 mmol, 1.0 eq.), $NaBH(OAc)_3$ (50 mg, 0.23 mmol, 1.5 eq.) and dry THF (2 mL). Purification by FC (EtOAc/MeOH/TEA 99:0:1 to 95:4:1) gave 53 mg (63%) of the title compound **23** as a pale-yellow solid. ^{1}H NMR (300 MHz, DMSO-d_6) δ 8.43 (t, J = 6.0 Hz, 1H), 8.32 (d, J = 8.1 Hz, 1H), 8.24 - 8.09 (m, 1H), 7.93 (dd, J= 6.4 Hz, J = 3.1 Hz, 1H), 7.87 - 7.76 (m, 2H), 7.75 (d, J = 7.4 Hz, 1H), 7.58 - 7.49 (m, 2H), 7.48 - 7.40 (m, 2H), 7.32 (t, J = 7.1 Hz, 1H), 7.24 (t, J = 7.0 Hz, 1H), 4.89 (t, J = 5.4 Hz, 1H), 4.83 (d, J = 6.0 Hz, 2H), 4.04 (t, J = 5.4 Hz, 2H), 3.83 (s, 2H), 3.71 (q, J = 5.4 Hz, 2H), 3.65 (s, 2H), 2.75 (bs, 4H), 2.64 (s, 3H). ^{13}C NMR (75 MHz, DMSO-d_6): δ 169.3, 162.1, 140.0, 139.5, 135.4, 134.9, 133.2, 130.8, 130.2, 128.5, 127.3, 126.1, 125.7, 125.4 (2xC), 125.3, 124.7, 123.5, 123.1, 120.1, 118.7, 115.9 (2xC), 60.1, 52.0, 51.5, 49.6, 49.2, 23.9, 21.8. 1 C-atom overlaps with DMSO-d_6 signal. ESI HRMS (m/z): calcd. for $C_{31}H_{32}N_5O_3$ $[M+H]^+$ 522.24997, found 522.24997.

1-(2-Hydroxyethyl)-5-((1-methanesulfonyl-1*H*-indol-3-yl)methyl)-*N*-(naphthalen-1-ylmethyl)-4,5,6,7-tetrahydro-1*H*-pyrazolo[4,3-*c*]pyridine-3-carboxamide (24). Compound **24** was synthesized employing the procedure described for compound **14**, using intermediate **78** (60 mg, 0.16 mmol, 1.0 eq.), TEA (16 mg, 0.16 mmol, 1.0 eq.) 1-methanesulfonyl-1*H*-indole-3-carbaldehyde (32 mg, 0.16 mmol, 1.0 eq.), AcOH (10 mg, 0.16 mmol, 1.0 eq.), $NaBH(OAc)_3$ (50 mg, 0.23 mmol, 1.5 eq.) and dry THF (2 mL). Purification by FC (EtOAc/MeOH 99:1 to 95:5) gave 48 mg (41%) of the title compound **24** as a pale-yellow solid. ^{1}H NMR (400 MHz, $CDCl_3$) δ 8.07 (dd, J = 7.6 Hz, 1.5 Hz, 1H), 7.90 (d, J = 8.2 Hz, 1H), 7.86 (dd, J = 7.0 Hz, 2.0 Hz, 1H), 7.79(t, J = 8.4 Hz, 2H), 7.56 - 7.34 (m, 6H),

7.30 (t, *J* = 7.6 Hz, 1H), 7.10 (t, *J* = 5.6 Hz, 1H), 5.00 (d, *J* = 5.6 Hz, 2H), 3.98 - 3.94 (m, 3H), 3.91 (s, 2H), 3.85 (d, *J* = 5.4 Hz, 2H), 3.11 (s, 3H), 2.81 (t, *J* = 5.6 Hz, 2H), 2.67 (t, *J* = 5.6 Hz, 2H). 2 protons could not be detected. ^{13}C NMR (101 MHz, $CDCl_3$): δ 162.3, 140.9, 139.5, 135.6, 134.0, 133.8, 131.6, 130.8, 128.8, 128.6, 126.8, 126.7, 126.1, 125.5, 125.3, 124.9, 123.7, 123.6, 120.8, 119.3, 117.1, 113.2, 61.4, 52.3, 51.1, 50.1, 49.0, 41.1, 40.8, 22.3. ESI HRMS (m/z): calcd. for $C_{30}H_{32}N_5O_4S$ $[M+H]^+$ 558.21695, found 558.21688.

1-(2-Hydroxyethyl)-5-((7-methoxy-1*H*-indol-3-yl)methyl)-*N*-(naphthalen-1-ylmethyl)-4,5,6,7-tetrahydro-1*H*-pyrazolo[4,3-*c*]pyridine-3-carboxamide (25). Compound **25** was synthesized employing the procedure described for compound **14**, using intermediate **78** (80 mg, 0.21 mmol, 1.0 eq.), TEA (21 mg, 0.21 mmol, 1.0 eq.), 7-methoxyindole-3-carboxaldehyde (33 mg, 0.21 mmol, 1.0 eq.), AcOH (13 mg, 0.21 mmol, 1.0 eq.), $NaBH(OAc)_3$ (67 mg, 0.32 mmol, 1.5 eq.) and dry THF (3 mL). Purification by FC (EtOAc/MeOH/TEA 99:0:1 to 95:4:1) gave 61 mg (57%) of the title compound **25** as a pale-pink solid. ^{1}H NMR (500 MHz, $CDCl_3$) δ 8.75 (s, 1H), 8.07 - 8.05 (m, 1H), 7.86 - 7.84 (m, 1H), 7.79 (d, *J* = 8.1 Hz, 1H), 7.49 - 7.45 (m, 3H), 7.41 - 7.38 (m, 1H), 7.33 (d, *J*= 8.0 Hz, 1H), 7.14 (t, *J*= 5.7 Hz, 1H), 7.10 (d, *J* = 2.2 Hz, 1H), 7.04 (t, *J* = 7.9 Hz, 1H), 6.64 (d, *J* = 7.7 Hz, 1H), 5.00 (d, *J* = 5.7 Hz, 1H), 3.95 (s, 2H), 3.94 (s, 5H), 3.81 (t, *J* = 5.2 Hz, 2H), 3.70 (t, *J* = 5.1 Hz, 2H), 2.73 (t, *J* = 5.7 Hz, 2H), 2.53 (t, *J* = 5.6 Hz, 2H). ^{13}C NMR (126 MHz, $CDCl_3$): δ 162.3, 146.3, 140.8, 139.8, 133.9, 133.8, 131.6, 129.4, 128.8, 128.6, 126.9, 126.8, 126.7, 126.1, 125.5, 123.8, 123.7, 120.0 117.7, 112.6, 112.1, 101.8, 61.2, 55.4, 52.5, 51.0, 49.9, 48.6, 41.1, 22.4. ESI HRMS (m/z): calcd. for $C_{30}H_{32}N_5O_3$ $[M+H]^+$ 510.24997, found 510.24997.

1-(2-Hydroxyethyl)-5-((7-methoxy-1-methyl-1*H*-indol-3-yl)methyl)-*N*-(naphthalen-1-ylmethyl)-4,5,6,7-tetrahydro-1*H*-pyrazolo[4,3-*c*]pyridine-3-carboxamide (26).

Compound **26** was synthesized employing the procedure described for compound **14**, using intermediate **78** (60 mg, 0.16 mmol, 1.0 eq.), TEA (16 mg, 0.16 mmol, 1.0 eq.) 7-methoxy-1-methyl-1*H*-indole-3-carbaldehyde (24 mg, 0.16 mmol, 1.0 eq.), AcOH (10 mg, 0.16 mmol, 1.0 eq.), $NaBH(OAc)_3$ (50 mg, 0.23 mmol, 1.5 eq.) and dry THF (2 mL). Purification by automated preparative chromatography (RP-C18, linear gradient from water/MeOH 90:10 to 15:85) gave 26 mg (31%) of the title compound **26** as a pale-yellow solid. ^{1}H NMR (500 MHz, $CDCl_3$) δ 8.06 (d, J = 8.1 Hz, 1H), 7.85 (dd, J = 7.4 Hz, 1.4 Hz, 1H), 7.79 (d, J = 8.1 Hz, 1H), 7.56 - 7.44 (m, 3H), 7.40 (t, J = 7.6 Hz, 1H), 7.25 (d, J = 6.5 Hz, 1H), 7.13 (t, J = 5.6 Hz, 1H), 7.01 (s, 1H), 7.00 (t, J = 8.1 Hz, 1H), 6.61 (d, J = 7.7 Hz, 1H), 4.99 (d, J = 5.6 Hz, 2H), 4.03 - 4.01 (m, 7H), 3.91-3.89 (m, 6H), 3.78 (d, J = 4.5 Hz, 2H), 2.85 (t, J = 4.9 Hz, 2H), 2.70 (t, J = 5.3 Hz, 2H). ^{13}C NMR (126 MHz, $CDCl_3$): δ 162.2, 148.0, 140.9, 139.3, 133.9, 133.7, 131.6, 130.8, 130.7, 128.8, 128.6, 126.8, 126.7 (2xC), 126.0, 125.5, 123.7, 120.1, 116.4, 112.0, 108.7, 102.5, 61.3, 55.5, 51.9, 49.2, 48.4, 41.1, 36.7, 21.9. ESI HRMS (m/z): calcd. for $C_{31}H_{34}N_5O_3$ $[M+H]^+$ 524.26562, found 524.26560.

Methyl 3-((1-(2-hydroxyethyl)-3-((naphthalen-1-ylmethyl)carbamoyl)-1,4,6,7-tetrahydro-5*H*-pyrazolo[4,3-*c*]pyridin-5-yl)methyl)-1*H*-indole-7-carboxylate (27).

Compound **78** (80 mg, 0.21 mmol, 1.0 eq.), methyl 1*H*-indole-7-carboxylate (40 mg, 0.21 mmol, 1.0 eq.) and TEA (21 mg, 0.21 mmol, 1.0 eq.) were dissolved in MeOH (2 mL). 37% aqueous solution of formaldehyde (19 mg, 0.21 mmol, 1.0 eq.) and $ZnCl_2$ (43 mg, 0.32 mmol, 1.5 eq.) were then added and the resulting mixture was stirred overnight at rt. The reaction mixture was concentrated *in vacuo*. Purification of the residue by FC (EtOAc/MeOH/TEA 99:0:1 to 93:6:1) gave 50 mg (44%) of the title compound **27** as a white solid. ^{1}H NMR (500 MHz, $CDCl_3$) δ 9.76 (s, 1H), 8.07 (d, J = 8.0 Hz, 1H), 7.98 (d, J = 7.7 Hz, 1H), 7.88 (d, J = 7.5 Hz, 1H), 7.85 (d, J = 7.2 Hz, 1H), 7.79 (d, J = 8.0 Hz, 1H), 7.52 - 7.46 (m, 3H), 7.40 (t, J = 7.5 Hz, 1H), 7.31 (bs, 1H), 7.14 (t, J = 7.7 Hz, 1H), 7.07 (t, J = 5.5 Hz, 2H), 3.99 - 3.93 (m,

10H), 3.82 (t, J = 4.9 Hz, 2H), 2.79 (t, J = 5.6 Hz, 2H), 2.64 (t, J = 5.6 Hz, 2H). ^{13}C NMR (91 MHz, $CDCl_3$): δ 168.0, 162.3, 141.0, 139.7, 136.4, 134.0, 133.8, 131.6, 129.1, 128.8, 128.6, 126.8, 126.7, 126.1, 125.5, 125.4, 125.1, 124.6, 123.8, 119.1, 117.5, 112.6, 112.5, 61.4, 52.5, 52.0, 51.1, 50.0, 48.8, 41.1, 22.4. ESI HRMS (m/z): calcd. for $C_{31}H_{32}N_5O_4$ $[M+H]^+$ 538.24488, found 538.24484.

1-(2-Hydroxyethyl)-5-((1*H*-indol-2-yl)methyl)-*N*-(naphthalen-1-ylmethyl)-4,5,6,7-tetrahydro-1*H*-pyrazolo[4,3-*c*]pyridine-3-carboxamide (28). Compound **28** was synthesized employing the procedure described for compound **14**, using intermediate **78** (80 mg, 0.21 mmol, 1.0 eq.), TEA (21 mg, 0.21 mmol, 1.0 eq.), indole-2-carboxaldehyde (30 mg, 0.21 mmol, 1.0 eq.), AcOH (13 mg, 0.21 mmol, 1.0 eq.), $NaBH(OAc)_3$ (67 mg, 0.32 mmol, 1.5 eq.) and dry THF (3 mL). Purification by FC (EtOAc/MeOH/TEA 99:0:1 to 93:6:1) gave 55 mg (53%) of the title compound **28** as a pale-pink solid. ^{1}H NMR (500 MHz, $CDCl_3$) δ 8.82 (s, 1H), 8.09 - 8.07 (m, 1H), 7.87 - 7.85 (m, 1H), 7.79 (d, J = 8.2 Hz, 1H), 7.57 (d, J = 7.8 Hz, 1H), 7.49 - 7.45 (m, 3H), 7.39 - 7.34 (m, 2H), 7.17 - 7.13 (m, 1H), 7.10-7.07 (m, 2H), 6.40 (s, 1H), 4.99 (d, J = 5.8 Hz, 2H), 3.91 (s, 2H), 3.89 - 3.87 (m, 4H), 3.78 (t, J = 4.8 Hz, 2H), 2.65 (t, J = 5.6 Hz, 2H), 2.49 (t, J = 5.6 Hz, 2H). ^{13}C NMR (126 MHz, $CDCl_3$): δ 162.1, 140.8, 139.6, 136.4, 135.8, 134.0, 133.8, 131.6, 128.8, 128.7, 128.5, 127.0, 126.7, 126.1, 125.5, 123.8, 121.7, 120.3, 119.7, 117.3, 111.0, 101.9, 61.2, 54.7, 51.2, 50.4, 48.5, 41.1, 22.2. ESI HRMS (m/z): calcd. for $C_{29}H_{30}N_5O_2$ $[M+H]^+$ 480.23940, found 480.23912.

1-(2-Hydroxyethyl)-N,5-bis(naphthalen-1-ylmethyl)-4,5,6,7-tetrahydro-1H-pyrazolo[4,3-*c*]pyridine-3-carboxamide (30). Compound **30** was synthesized employing the procedure described for compound **14**, using intermediate **78** (120 mg, 0.31 mmol, 1.0 eq.), TEA (31 mg, 0.31 mmol, 1.0 eq.), 1-naphthaldehyde (48 mg, 0.31 mmol, 1.0 eq.), AcOH (19 mg, 0.31 mmol, 1.0 eq.), $NaBH(OAc)_3$ (100 mg, 0.46 mmol, 1.5 eq.) and dry THF (5 mL). Purification

by FC (EtOAc/MeOH/TEA 99:0:1 to 95:4:1) gave 60 mg (39%) of the title compound **30** as a pale-yellow solid. ^{1}H NMR (500 MHz, $CDCl_3$) δ 8.30 (dd, J = 7.4 Hz, 2.1 Hz, 1H), 8.08 (d, J = 8.2 Hz, 1H), 7.87 - 7.83 (m, 2H), 7.80 (d, J = 8.2 Hz, 2H), 7.54 - 7.46 (m, 6H), 7.42 (ddd, J = 8.0 Hz, 7.0 Hz, 5.6 Hz, 2H), 7.09 (t, J = 5.7 Hz, 1H), 5.01 (d, J = 5.7 Hz, 2H), 4.15 (s, 2H), 3.99 (s, 2H), 3.91 (t, J = 4.4 Hz, 2H), 3.82 (t, J = 5.1 Hz, 2H), 2.77 (t, J = 5.7 Hz, 2H), 2.57 (t, J = 5.7 Hz, 2H). ^{13}C NMR (126 MHz, $CDCl_3$) δ 162.3, 140.9, 139.9, 134.3, 134.0, 133.9, 133.8, 132.7, 131.6, 128.8, 128.6, 128.5, 128.2, 127.6, 126.8, 126.7, 126.1, 126.0, 125.8, 125.5, 125.4, 124.9, 123.8, 117.7, 61.4, 60.2, 50.9, 50.5, 48.8, 41.1, 22.4. ESI HRMS (m/z): calcd. for $C_{31}H_{31}N_4O_2$ $[M+H]^+$ 491.24415, found 491.24404.

1-(2-Hydroxyethyl)-5-((4-hydroxynaphthalen-1-yl)methyl)-*N*-(naphthalen-1-ylmethyl)-4,5,6,7-tetrahydro-1*H*-pyrazolo[4,3-*c*]pyridine-3-carboxamide (31). Compound **31** was synthesized employing the procedure described for compound **14**, using intermediate **78** (60 mg, 0.16 mmol, 1.0 eq.), TEA (16 mg, 0.16 mmol, 1.0 eq.), 4-hydroxy-1-naphthaldehyde (27 mg, 0.16 mmol, 1.0 eq.), AcOH (10 mg, 0.16 mmol, 1.0 eq.), $NaBH(OAc)_3$ (50 mg, 0.23 mmol, 1.5 eq.) and dry THF (2 mL). Purification by FC (EtOAc/MeOH/TEA 99:0:1 to 95:4:1) gave 40 mg (49%) of the title compound **31** as a white solid. ^{1}H NMR (500 MHz, DMSO-d_6) δ 10.09 (s, 1H), 8.41 (t, J = 5.5 Hz, 1H), 8.26 – 8.09 (m, 3H), 7.96 – 7.93 (m, 1H), 7.83 (dd, J = 7.1, 2.0 Hz, 1H), 7.60 – 7.37 (m, 6H), 7.25 (d, J = 7.5 Hz, 1H), 6.82 (d, J = 7.5 Hz, 1H), 4.89 (t, J = 4.9 Hz, 1H), 4.83 (d, J = 6.1 Hz, 2H), 4.03 (t, J = 4.9 Hz, 2H), 3.95 (s, 2H), 3.77 – 3.65 (m, 2H), 3.58 (s, 2H), 2.76 (bs, 2H), 2.70 (bs, 2H). ^{13}C NMR (101 MHz, DMSO-d_6) δ 162.5, 153.4, 140.4, 140.0, 135.4, 133.7, 133.7, 131.3, 128.9, 128.6, 127.8, 126.6, 126.3, 126.2, 125.8, 125.8, 125.4, 125.3, 124.8, 124.7, 124.0, 122.7, 116.4, 107.4, 60.5, 60.1, 52.0, 49.8, 49.7, 22.28. ESI HRMS (m/z): calcd. for $C_{31}H_{31}N_4O_3$ $[M+H]^+$ 507.23907, found 507.23902.

5-((4-Hydroxy-5,6,7,8-tetrahydronaphthalen-1-yl)methyl)-1-(2-hydroxyethyl)-*N*-(naphthalen-1-ylmethyl)-4,5,6,7-tetrahydro-1*H*-pyrazolo[4,3-*c*]pyridine-3-carboxamide (32). Compound **32** was synthesized employing the procedure described for compound **14**, using intermediate **78** (360 mg, 0.93 mmol, 1.0 eq.), TEA (93 mg, 0.93 mmol, 1.0 eq.), 4-methoxy-5,6,7,8-tetrahydronaphthalene-1-carbaldehyde (176 mg, 0.93 mmol, 1.0 eq.), AcOH (57 mg, 0.93 mmol, 1.0 eq.), $NaBH(OAc)_3$ (300 mg, 1.38 mmol, 1.5 eq.) and dry THF (10 mL). Purification by FC (EtOAc/MeOH/TEA 99:0:1 to 95:4:1) gave 265 mg (56%) of the title compound **32** as a pale-white solid. ^{1}H NMR (400 MHz, $CDCl_3$) δ 8.08 (d, J = 7.9 Hz, 1H), 7.86 (dd, J = 7.3 Hz, 2.0 Hz, 1H), 7.80 (d, J = 8.1 Hz, 1H), 7.55 - 7.46 (m, 3H), 7.43 - 7.40 (m, 1H), 6.64 (d, J = 8.3 Hz, 1H), 5.01 (d, J = 5.7 Hz, 2H), 3.93 (t, J = 5.1 Hz, 2H), 3.86 - 3.81 (m, 4H), 3.81 (s, 3H), 3.62 (s, 2H), 2.82 (bs, 2H), 2.71 (t, J = 5.5 Hz, 2H), 2.66 (bs, 2H), 2.60 (t, J = 5.5 Hz, 2H), 1.75 (t, J = 2.9 Hz, 4H). ^{13}C NMR (101 MHz, $CDCl_3$): δ 162.3, 156.8, 140.9, 139.9, 138.1, 134.0, 133.8, 131.7, 128.8, 128.6, 128.2, 127.8, 126.8, 126.7, 126.4, 126.0, 125.5, 123.8, 117.9, 106.3, 61.4, 59.5, 55.3, 50.9, 50.3, 48.6, 41.1, 26.4, 23.7, 22.9, 22.5 (2xC). ESI HRMS (m/z): calcd. for $C_{32}H_{37}N_4O_3$ $[M+H]^+$ 525.28602, found 525.28590.

1-(2-Hydroxyethyl)-5-((4-(methylthio)naphthalen-1-yl)methyl)-*N*-(naphthalen-1-ylmethyl)-4,5,6,7-tetrahydro-1*H*-pyrazolo[4,3-*c*]pyridine-3-carboxamide (33). Compound **33** was synthesized employing the procedure described for compound **14**, using intermediate **78** (60 mg, 0.16 mmol, 1.0 eq.), TEA (16 mg, 0.16 mmol, 1.0 eq.), 4-methylthio-1-naphthaldehyde (32 mg, 0.16 mmol, 1.0 eq.), AcOH (10 mg, 0.16 mmol, 1.0 eq.), $NaBH(OAc)_3$ (50 mg, 0.23 mmol, 1.5 eq.) and dry THF (2 mL). Purification by FC (EtOAc/MeOH/TEA 99:0:1 to 95:4:1) gave 37 mg (43%) of the title compound **33** as a white solid. ^{1}H NMR (400 MHz, $CDCl_3$) δ 8.34 - 8.26 (m, 2H), 8.07 (dd, J = 7.8 Hz, 1.2 Hz, 1H), 7.86 (dd, J = 7.2 Hz, 2.2 Hz, 1H), 7.79 (d, J = 8.1 Hz, 1H), 7.56 - 7.38 (m, 7H), 7.32 (d, J =

7.5 Hz, 1H), 7.09 (t, *J* = 5.7 Hz, 1H), 5.00 (d, *J* = 5.7 Hz, 2H), 4.12 (s, 2H), 3.97 (bs, 2H), 3.90 (dd, *J* = 5.6 Hz, 4.0 Hz, 2H), 3.81 (dd, *J* = 5.6 Hz, 4.0 Hz, 2H), 2.78 (t, *J* = 5.6 Hz, 2H), 2.60-2.56 (m, 2H), 2.58 (s, 3H). ^{13}C NMR (101 MHz, $CDCl_3$): δ 162.3, 140.9, 139.8, 136.1, 134.0, 133.8, 132.8, 132.1, 131.6, 128.8, 128.6, 127.7, 126.8, 126.7, 126.4, 126.1, 126.0, 125.5, 124.8, 123.8, 123.0, 117.4, 61.4, 60.0, 51.0, 50.4, 48.9, 41.1, 22.4, 16.3. ESI HRMS (m/z): calcd. for $C_{32}H_{33}N_4O_2S$ $[M+H]^+$ 537.23187, found 537.23185.

1-(2-Hydroxyethyl)-5-((4-(methylsulfinyl)naphthalen-1-yl)methyl)-*N*-(naphthalen-1-ylmethyl)-4,5,6,7-tetrahydro-1*H*-pyrazolo[4,3-*c*]pyridine-3-carboxamide (34).

Compound **34** was synthesized employing the procedure described for compound **14**, using intermediate **78** (80 mg, 0.21 mmol, 1.0 eq.), TEA (21 mg, 0.21 mmol, 1.0 eq.), 4-(methylsulfinyl)-1-naphthaldehyde (46 mg, 0.21 mmol, 1.0 eq.), AcOH (13 mg, 0.21 mmol, 1.0 eq.), $NaBH(OAc)_3$ (67 mg, 0.32 mmol, 1.5 eq.) and dry THF (3 mL). Purification by FC (EtOAc/MeOH/TEA 99:0:1 to 95:4:1) gave 56 mg (48%) of the title compound **34** as a white solid. ^{1}H NMR (500 MHz, $CDCl_3$) δ 8.40-8.38 (m, 1H), 8.11 (d, *J* = 7.4 Hz, 1H), 8.06 (d, *J* = 8.1 Hz, 1H), 7.94 - 7.90 (m, 1H), 7.84 (dd, *J* = 7.4 Hz, 1.9 Hz, 1H), 7.78 (d, *J* = 8.1 Hz, 1H), 7.72 (d, *J* = 7.0 Hz, 1H), 7.60-7.54 (m, 2H), 7.53 - 7.44 (m, 3H), 7.39 (dd, *J* = 8.1 Hz, 7.1 Hz, 1H), 7.17 (t, *J* = 5.6 Hz, 2H), 4.99 (d, *J* = 5.6 Hz, 2H), 4.20 (s, 2H), 4.02 (q, *J* = 14.9 Hz, 2H), 3.93 (t, *J* = 4.9 Hz, 2H), 3.83 (t, *J* = 4.9 Hz, 2H), 2.83 (s, 3H), 2.81 (bs, 2H), 2.65 (bs, 2H). ^{13}C NMR (75 MHz, $CDCl_3$): δ 162.3, 141.5, 140.9, 139.6, 133.9, 133.7, 132.7, 131.6, 129.1, 128.8, 128.6, 127.4, 127.4, 127.2, 126.9, 126.8, 126.7, 126.0, 126.0, 125.5, 123.7, 121.9, 121.8, 117.1, 61.3, 59.8, 51.1, 50.4, 49.0, 43.0, 41.0, 22.3. ESI HRMS (m/z): calcd. for $C_{32}H_{33}N_4O_3S$ $[M+H]^+$ 553.22679, found 553.22666.

5-((4-(Dimethylamino)naphthalen-1-yl)methyl)-1-(2-hydroxyethyl)-*N*-(naphthalen-1-ylmethyl)-4,5,6,7-tetrahydro-1*H*-pyrazolo[4,3-*c*]pyridine-3-carboxamide (35).

Compound **78** (120 mg, 0.31 mmol, 1.0 eq.), was suspended in dry 1,2-*d*ichloroethane (3 mL), followed by addition of TEA (31 mg, 0.31 mmol, 1.0 eq.). The mixture was stirred for 0.5 h and 4-*d*imethylaminonaphthaldehyde (62 mg, 0.31 mmol, 1.0 eq.), AcOH (19 mg, 0.31 mmol, 1.0 eq.) and $NaBH(OAc)_3$ (100 mg, 0.46 mmol, 1.5 eq.) were added. After stirring for 12 h, the mixture was quenched with saturated aqueous solution of $NaHCO_3$ (5 mL) and extracted with DCM (2x5 mL). The combined organic extracts were washed with water (5 mL), brine (5 mL), dried over anhydrous Na_2SO_4, filtered and concentrated *in vacuo*. The residue was purified by FC (EtOAc/MeOH/TEA 99:0:1 to 93:6:1) to yield 57 mg (34%) of the title compound **35** as a white solid. ^{1}H NMR (400 MHz, $CDCl_3$) δ 8.28 - 8.26 (m, 2H), 8.08 (dd, J = 8.1 Hz, 1.1 Hz, 1H), 7.86 (dd, J= 7.5 Hz, 2.1 Hz, 1H), 7.79 (d, J = 8.1 Hz, 1H), 7.54 - 7.45 (m, 5H), 7.40 (d, J = 8.1 Hz, 1H), 7.39 (t, J = 7.5 Hz, 1H), 7.10 (t, J = 5.7 Hz, 1H), 7.01 (d, J = 7.5 Hz, 1H), 5.01 (d, J = 5.7 Hz, 2H), 4.08 (s, 2H), 3.97 (s, 2H), 3.89 (dd, J = 5.6 Hz, J = 4.0 Hz, 2H), 3.80 (t, J = 5.2 Hz, 2H), 2.90 (s, 6H), 2.78 (t, J = 5.6 Hz, 2H), 2.58 (t, J = 5.6 Hz, 2H). ^{13}C NMR (126 MHz, $CDCl_3$): δ 162.3, 151.0, 140.9, 139.9, 134.0, 133.9, 133.8, 131.6, 129.3, 128.8, 128.6, 127.9, 126.8, 126.7, 126.0 (2xC), 125.9, 125.5, 125.3, 125.0, 124.7 (2xC), 123.8, 117.7, 113.4, 61.3, 60.2, 51.0, 50.4, 45.4 (2xC), 41.1, 22.4. ESI HRMS (m/z): calcd. for $C_{33}H_{36}N_5O_2$ $[M+H]^+$ 534.28635, found 534.28633.

5-Benzyl-1-(2-hydroxyethyl)-*N*-(naphthalen-1-ylmethyl)-4,5,6,7-tetrahydro-1*H*-pyrazolo[4,3-*c*]pyridine-3-carboxamide (36). Compound **36** was synthesized employing the procedure described for compound **14**, using intermediate **78** (80 mg, 0.21 mmol, 1.0 eq.), TEA (21 mg, 0.21 mmol, 1.0 eq.), benzaldehyde (22 mg, 0.21 mmol, 1.0 eq.), AcOH (13 mg, 0.21 mmol, 1.0 eq.), $NaBH(OAc)_3$ (67 mg, 0.32 mmol, 1.5 eq.) and dry THF (3 mL). Purification by FC (EtOAc/MeOH/TEA 99:0:1 to 95:4:1) gave 57 mg (62%) of the title compound **36** as a white solid. ^{1}H NMR (500 MHz, $CDCl_3$) δ 8.07 (d, J = 7.9 Hz, 1H), 7.87 (dd, J = 7.4 Hz, 1.9 Hz, 1H), 7.81 (d, J = 8.1 Hz, 1H), 7.54 - 7.47 (m, 3H), 7.44 - 7.40 (m,

1H), 7.39 - 7.37 (m, 2H), 7.33 (t, *J* = 7.4 Hz, 2H), 7.28 (dt, *J* = 8.2 Hz, 1.8 Hz, 1H), 7.05 (t, *J* = 7.2 Hz, 1H), 5.01 (d, *J* = 5.7 Hz, 2H), 3.96 (t, *J* = 5.3 Hz, 2H), 3.87 (s, 2H), 3.85 (t, *J* = 5.6 Hz, 2H), 3.76 (s, 2H), 2.73 (t, *J* = 5.6 Hz, 2H), 2.66 (t, *J* = 5.4 Hz, 2H). ^{13}C NMR (126 MHz, $CDCl_3$): δ 162.2, 141.0, 139.7, 138.2, 134.0, 133.8, 131.6, 129.3 (2xC), 128.8, 128.7, 128.5 (2xC), 127.4, 126.8, 125.7, 126.1, 125.5, 123.8, 117.6, 62.1, 61.4, 51.0, 50.1, 48.8, 41.1, 22.4. ESI HRMS (m/z): calcd. for $C_{27}H_{29}N_4O_2$ $[M+H]^+$ 441.22850, found 441.22865.

1-(2-Hydroxyethyl)-5-(4-methylbenzyl)-*N*-(naphthalen-1-ylmethyl)-4,5,6,7-tetrahydro-1*H*-pyrazolo[4,3-*c*]pyridine-3-carboxamide (37). Compound **37** was synthesized employing the procedure described for compound **14**, using intermediate **78** (80 mg, 0.21 mmol, 1.0 eq.), TEA (21 mg, 0.21 mmol, 1.0 eq.), 4-methylbenzaldehyde (24 mg, 0.21 mmol, 1.0 eq.), AcOH (13 mg, 0.21 mmol, 1.0 eq.), $NaBH(OAc)_3$ (67 mg, 0.32 mmol, 1.5 eq.) and dry THF (3 mL). Purification by FC (EtOAc/MeOH/TEA 99:0:1 to 95:4:1) gave 54 mg (57%) of the title compound **37** as a white solid. ^{1}H NMR (300 MHz, $CDCl_3$) δ 8.11 - 8.04 (m, 1H), 7.88 - 7.85 (m, 1H), 7.81 (d, *J* = 8.0 Hz, 1H), 7.57 - 7.37 (m, 4H), 7.26 (d, *J* = 7.9 Hz, 1H), 7.14 (d, *J* = 7.8 Hz, 1H), 7.04 (t, *J* = 5.7 Hz, 1H), 5.02 (d, *J* = 5.7 Hz, 2H), 3.99 - 3.93 (m, 2H), 3.90-3.82 (m, 4H), 3.73 (s, 2H), 2.73 (t, *J* = 5.1 Hz, 2H), 2.66 (t, *J* = 5.0 Hz, 2H), 2.35 (s, 3H). ^{13}C NMR (91 MHz, $CDCl_3$): δ 162.2, 141.0, 139.6, 137.1, 134.6, 134.0, 133.8, 131.6, 129.3 (2xC), 129.3 (2xC), 128.8, 128.6, 126.8, 126.7, 126.1, 125.5, 123.8, 117.3, 61.7, 61.4, 51.1, 50.0, 48.7, 41.1, 22.3, 21.3. ESI HRMS (m/z): calcd. for $C_{28}H_{31}N_4O_2$ $[M+H]^+$ 455.24415, found 455.24392.

1-(2-Hydroxyethyl)-5-(4-ethylbenzyl)-*N*-(naphthalen-1-ylmethyl)-4,5,6,7-tetrahydro-1*H*-pyrazolo[4,3-*c*]pyridine-3-carboxamide (38). Compound **38** was synthesized employing the procedure described for compound **14**, using intermediate **78** (80 mg, 0.21 mmol, 1.0 eq.), TEA (21 mg, 0.21 mmol, 1.0 eq.), 4-ethylbenzaldehyde (28 mg, 0.21 mmol, 1.0 eq.), AcOH

(13 mg, 0.21 mmol, 1.0 eq.), $NaBH(OAc)_3$ (67 mg, 0.32 mmol, 1.5 eq.) and dry THF (3 mL). Purification by FC (EtOAc/MeOH/TEA 99:0:1 to 95:4:1) gave 55 mg (56%) of the title compound **38** as a pale-yellow solid. ^{1}H NMR (360 MHz, $CDCl_3$) δ 8.07 (d, J = 8.2 Hz, 1H), 7.86 (dd, J = 6.7 Hz, 1.9 Hz, 1H), 7.80 (d, J = 8.0 Hz, 1H), 7.57 - 7.37 (m, 4H), 7.29 (d, J = 7.9 Hz, 2H), 7.17 (d, J = 7.9 Hz, 2H), 7.07 (t, J = 5.3 Hz, 1H), 5.01 (t, J = 5.6 Hz, 2H), 3.94 (t, J = 4.8 Hz, 2H), 3.89 (s, 2H), 3.84 (t, J = 4.5 Hz, 2H), 3.74 (s, 2H), 2.89 (br. s, 1H), 2.73 (t, J = 5.3 Hz, 2H), 2.68 - 2.62 (m, 4H), 1.24 (t, J = 7.6 Hz, 3H). ^{13}C NMR (91 MHz, $CDCl_3$): δ 162.2, 143.4, 141.0, 139.7, 135.3, 134.0, 133.8, 131.7, 129.3 (2xC), 128.8, 128.6, 128.0 (2xC), 126.8, 126.7, 126.1, 125.5, 123.8, 117.6, 61.7, 61.4, 51.0, 50.0, 48.7, 41.1, 28.7, 22.4, 15.7. ESI HRMS (m/z): calcd. for $C_{29}H_{33}N_4O_2$ $[M+H]^+$ 469.25980, found 469.25967.

1-(2-Hydroxyethyl)-5-(4-isopropylbenzyl)-*N*-(naphthalen-1-ylmethyl)-4,5,6,7-tetrahydro-1*H*-pyrazolo[4,3-*c*]pyridine-3-carboxamide (39). Compound **39** was synthesized employing the procedure described for compound **14**, using intermediate **78** (80 mg, 0.21 mmol, 1.0 eq.), TEA (21 mg, 0.21 mmol, 1.0 eq.), 4-isopropylbenzaldehyde (31 mg, 0.21 mmol, 1.0 eq.), AcOH (13 mg, 0.21 mmol, 1.0 eq.), $NaBH(OAc)_3$ (67 mg, 0.32 mmol, 1.5 eq.) and dry THF (3 mL). Purification by FC (EtOAc/MeOH/TEA 99:0:1 to 95:4:1) gave 67 mg (65%) of the title compound **39** as a white solid. ^{1}H NMR (250 MHz, $CDCl_3$) δ 8.09 - 8.05 (m, 1H), 7.87 - 7.78 (m, 2H), 7.54 - 7.37 (m, 4H), 7.30 (d, J = 8.0 Hz, 2H), 7.19 (d, J = 8.0 Hz, 2H), 7.11 (t, J = 5.4 Hz, 1H), 4.99 (d, J = 5.7 Hz, 2H), 3.87 (bs, 4H), 3.79 (t, J = 5.2 Hz, 2H), 2.91 (sept, J = 6.9 Hz, 1H), 2.72 (t, J = 4.9 Hz, 2H), 2.65 (t, J = 4.9 Hz, 2H), 1.26 (d, J = 6.9 Hz, 6H). ^{13}C NMR (63 MHz, $CDCl_3$): δ 162.2, 148.0, 141.0, 139.6, 135.3, 134.0, 133.8, 131.6, 129.3 (2xC), 128.8, 128.6, 126.8, 126.7, 126.6 (2xC), 126.0, 125.5, 123.8, 117.5, 61.7, 61.3, 51.0, 50.0, 48.8, 41.1, 33.9, 24.2 (2xC), 22.4. ESI HRMS (m/z): calcd. for $C_{30}H_{35}N_4O_2$ $[M+H]^+$ 483.27545, found 483.27524.

1-(2-Hydroxyethyl)-5-(4-ethoxybenzyl)-*N*-(naphthalen-1-ylmethyl)-4,5,6,7-tetrahydro-1*H*-pyrazolo[4,3-*c*]pyridine-3-carboxamide (40). Compound **40** was synthesized employing the procedure described for compound **14**, using intermediate **78** (80 mg, 0.21 mmol, 1.0 eq.), TEA (21 mg, 0.21 mmol, 1.0 eq.), 4-ethoxybenzaldehyde (33 mg, 0.21 mmol, 1.0 eq.), AcOH (13 mg, 0.21 mmol, 1.0 eq.), $NaBH(OAc)_3$ (67 mg, 0.32 mmol, 1.5 eq.) and dry THF (3 mL). Purification by FC (EtOAc/MeOH/TEA 99:0:1 to 95:4:1) gave 62 mg (63%) of the title compound **40** as a white solid. ^{1}H NMR (500 MHz, $CDCl_3$) δ 8.07 (d, J = 7.9 Hz, 1H), 7.87 (dd, J = 7.4 Hz, 2.0 Hz, 1H), 7.81 (d, J = 8.1 Hz, 1H), 7.55 - 7.45 (m, 3H), 7.42 (dd, J = 8.1 Hz, J = 7.0 Hz, 1H), 7.27 (d, J = 8.9 Hz, 2H), 7.04 (t, J = 5.6 Hz, 1H), 6.85 (d, J = 8.7 Hz, 2H), 5.01 (d, J = 5.7 Hz, 2H), 4.03 (q, J = 7.0 Hz. 2H), 3.95 (t, J = 5.3 Hz, 2H), 3.86 - 3.84 (m, 4H), 3.69 (s, 3H), 2.72 (t, J = 5.5 Hz, 2H), 2.65 (t, J = 5.3 Hz, 2H), 1.41 (t, J = 7.0 Hz, 3H). ^{13}C NMR (126 MHz, $CDCl_3$): δ 162.2, 158.3, 140.9, 139.7, 134.0, 133.8, 131.6, 130.5 (2x), 130.1, 128.1, 128.7, 126.8, 126.7, 126.1, 125.5, 123.8, 117.6, 114.4 (2x), 63.5, 61.5, 61.4, 51.0, 50.0, 48.6, 41.1, 22.4, 15.0. ESI HRMS (m/z): calcd. for $C_{29}H_{33}N_4O_3$ $[M+H]^+$ 485.25472, found 485.25447.

1-(2-Hydroxyethyl)-5-(4-chlorobenzyl)-*N*-(naphthalen-1-ylmethyl)-4,5,6,7-tetrahydro-1*H*-pyrazolo[4,3-*c*]pyridine-3-carboxamide (41). Compound **41** was synthesized employing the procedure described for compound **14**, using intermediate **78** (80 mg, 0.21 mmol, 1.0 eq.), TEA (21 mg, 0.21 mmol, 1.0 eq.), 4-chlorobenzaldehyde (29 mg, 0.21 mmol, 1.0 eq.), AcOH (13 mg, 0.21 mmol, 1.0 eq.), $NaBH(OAc)_3$ (67 mg, 0.32 mmol, 1.5 eq.) and dry THF (3 mL). Purification by FC (EtOAc/MeOH/TEA 99:0:1 to 95:4:1) gave 50 mg (50%) of the title compound **41** as a pale-yellow solid. ^{1}H NMR (500 MHz, DMSO-d_6) δ 8.44 (t, J = 5.8 Hz, 1H), 8.19 (d, J = 7.6 Hz, 1H), 7.93 (d, J = 7.1 Hz, 1H), 7.82 (t, J = 4.6 Hz, 1H), 7.55 - 7.51 (m, 2H), 7.45 (d, J = 4.6Hz, 2H), 7.37 (*virt.* q, $J = J \approx$ 8.3 Hz, 4H), 4.90 (t, J = 5.2 Hz,1H), 4.84 (d, J = 5.8 Hz, 2H), 4.04 (t, J = 5.2 Hz, 2H), 3.71 (d, J = 5.2 Hz, 2H), 3.66 (s,

2H), 3.54 (s, 2H), 2.73 - 2.70 (m, 4H). ^{13}C NMR (126 MHz, DMSO-d_6): δ 162.1, 140.3, 139.4, 137.9, 135.0 ,133.3, 131.5, 130.8, 130.4 (2xC), 128.5, 128.2 (2xC), 127.3, 126.2, 125.7, 125.4 (2xC), 123.5, 115.8, 60.2 (2xC), 51.6, 49.2, 49.2, 21.8. 1 CH_2-group overlaps with the DMSO-signal. ESI HRMS (m/z): calcd. for $C_{27}H_{28}ClN_4O_2$ $[M+H]^+$ 475.18953, found 475.18939.

1-(2-Hydroxyethyl)-*N*-(naphthalen-1-ylmethyl)-5-(4-(trifluoromethoxy)benzyl)-4,5,6,7-tetrahydro-1*H*-pyrazolo[4,3-*c*]pyridine-3-carboxamide (42). Compound **42** was synthesized employing the procedure described for compound **14**, using intermediate **78** (80 mg, 0.21 mmol, 1.0 eq.), TEA (21 mg, 0.21 mmol, 1.0 eq.), 4-trifluoromethyoxybenzaldehyde (37 mg, 0.21 mmol, 1.0 eq.), AcOH (13 mg, 0.21 mmol, 1.0 eq.), $NaBH(OAc)_3$ (67 mg, 0.32 mmol, 1.5 eq.) and dry THF (3 mL). Purification by FC (EtOAc/MeOH/TEA 99:0:1 to 95:4:1) gave 70 mg (64%) of the title compound **42** as a pale-yellow solid. ^{1}H NMR (500 MHz, $CDCl_3$) δ 8.08 (dd, J = 8.0 Hz, 1.1 Hz, 1H), 7.87 (dd, J = 7.3 Hz, 2.0 Hz, 1H), 7.81 (d. J = 8.0 Hz, 1H), 7.55 - 7.47 (m, 3H), 7.44 (d, J = 8.0 Hz, 1H), 7.40 (d, J = 8.7 Hz, 2H), 7.18 (d, J = 8.0 Hz, 2H), 7.02 (t, J = 5.7 Hz, 1H), 5.02 (d, J = 5.7 Hz, 2H), 4.00 (d, J = 5.3 Hz, 2H), 3.92 - 3.89 (m, 2H), 3.88 (s, 2H), 3.76 (s, 2H), 2.74 (t, J = 5.5 Hz, 2H), 2.68 (t, J = 5.5 Hz, 2H). ^{13}C NMR (91 MHz, $CDCl_3$): δ 162.2, 148.5, 141.0, 139.6, 137.3, 134.0, 133.8, 131.7, 130.3 (2xC), 128.8, 128.7, 126.8, 126.7, 126.1, 125.5, 123.8, 121.0 (2xC), 117.5, 61.4, 61.2, 51.0, 50.1, 49.0, 41.1, 22.5. CF_3-signal could not be detected. ESI HRMS (m/z): calcd. for $C_{28}H_{28}F_3N_4O_3$ $[M+H]^+$ 525.21080, found 525.21064.

5-(3,4-Dimethoxybenzyl)-1-(2-hydroxyethyl)-*N*-(naphthalen-1-ylmethyl)-4,5,6,7-tetrahydro-1*H*-pyrazolo[4,3-*c*]pyridine-3-carboxamide (43). Compound **43** was synthesized employing the procedure described for compound **14**, using intermediate **78** (80 mg, 0.21 mmol, 1.0 eq.), TEA (21 mg, 0.21 mmol, 1.0 eq.), 3,4-*d*imethoxybenzaldehyde (37

mg, 0.21 mmol, 1.0 eq.), AcOH (13 mg, 0.21 mmol, 1.0 eq.), $NaBH(OAc)_3$ (67 mg, 0.32 mmol, 1.5 eq.) and dry THF (3 mL). Purification by FC (EtOAc/MeOH/TEA 99:0:1 to 95:4:1) gave 34 mg (32%) of the title compound **43** as a white solid. ^{1}H NMR (300 MHz, $CDCl_3$) δ 8.07 (dd, J = 6.6 Hz, 2.4 Hz, 1H), 7.86 (dd, J = 6.3 Hz, 3.1 Hz, 1H), 7.80 (d, J = 7.9 Hz, 1H), 7.58 - 7.35 (m, 4H), 7.10 (t, J = 5.6 Hz, 1H), 6.94 (d, 1.6 Hz, 1H), 6.88 (dd, J = 8.1 Hz, 1.6 Hz, 1H), 6.81 (d, J = 8.1 Hz, 1H), 5.00 (d, J = 5.6 Hz, 2H), 3.96 - 3.88 (m, 3H), 3.87 (s, 3H), 3.87 (s, 3H), 3.85 -3.79 (m, 3H), 3.69 (s, 2H), 2.69 (d, J = 4.8 Hz, 2H), 2.64 (d, J = 4.8 Hz, 2H). ^{13}C NMR (75 MHz, $CDCl_3$): δ 162.2, 149.1, 148.4, 141.0, 139.7, 134.0, 133.8, 131.6, 131.0, 128.8, 128.6, 126.8, 126.7, 126.0, 125.5, 123.8, 121.4, 117.6, 112.3, 111.0, 61.8, 61.3, 56.1, 51.0, 50.1, 48.6, 41.1, 22.4. ESI HRMS (m/z): calcd. for $C_{29}H_{33}N_4O_4$ $[M+H]^+$ 501.24963, found 501.24950.

5-(3,4-Dichlorobenzyl)-1-(2-hydroxyethyl)-*N*-(naphthalen-1-ylmethyl)-4,5,6,7-tetrahydro-1*H*-pyrazolo[4,3-*c*]pyridine-3-carboxamide (44). Compound **44** was synthesized employing the procedure described for compound **14**, using intermediate **78** (80 mg, 0.21 mmol, 1.0 eq.), TEA (21 mg, 0.21 mmol, 1.0 eq.), 3,4-*d*ichlorobenzaldehyde (36 mg, 0.21 mmol, 1.0 eq.), AcOH (13 mg, 0.21 mmol, 1.0 eq.), $NaBH(OAc)_3$ (67 mg, 0.32 mmol, 1.5 eq.) and dry THF (3 mL). Purification by FC (EtOAc/MeOH/TEA 99:0:1 to 95:4:1) gave 55 mg (50%) of the title compound **44** as a pale-yellow solid. ^{1}H NMR (500 MHz, $CDCl_3$) δ 8.06 (d, J = 7.8 Hz, 1H), 7.86 (dd, J = 6.9 Hz, 2.2 Hz, 1H), 7.80 (d, J = 8.1 Hz, 1H), 7.53 - 7.45 (m, 5H), 7.41 (d, J = 8.0 Hz, 1H), 7.38 (d, J = 8.1 Hz, 1H), 7.20 (dd, J = 8.1 Hz, 1.8 Hz, 1H), 7.10 (t, J = 5.7 Hz, 1H), 4.99 (d, J = 5.7 Hz), 3.94 (t, J = 4.5 Hz, 2H), 3.85 - 3.83 (m, 4H), 3.68 (s, 2H), 2.71 (t, J = 5.4 Hz), 2.65 (t, J = 5.4 Hz, 2H), 2.16 (s, 1H). ^{13}C NMR (126 MHz, $CDCl_3$): δ 162.2, 140.0, 139.5, 139.0, 134.0, 133.8, 132.6, 131.6, 131.2, 130.8, 130.5, 128.8, 128.6, 128.3, 126.8, 126.7, 126.1, 125.5, 123.7, 117.3, 61.3, 60.8, 51.0,

50.0, 49.0, 41.1, 22.4. ESI HRMS (m/z): calcd. for $C_{27}H_{27}Cl_2N_4O_2$ $[M+H]^+$ 509.15056, found 509.15037.

5-((2,3-dihydro-1*H*-inden-2-yl)methyl)-1-(2-hydroxyethyl)-*N*-(naphthalen-1-ylmethyl)-4,5,6,7-tetrahydro-1*H*-pyrazolo[4,3-*c*]pyridine-3-carboxamide (45). Compound **45** was synthesized employing the procedure described for compound **14**, using intermediate **78** (80 mg, 0.21 mmol, 1.0 eq.), TEA (21 mg, 0.21 mmol, 1.0 eq.), 2,3-*d*ihydro-1H-indene-2-carbaldehyde (31 mg, 0.21 mmol, 1.0 eq.), AcOH (13 mg, 0.21 mmol, 1.0 eq.), $NaBH(OAc)_3$ (67 mg, 0.32 mmol, 1.5 eq.) and dry THF (3 mL). Purification by FC (EtOAc/MeOH/TEA 99:0:1 to 95:4:1) gave 71 mg (70%) of the title compound **45** as a white solid. ^{1}H NMR (300 MHz, $CDCl_3$) δ 8.14 - 8.05 (m, 1H), 7.87 (dd, J = 7.0 Hz, 2.4 Hz, 1H), 7.81 (d, J = 8.0 Hz, 1H), 7.58 - 7.47 (m, 3H), 7.44 (d, J = 8.0 Hz, 1H), 7.23 - 7.17 (m, 2H), 7.16 - 7.11 (m, 2H), 7.05 (t, J = 5.7 Hz, 1H), 5.03 (d, J = 5.7 Hz, 2H), 4.04 - 3.95 (m, 2H), 3.92 - 3.85 (m, 4H), 3.12 (d, J = 7.3 Hz, 1H), 3.07 (d, J = 7.6 Hz, 1H), 2.90-2.76 (m, 5H), 2.71 (t, J = 6.5 Hz, 3H), 2.64 (d, J = 7.3 Hz, 2H). ^{13}C NMR (75 MHz, $CDCl_3$): δ 162.2, 143.0 (2xC), 140.9, 139.5, 133.9, 133.8, 131.6, 128.8, 128.6, 126.8, 126.7, 126.3 (2xC), 126.0, 125.5, 124.7 (2xC), 123.8, 117.1, 62.8, 61.2, 51.1, 50.1, 49.7, 41.0, 37.9 (2xC), 37.1, 22.1. ESI HRMS (m/z): calcd. for $C_{30}H_{33}N_4O_2$ $[M+H]^+$ 481.25980, found 481.25949.

2-((4-Methoxynaphthalen-1-yl)methyl)-9-(naphthalen-1-ylmethyl)-1,2,3,4,8,9-hexahydropyrido[4',3':3,4]pyrazolo[1,5-*a*]pyrazin-10(7*H*)-one (46). To a stirred, cooled (ice-salt bath) solution of compound **80** (75 mg, 0.14 mol, 1.0 eq.), DIPEA (57 mg, 0.44 mmol, 3.0 eq.) and DMAP (1 mg, 5 mol%) in dry DCM (2 mL) was added methanesulfonly chloride (37 mg, 0.28 mmol, 2.0 eq.). The reaction mixture was allowed to reach rt and stirred for 1 h. The solution was washed with water (0.5 mL), brine (0.5 mL), dried over anhydrous Na_2SO_4, filtered and concentrated *in vacuo*. The residue was redissolved in dry

toluene (2x1 mL) and evaporated *in vacuo*. The obtained brown oil was dissolved in dry THF (0.5 mL). The solution was cooled (ice-salt bath) and *t*BuOK (31 mg, 0.28 mmol, 2.0 eq.) was added in portions. The reaction mixture was allowed to warm to rt, stirred overnight followed by quenching with saturated aqueous solution of NH_4Cl (1 mL). The mixture was extracted with AcOEt (2x1 mL) and the combined organic extracts were washed with brine, dried over anhydrous Na_2SO_4, filtered and evaporated *in vacuo*. Purification of the residue by FC (hexane/EtOAc 1:1 to 0:1) gave 40 mg (57%) of the title compound **46** as a beige solid. ^{1}H NMR (500 MHz, $CDCl_3$) δ 8.29 (dd, J = 8.5 Hz, 1.2 Hz, 2H), 8.08 (dd, J = 6.7 Hz, 2.2 Hz, 1H), 7.88 (dd, J = 6.7 Hz, 2.9 Hz, 1H), 7.85 (dd, J = 7.5 Hz, 1.9 Hz, 1H), 7.56 - 7.45 (m, 5H), 7.45 (d, J = 7.0 Hz, 1H), 7.39 (d, J = 7.7 Hz, 1H), 6.76 (d, J = 7.7 Hz, 1H), 5.16 (s, 2H), 4.08 (s, 2H), 4.07 (d, J = 6.2 Hz, 2H), 4.01 (s, 3H), 3.97 (s, 2H), 3.55 - 3.52 (m, 2H), 2.84 (t, J = 5.7 Hz, 2H), 2.74 (t, J = 5.7 Hz, 2H). ^{13}C NMR (126 MHz, $CDCl_3$) δ 158.5, 155.4, 148.3, 134.1, 133.5, 131.8, 131.8, 129.3, 128.9, 128.8, 128.1, 127.8, 127.1, 126.5, 126.4, 126.3, 126.1, 125.2, 125.1, 124.8, 123.9, 122.3, 119.1, 103.0, 60.5, 55.6, 50.0 (2xC), 46.9, 46.1, 43.9, 24.0. ESI HRMS (m/z): calcd. for $C_{32}H_{31}N_4O_2$ $[M+H]^+$ 503.24415, found 503.24455.

8-((4-Methoxynaphthalen-1-yl)methyl)-2-(naphthalen-1-ylmethyl)-1,2,6,7,8,9-hexahydro-3*H*-imidazo[1',5':1,5]pyrazolo[4,3-*c*]pyridin-3-one (47). To a stirred, cooled (ice-salt bath) solution of compound **83** (100 mg, 0.22 mmol, 1.0 eq.) in dry DCM (5 mL) was added CDI (42 mg, 0.26 mmol, 1.2 eq.). The reaction mixture was allowed to reach rt, stirred overnight and evaporated *in vacuo*. Purification by automated preparative chromatography (SiO_2, linear gradient hexane/EtOAc 1:0 to 0:1) gave 35 mg (33%) of the title compound **47** as a white solid. ^{1}H NMR (400 MHz, $CDCl_3$) δ 8.31 – 8.23 (m, 1H), 8.21 – 8.12 (m, 2H), 7.92 – 7.92 (m, 2H), 7.59 – 7.48 (m, 2H), 7.48 – 7.39 (m, 4H), 7.31 (d, J = 8.5 Hz, 1H), 6.72 (d, J = 7.8 Hz, 1H), 5.12 (s, 2H), 4.03 - 3.95 (m, 5H), 3.90 (s, 2H), 3.34 (s, 2H), 2.90 (s, 4H). ^{13}C NMR (101 MHz, $CDCl_3$) δ 155.5, 149.4, 135.5 (bs), 134.0, 133.3,

131.4, 131.0, 129.5, 128.8, 127.8, 127.3, 126.5, 126.4, 125.9, 125.1, 124.4 (bs), 123.5, 122.3, 102.8, 76.7 (bs), 60.1, 55.5, 50.5, 47.8 (bs), 46.1, 42.8, 24.4 (bs). ESI HRMS (m/z): calcd. for $C_{31}H_{29}N_4O_2$ $[M+H]^+$ 489.22850; found 489.22856.

2-(5-((4-Methoxynaphthalen-1-yl)methyl)-3-(((naphthalen-1-ylmethyl)amino)methyl)-4,5,6,7-tetrahydro-1*H*-pyrazolo[4,3-*c*]pyridin-1-yl)ethan-1-ol (48). Compound **48** was synthesized employing the procedure described for compound **14**, using intermediate **86** (40 mg, 0.11 mmol, 1.0 eq.), 1-naphthaldehyde (17 mg, 0.11 mmol, 1.0 eq.), AcOH (7 mg, 0.11 mmol, 1.0 eq.), $NaBH(OAc)_3$ (34 mg, 0.16 mmol, 1.5 eq.) and dry THF (1 mL). Purification by FC (DCM/MeOH/7 M solution of NH_3 in MeOH 99:0:1 to 94:5:1) gave 17 mg (30%) of the title compound **48** as a white solid. ^{1}H NMR (500 MHz, DMSO-d_6) δ 8.21 (d, J = 8.5 Hz, 1H), 8.17 (d, J = 7.9 Hz, 1H), 8.12 (d, J = 7.4 Hz, 1H), 7.91 (dd, J = 6.8 Hz, 2.3 Hz, 1H), 7.81 (d, J = 8.1 Hz, 1H), 7.54 - 7.37 (m, 7H), 7.33 (d, J = 7.8 Hz, 1H), 6.87 (d, J = 7.8 Hz, 1H), 4.79 (t, J = 5.4 Hz, 1H), 4.11 (s, 2H), 3.96 (s, 3H), 3.92 (bs, 4H), 3.67 - 3.60 (m, 4H), 3.41 (s, 2H), 2.73 (t, J = 5.7 Hz, 2H), 2.63 (t, J = 5.7 Hz, 2H). ^{13}C NMR (126 MHz, DMSO-d_6) δ 154.5, 144.9, 137.7, 136.0, 133.4, 132.9, 131.5, 128.3, 127.7, 127.2, 126.2, 126.1, 125.9, 125.8, 125.6, 125.3, 125.2, 125.1, 125.0, 124.2, 121.7, 112.3, 103.4, 60.4, 59.6, 55.5, 50.7, 50.0, 49.5, 48.9, 45.4, 21.8. ESI HRMS (m/z): calcd. for $C_{32}H_{35}N_4O_2$ $[M+H]^+$ 507.27545, found 507.27562.

***N*-((1-(2-Hydroxyethyl)-5-((4-methoxynaphthalen-1-yl)methyl)-4,5,6,7-tetrahydro-1*H*-pyrazolo[4,3-*c*]pyridin-3-yl)methyl)naphthalene-1-sulfonamide (49).** To a stirred, cooled (ice-salt bath) solution of compound **86** (40 mg, 0.11 mol, 1.0 eq.), TEA (16 mg, 0.16 mmol, 1.5 eq.) and DMAP (1 mg, 5 mol%) in dry DCM (1 mL) was added naphthalene-1-sulfonyl chloride (25 mg, 0.11 mmol, 1.0 eq.). The reaction mixture was allowed to reach rt and stirred overnight. The solution was washed with water (0.5 mL), brine (0.5 mL), dried over

anhydrous Na_2SO_4, filtered and concentrated *in vacuo*. Purification by FC (EtOAc/MeOH 99:1 to 95:5) gave 35 mg (57%) of the title compound **49** as a white solid. ^{1}H NMR (500 MHz, $CDCl_3$) δ 8.61 (d, J = 8.3 Hz, 1H), 8.30 (d, J = 7.9 Hz, 1H), 8.16 (d, J = 7.2 Hz, 1H), 8.12 (d, J = 8.3 Hz, 1H), 7.96 (d, J = 8.3 Hz, 1H), 7.86 (d, J = 7.6 Hz, 1H), 7.59 - 7.45 (m, 4H), 7.41 (t, J = 7.8 Hz, 1H), 7.32 (d, J = 7.8 Hz, 1H), 6.76 (d, J = 7.8 Hz, 1H), 6.22 (bs, 1H), 4.01 (s, 2H), 3.91 (s, 2H), 3,84 (d, J = 4.9 Hz, 2H), 3.77 (t, J = 4.9 Hz, 2H), 3.62 (t, J = 4.9 Hz, 2H), 3.29 (bs, 2H), 2.66 (t, J = 5.2 Hz, 2H), 2.46 (t, J = 5.5 Hz, 2H). ^{13}C NMR (126 MHz, $CDCl_3$): δ 155.6, 142.2, 138.8, 134.6, 134.2, 134.1, 133.4, 129.6, 129.0, 128.3, 128.2, 128.1, 126.9, 126.7, 126.1, 125.2, 124.7, 124.5, 124.2, 122.5, 119.9, 112.9, 103.1, 61.3, 59.7, 55.7, 50.2, 49.1, 48.7, 39.6, 22.0. ESI HRMS (m/z): calcd. for $C_{31}H_{33}N_4O_4S$ $[M+H]^+$ 557.22170, found 557.22161.

5-((4-Methoxynaphthalen-1-yl)methyl)-1-(2-(methylamino)ethyl)-*N*-(naphthalen-1-ylmethyl)-4,5,6,7-tetrahydro-1*H*-pyrazolo[4,3-*c*]pyridine-3-carboxamide (51).

Compound **87** (120 mg, 0.18 mmol, 1.0 eq.) was dissolved in DCM (1 mL), followed by addition of 33% ethanolic solution of $MeNH_2$ (2 mL,15.60 mmol, 86.6 eq.). The mixture was refluxed for 4 h, cooled to rt and evaporated *in vacuo*. Purification by FC (DCM/MeOH/7 M solution of NH_3 in MeOH 99:0:1 to 94:5:1) gave 44 mg (46%) of the title compound **51** as a pale-yellow solid. ^{1}H NMR (400 MHz, DMSO-d_6) δ 8.42 (t, J = 6.0 Hz, 1H), 8.24 (d, J = 7.9 Hz, 1H), 8.18 (d, J = 8.8 Hz, 1H), 7.93 (dd, J = 6.0 Hz, 3.2 Hz, 1H), 7.86 - 7.78 (m, 1H), 7.56 - 7.45 (m, 5H), 7.43 (d, J = 5.3 Hz, 2H), 7.37 (d, J = 7.9 Hz, 1H), 6.90 (d, J = 7.9 Hz, 1H), 4.83 (d, J = 6.0 Hz, 2H), 4.02 (t, J = 6.0 Hz, 2H), 3.98 (s, 2H), 3.96 (s, 2H), 3.58 (s, 2H), 2.80 (d, J = 6.1 Hz, 2H), 2.77 (d, J = 6.1 Hz, 2H), 2.67 (t, J = 5.1 Hz, 2H), 2.23 (s, 3H). ^{13}C NMR (101 MHz, DMSO-d_6) δ 162.1, 154.5, 139.9, 139.0, 134.9, 133.2, 132.8, 130.8, 128.4, 127.8, 127.3, 126.2, 126.1, 126.0, 125.7, 125.4, 125.3, 125.2, 125.0, 124.9, 123.4, 121.7, 116.0,

103.4, 59.5, 55.4, 51.0, 49.3, 49.2, 48.5, 35.8, 28.1, 21.7. ESI HRMS (m/z): calcd. for $C_{33}H_{36}N_5O_2$ $[M+H]^+$ 534.28635, found 534.28647.

1-(2-(Isopropylamino)ethyl)-5-((4-methoxynaphthalen-1-yl)methyl)-*N*-(naphthalen-1-ylmethyl)-4,5,6,7-tetrahydro-1*H*-pyrazolo[4,3-*c*]pyridine-3-carboxamide (52). To a solution of compound **50** (100 mg, 0.19 mmo) in dry THF (2 mL) was added acetone (11 mg, 0.19 mmol, 1.0 eq.), AcOH (11 mg, 0.19 mol, 1.0 eq.) and $NaBH(OAc)_3$ (60 mg, 0.28 mmol, 1.5 eq.). The reaction mixture was stirred overnight at rt, followed by addition of saturated aqueous solution of $NaHCO_3$ (1 mL). The mixture was extracted with EtOAc (2x2 mL) and the combined organic phase was washed with water (1 mL), brine (1 mL), dried over anhydrous Na_2SO_4, filtered and concentrated *in vacuo*. Purification by FC (DCM/MeOH/7 M solution of NH_3 in MeOH 99:0:1 to 94:5:1) gave 85 mg (80%) of the title compound **52** as a white solid. ^{1}H NMR (500 MHz, DMSO-d_6) δ 8.44 (t, J = 6.2 Hz, 1H), 8.24 (d, J = 7.9 Hz, 1H), 8.17 (d, J = 7.9 Hz, 2H), 7.92 (dd, J = 6.5 Hz, 2.8 Hz, 1H), 7.84 - 7.77 (m, 1H), 7.57 - 7.46 (m, 4H), 7.45 - 7.40 (m, 2H), 7.37 (d, J = 7.9 Hz, 1H), 6.89 (d, J = 7.9 Hz, 1H), 4.82 (d, J = 6.1 Hz, 2H), 4.00 (t, J = 6.6 Hz, 2H), 3.98 (s, 2H), 3.96 (s, 3H), 3.58 (s, 2H), 2.82 (t, J = 6.6 Hz, 2H), 2.77 (t, J = 5.4 Hz, 2H), 2.68 (t, J = 5.1 Hz, 2H), 2.61 (sept, J = 6.2 Hz, 1H), 0.90 (d, J = 6.2 Hz, 6H). ^{13}C NMR (126 MHz, DMSO-d_6) δ 162.1, 154.5, 139.9, 139.0, 135.0, 133.2, 132.9, 130.8, 128.5, 127.8, 127.3, 126.2, 126.2, 126.0, 125.7, 125.4, 125.2, 125.2, 125.0, 125.0, 123.5, 121.7, 116.0, 103.4, 59.5, 55.5, 49.4, 49.3, 49.3, 47.8, 46.5, 22.8 (2xC), 21.8. 1 C-atom overlaps with DMSO-d_6 signal. ESI HRMS (m/z): calcd. for $C_{35}H_{40}N_5O_2$ $[M+H]^+$ 562.31765, found 562.31897.

1-(Azetidin-3-yl)-5-((4-methoxynaphthalen-1-yl)methyl)-*N*-(naphthalen-1-ylmethyl)-4,5,6,7-tetrahydro-1*H*-pyrazolo[4,3-*c*]pyridine-3-carboxamide (53). Compound **88** (240 mg, 0.38 mmol) was stirred in 4 M solution of HCl in 1,4-dioxane (2 mL) for 4 h at rt. The

solution was concentrated *in vacuo* and the residue was partitioned between DCM (2 mL) and saturated aqueous solution of $NaHCO_3$ (1 mL). The phases were separated and the organic layer was dried over anhydrous Na_2SO_4, filtered and evaporated *in vacuo*. Purification by FC (DCM/MeOH/7 M solution of NH_3 in MeOH 99:0:1 to 93:6:1) gave 123 mg (61%) of the title compound **53** as a pale-yellow solid. ^{1}H NMR (400 MHz, DMSO-d_6) δ 8.43 (t, J = 5.9 Hz, 1H), 8.23 (d, J = 7.9 Hz, 1H), 8.17 (d, J = 8.1 Hz, 2H), 7.94 - 7.92 (m, 1H), 7.82 (t, J = 4.6 Hz, 1H), 7.56 - 7.41 (m, 6H), 7.37 (d, J = 7.9 Hz, 2H), 6.90 (d, J = 7.9 Hz, 1H), 5.07 (p, J = 7.3 Hz, 1H), 4.85 (d, J = 5.9 Hz, 2H), 3.98 (s, 3H), 3.96 (s, 4H), 3.63 (t, J = 7.3 Hz, 2H), 3.57 (s, 2H), 2.76 (t, J = 5.3 Hz, 2H), 2.65 (t, J = 5.3 Hz, 2H). ^{13}C NMR (101 MHz, DMSO-d_6) δ 162.0, 154.5, 140.1, 138.6, 134.9, 133.2, 132.8, 130.8, 128.5, 127.7, 127.3, 126.2, 126.1, 125.9, 125.7, 125.4, 125.4, 125.2, 125.0, 124.9, 123.4, 121.6, 116.4, 103.4, 59.4, 55.5, 52.7 (2xC), 51.4, 49.1 (2xC), 21.5. 1 signal overlaps with DMSO-d_6. ESI HRMS (m/z): calcd. for $C_{33}H_{34}N_5O_2$ $[M+H]^+$ 532.27070, found 532.27141.

1-(2-(Dimethylamino)ethyl)-5-((4-methoxynaphthalen-1-yl)methyl)-*N*-(naphthalen-1-ylmethyl)-4,5,6,7-tetrahydro-1*H*-pyrazolo[4,3-*c*]pyridine-3-carboxamide (54). To a solution of compound **50** (80 mg, 0.15 mmo) in dry THF (1 mL) was added 37% aqueous solution of formaldehyde (36 mg, 0.46 mmol, 3.0 eq.) and $NaBH(OAc)_3$ (131 mg, 0.62 mmol, 4.0 eq.). The reaction mixture was stirred overnight at rt, followed by addition of saturated aqueous solution of $NaHCO_3$ (1 mL). The mixture was extracted with EtOAc (2x1 mL) and the combined organic phase was washed with water (1 mL), brine (1 mL), dried over anhydrous Na_2SO_4, filtered and concentrated *in vacuo*. Purification by FC (DCM/MeOH/7 M solution of NH_3 in MeOH 99:0:1 to 94:5:1) gave 68 mg (83%) of the title compound **54** as a white solid. ^{1}H NMR (500 MHz, DMSO-d_6) δ 8.43 (t, J = 6.2 Hz, 1H), 8.23 (d, J = 7.8 Hz, 1H), 8.17 (d, J = 7.8 Hz, 2H), 7.93 (dd, J = 5.9 Hz, 2.4 Hz, 1H), 7.81 (dd, J = 6.9 Hz, 2.4 Hz, 1H), 7.56 - 7.44 (m, 4H), 7.44 - 7.40 (m, 2H), 7.37 (d, J = 7.8 Hz, 1H),

6.90 (d, *J* = 7.8 Hz, 1H), 4.82 (d, *J* = 6.2 Hz, 2H), 4.05 (t, *J* = 6.7 Hz, 2H), 3.98 (s, 2H), 3.96 (s, 3H), 3.57 (s, 2H), 2.77 (t, *J* = 5.4 Hz, 2H), 2.68 (t, *J* = 5.4 Hz, 2H), 2.56 (t, *J* = 6.7 Hz, 2H), 2.12 (s, 6H). ^{13}C NMR (126 MHz, DMSO-d_6) δ 162.1, 154.4, 139.9, 139.0, 135.0, 133.3, 132.9, 130.8, 128.5, 127.9, 127.3, 126.3, 126.2, 126.0, 125.7, 125.4, 125.3, 125.2, 125.1, 125.0, 123.5, 121.7, 116.1, 103.4, 59.5, 58.4, 55.5, 49.4, 49.3, 47.1 (2xC), 45.3, 21.7. 1 C-atom overlaps with DMSO-d_6 signal. ESI HRMS (m/z): calcd. for $C_{34}H_{38}N_5O_2$ $[M+H]^+$ 548.30200, found 548.30223.

1-(2-(1*H*-Imidazol-1-yl)ethyl)-5-((4-methoxynaphthalen-1-yl)methyl)-*N*-(naphthalen-1-ylmethyl)-4,5,6,7-tetrahydro-1*H*-pyrazolo[4,3-*c*]pyridine-3-carboxamide (55). A mixture of compound **87** (132 mg, 0.20 mmol, 1 eq.), imidazole (21 mg, 0.30 mmol, 1.5 eq.) and Cs_2CO_3 (98 mg, 0.30 mmol, 1.5 eq.) in dry DMF (2 mL) was stirred for 2 h at 60 °C. The reaction mixture was cooled and partitioned between EtOAc (15 mL) and water (40 mL). The aqueous phase was extracted with EtOAc (2x10 mL). The combined organic layers were washed with water (2x10 mL), brine (2x10 mL), dried over anhydrous Na_2SO_4, filtered and evaporated *in vacuo*. Purification by FC (DCM/MeOH/7 M solution of NH_3 in MeOH 99:0:1 to 94:5:1) gave 77 mg (67%) of the title compound **55** as a white solid. ^{1}H NMR (500 MHz, $CDCl_3$) δ 8.27 (d, *J* = 8.0 Hz, 1H), 8.20 (d, *J* = 8.2 Hz, 1H), 8.10 (d, *J* = 8.2 Hz, 1H), 7.88 (d, *J* = 8.0 Hz, 1H), 7.82 (d, *J* = 8.2 Hz, 1H), 7.55 (dd, *J* = 6.8 Hz, 1.1 Hz, 1H), 7.53 - 7.48 (m, 3H), 7.48 - 7.42 (m, 2H), 7.34 (d, *J* = 7.8 Hz, 1H), 7.14 (s, 1H), 7.07(t, *J* = 5.6 Hz, 1H), 6.93 (s, 1H), 6.73 (d, *J* = 7.8 Hz, 1H), 6.43 (s, 1H), 5.03 (d, *J* = 5.6 Hz, 2H), 4.21 (t, *J* = 5.2 Hz, 2H), 4.04 (s, 2H), 4.02 (t, *J* = 5.2 Hz, 2H), 3.98 (s, 3H), 3.92 (s, 2H), 2.05 (t, *J* = 5.4 Hz, 2H), 1.98 (t, *J* = 5.4 Hz, 2H). ^{13}C NMR (126 MHz, $CDCl_3$): δ 162.2, 155.4, 141.6, 140.3, 137.0, 133.9, 133.7, 133.4, 131.6, 129.8, 128.8, 128.7, 128.1, 126.9, 126.8, 126.5, 126.1, 126.0, 125.5, 125.5, 125.1, 124.7, 123.7, 122.3, 119.1, 117.2, 103.0, 59.6, 55.6, 50.0, 49.8, 48.4,

46.6, 41.1, 21.2. ESI HRMS (m/z): calcd. for $C_{35}H_{35}N_6O_2$ $[M+H]^+$ 571.28160, found 571.28301.

1-(2-(1*H*-Pyrazol-1-yl)ethyl)-5-((4-methoxynaphthalen-1-yl)methyl)-*N*-(naphthalen-1-ylmethyl)-4,5,6,7-tetrahydro-1*H*-pyrazolo[4,3-*c*]pyridine-3-carboxamide (56).

Compound **56** was synthesized employing the procedure described for compound **55**, using intermediate **87** (132 mg, 0.20 mmol, 1 eq.), pyrazole (21 mg, 0.30 mmol, 1.5 eq.), Cs_2CO_3 (98 mg, 0.30 mmol, 1.5 eq.) and dry DMF (2 mL). Purification by FC (DCM/MeOH/7 M solution of NH_3 in MeOH 99:0:1 to 94:5:1) gave 66 mg (57%) of the title compound **56** as a white solid. ^{1}H NMR (500 MHz, $CDCl_3$) δ 8.28 (d, J = 7.8 Hz, 1H), 8.21 (d, J = 7.8 Hz, 1H), 8.12 (d, J = 8.2 Hz, 1H), 7.89 (d, J = 7.8 Hz, 1H), 7.84 (d, J = 8.2 Hz, 1H), 7.60-7.42 (m, 7H), 7.32 (d, J = 6.1 Hz, 1H), 7.08 (t, J = 5.1 Hz, 1H), 6.77 (d, 1.5 Hz, 1H), 6.73 (d, J = 7.8 Hz, 1H), 6.06 (bs, 1H), 5.05 (d, J = 5.5 Hz, 2H), 4.42 (t, J = 5.5 Hz, 2H), 4.22 (t, J = 5.0 Hz, 2H), 4.00 (s, 5H), 3.89 (s, 2H), 2.58 (bs, 2H), 1.98 (bs, 2H). ^{13}C NMR (126 MHz, $CDCl_3$): δ 162.4, 155.4, 141.5, 140.5, 140.4, 134.0, 133.8, 133.5, 131.7, 130.3, 128.8, 128.7, 127.8, 126.9, 126.7, 126.4, 126.1 (2xC), 126.1, 125.6, 125.1, 124.8, 123.8, 122.3, 117.0, 105.9, 103.0, 59.7, 55.6, 51.9, 50.0, 49.2, 48.5, 41.1, 21.2. ESI HRMS (m/z): calcd. for $C_{35}H_{35}N_6O_2$ $[M+H]^+$ 571.28160, found 571.28301.

5-((4-Methoxynaphthalen-1-yl)methyl)-1-(2-morpholinoethyl)-*N*-(naphthalen-1-ylmethyl)-4,5,6,7-tetrahydro-1*H*-pyrazolo[4,3-*c*]pyridine-3-carboxamide (57).

Compound **57** was synthesized employing the procedure described for compound **55**, using intermediate **87** (132 mg, 0.20 mmol, 1 eq.), morpholine (26 mg, 0.30 mmol, 1.5 eq.), Cs_2CO_3 (98 mg, 0.30 mmol, 1.5 eq.) and dry DMF (2 mL). Purification by FC (DCM/MeOH/7 M solution of NH_3 in MeOH 99:0:1 to 98:1:1) gave 41 mg (35%) of the title compound **57** as a white solid. ^{1}H NMR (500 MHz, $CDCl_3$) δ 8.33 – 8.27 (m, 2H), 8.13 (d, J

= 8.1 Hz, 1H), 7.90 (dd, *J* = 7.7, 1.7 Hz, 1H), 7.84 (d, *J* = 8.2 Hz, 1H), 7.61 – 7.43 (m, 6H), 7.40 (d, *J* = 7.8 Hz, 1H), 7.07 (t, *J* = 5.7 Hz, 1H), 6.78 (d, *J* = 7.8 Hz, 1H), 5.06 (d, *J* = 5.7 Hz, 2H), 4.10 (s, 2H), 4.03 (s, 3H), 4.02 – 3.93 (m, 4H), 3.64 (t, *J* = 4.7 Hz, 4H), 2.81 (t, *J* = 5.7 Hz, 2H), 2.71 - 2.61 (m, 4H), 2.40 (t, *J* = 4.7 Hz, 4H). ^{13}C NMR (91 MHz, $CDCl_3$) δ 162.5, 155. 3, 140.5, 139.2, 133.9, 133.4, 131.6, 129.8, 128.7, 128.4, 127.7, 126.6, 126.6, 126.4, 126.2, 126.0, 125.9, 125.4, 125.0, 124.7, 123.7, 122.2, 117.5, 102.9, 66.9, 60.0, 58.0, 55.5, 53.8, 50.3, 48.6, 47.0, 40.9, 22.5. ESI HRMS (m/z): calcd. for $C_{36}H_{40}N_5O_3$ $[M+H]^+$ 590.31257, found 590.31338.

1-(2-Acetamidoethyl)-5-((4-methoxynaphthalen-1-yl)methyl)-*N*-(naphthalen-1-ylmethyl)-4,5,6,7-tetrahydro-1*H*-pyrazolo[4,3-*c*]pyridine-3-carboxamide (58). A solution of compound **50** (60 mg, 0.11 mmol, 1.0 eq.) in acetic anhydride (100 mg, 0.99 mmol, 9.0 eq.) was heated at 80 °C for 1 h. The mixture was evaporated *in vacuo* and the residue was purified by FC (EtOAc/MeOH 99:1 to 95:5) to give 45 mg (73%) of the title compound **58** as a white solid. ^{1}H NMR (400 MHz, $CDCl_3$) δ 8.28 (dd, *J* = 6.6 Hz, 2.0 Hz, 1H), 8.23 (dd, *J* = 7.1 Hz, 2.0 Hz, 1H), 8.09 (dd, *J* = 8.7 Hz, 1.3 Hz, 1H), 7.86 (dd, *J* = 7.1 Hz, 2.3 Hz, 1H), 7.80 (d, *J* = 8.1 Hz, 1H), 7.55 - 7.38 (m, 6H), 7.33 (d, *J* = 7.8 Hz, 1H), 7.08 (t, *J* = 5.6 Hz, 1H), 6.73 (d, *J* = 7.8 Hz, 1H), 5.82 (t, *J* = 5.6 Hz, 1H), 5.01 (d, *J* = 5.6 Hz, 2H), 4.05 (s, 2H), 4.00 (s, 3H), 3.95 - 3.88 (m, 4H), 3.48 (q, *J* = 5.8 Hz, 2H), 2.72 (t, *J* = 5.5 Hz, 2H), 2.52 (t, *J* = 5.5 Hz, 2H), 1.75 (s, 3H). ^{13}C NMR (101 MHz, $CDCl_3$) δ 170.6, 162.4, 155.4, 141.0, 139.8, 134.0, 133.9, 133.5, 131.6, 128.9, 128.6, 127.9, 126.9, 126.7, 126.4, 126.1, 126.1, 126.1, 125.6, 125.1, 124.7, 123.7, 122.4, 117.8, 103.0, 60.2, 55.6, 50.2, 48.9, 48.0, 41.1, 39.2, 23.1, 22.4. ESI HRMS (m/z): calcd. for $C_{34}H_{36}N_5O_3$ $[M+H]^+$ 562.28127, found 562.28196.

(2-(5-((4-methoxynaphthalen-1-yl)methyl)-3-((naphthalen-1-ylmethyl)carbamoyl)-4,5,6,7-tetrahydro-1*H*-pyrazolo[4,3-*c*]pyridin-1-yl)ethyl)glycine (59). The solution of

compound 59 (37 mg, 0.06 mmol, 1.0 eq.) and NaOH (12 mg, 0.30 mmol, 5.0 eq.) in MeOH (1 mL)/water (0.1 mL) was stirred at rt for 2 h. The reaction mixture was evaporated *in vacuo* and the residue was partitioned between DCM (1 mL) and saturated aqueous solution of NH_4Cl. The aqueous phase was washed with DCM (2x0.5 mL) and the combined organic phase was dried over anhydrous Na_2SO_4, filtered and concentrated *in vacuo*. Purification by automated preparative chromatography (RP-C18, linear gradient from water/MeOH 90:10 to 15:85) gave 20 mg (58%) of the title compound **59** as a white solid. ^{1}H NMR (500 MHz, DMSO-d_6) δ 8.68(t, J = 6.2 Hz, 1H), 8.23 (d, J = 8.3 Hz, 1H), 8.18 (dd, J = 12.8 Hz, 8.1 Hz, 2H), 7.92 (d, J = 7.1 Hz, 1H), 7.80 (d, J = 5.0 Hz, 1H), 7.56 - 7.45 (m, 5H), 7.45 - 7.41 (m, 2H), 7.38 (d, J = 7.8 Hz, 1H), 6.90 (d, J = 7.8 Hz, 1H), 4.83 (d, J = 6.2 Hz, 2H), 4.18 (t, J = 6.2 Hz, 2H), 3.99 (s, 2H), 3.96 (s, 3H), 3.58 (s, 2H), 3.25 (s, 2H), 3.17 (t, J = 6.2 Hz, 2H), 2.79 (t, J = 4.3 Hz, 2H), 2.69 (t, J = 4.3 Hz, 2H). ^{13}C NMR (101 MHz, DMSO-d_6) δ 169.1, 161.9, 154.5, 140.2, 139.3, 134.8, 133.2, 132.8, 130.7, 130.5, 128.4, 127.8, 127.2, 126.2, 126.2, 125.9, 125.7, 125.2, 125.1, 125.0, 124.9, 123.5, 121.7, 116.1, 103.4, 59.3, 55.5, 49.7, 49.1 (2xC), 46.8, 46.0, 21.4. 1 C-atom overlaps with DMSO-d_6 signal. ESI HRMS (m/z): calcd. for $C_{34}H_{36}N_5O_4$ $[M+H]^+$ 578.27618, found 578.27710.

Methyl (2-(5-((4-methoxynaphthalen-1-yl)methyl)-3-((naphthalen-1-ylmethyl)carbamoyl)-4,5,6,7-tetrahydro-1*H*-pyrazolo[4,3-*c*]pyridin-1-yl)ethyl)glycinate (60). A mixture of compound **87** (70 mg, 0.10 mmol, 1.0 eq.), methyl glycinate hydrochloride (50 mg, 0.40 mmol, 4.0 eq.) and K_2CO_3 (110 mg, 0.80 mmol, 8.0 eq.) in MeCN (2 mL) was stirred at reflux overnight. The reaction mixture was cooled, filtered and evaporated *in vacuo*. The residue was partitioned between AcOEt (2 mL) and water (0.5 mL). The layers were separated and the organic phase was washed with brine (1 mL), dried over anhydrous Na_2SO_4, filtered and concentrated *in vacuo*. Purification by FC (EtOAc/MeOH 99:1 to 92:8) gave 88 mg (57%) of the title compound **60** as a white solid. ^{1}H NMR (500 MHz, DMSO-d_6)

δ 8.40 (t, J = 6.2 Hz, 1H), 8.23 (d, J = 8.5 Hz, 1H), 8.17 (dd, J = 8.7 Hz, 1.3 Hz, 2H), 7.94 - 7.91 (m, 1H), 7.82 (dd, J = 7.1 Hz, 2.3 Hz, 1H), 7.56 - 7.45 (m, 4H), 7.44 - 7.40 (m, 2H), 7.38 (d, J = 7.8 Hz, 1H), 6.91 (d, J = 7.8 Hz, 1H), 4.82 (d, J = 6.2 Hz, 2H), 4.03 (t, J = 6.2 Hz, 2H), 3.99 (s, 2H), 3.97 (s, 3H), 3.57 (s, 2H), 3.56 (s, 3H), 3.29 (s, 2H), 2.88 (t, J = 6.3 Hz, 2H), 2,78 (t, J = 5.8 Hz, 2H), 2.69 (t, J = 5.8 Hz, 2H). ^{13}C NMR (126 MHz, DMSO-d_6) δ 172.6, 162.1, 154.5, 139.9, 139.1, 134.9, 133.2, 132.8, 130.8, 128.5, 127.8, 127.3, 126.3, 126.2, 126.0, 125.7, 125.4, 125.2 (2xC), 125.1, 125.0, 123.5, 121.7, 116.0, 103.4, 59.5, 55.5, 51.3, 49.7, 49.3, 49.3, 48.9, 48.2, 21.7. 1 C-atom overlaps with DMSO-d_6 signal. ESI HRMS (m/z): calcd. for $C_{35}H_{38}N_5O_4$ $[M+H]^+$ 592.29183, found 592.29275.

1-(2-Hydroxyethyl)-5-((4-methoxynaphthalen-1-yl)methyl)-5-methyl-3-((naphthalen-1-ylmethyl)carbamoyl)-4,5,6,7-tetrahydro-1*H*-pyrazolo[4,3-*c*]pyridin-5-ium iodide (62). To a cooled (ice-salt bath) solution of compound **29** (100 mg, 0.19 mmol, 1.0 eq.) in acetone (0.5 mL) was added MeI (41 mg, 0.288 mmol, 1.5 eq.). The reaction mixture was allowed to reach rt and stirred overnight. The resulting precipitate was filtered off, washed with EtOAc and further purified by automated preparative chromatography (RP-C18, linear gradient from water/MeOH 90:10 to 40:60) to give 63 mg (50%) of the title compound **62** as a white solid. ^{1}H NMR (500 MHz, DMSO-d_6) δ 8.85 (d, J = 6.2 Hz, 1H), 8.32 (d, J = 8.5 Hz, 1H), 8.27 (dd, J = 8.5 Hz, 1.5 Hz, 1H), 8.24 (dd, J = 7.9 Hz, 1.5 Hz, 1H), 7.96 (dd, J = 7.3 Hz, 1.8 Hz, 1H), 7.85 (dd, J = 6.8 Hz, 2.7 Hz, 1H), 7.74 (d, J = 8.1 Hz, 1H), 7.62 - 7.53 (m, 4H), 7.51 - 7.45 (m, 2H), 7.12 (d, J = 8.1 Hz, 1H), 5.14 (q, 13.6 Hz, 2H), 4.98 (t, J = 5.6 Hz, 1H), 4.87 (d, J = 6.2 Hz, 2H), 4.73 (q, J = 15.2 Hz, 2H), 4.16 (t, J = 5.2 Hz, 2H), 4.04 (s, 3H), 3.85 - 3.80 (m, 2H), 3.76 (q, J = 5.4 Hz, 2H), 3.31 (dt, 17.0 Hz, J = 5.0 Hz, 1H), 3.12 (dt, 17.0 Hz, J = 7.5 Hz, 1H), 2.96 (bs, 3H). ^{13}C NMR (75 MHz, DMSO-d_6) δ 161.3, 156.9, 141.1, 135.9, 134.7, 134.7, 133.9, 133.3, 130.8, 128.5, 127.7, 127.4, 126.2, 125.7, 125.7, 125.5, 125.4, 125.2,

123.8, 123.5, 122.3, 115.5, 109.1, 104.0, 62.6, 62.6, 60.0, 56.7, 56.6, 56.0, 52.3, 45.8, 17.7. ESI HRMS (m/z): calcd. for $C_{33}H_{35}N_4O_3$ $[M+H]^+$ 535.27037, found 535.27027.

1-(2-Hydroxyethyl)-5-((4-methoxynaphthalen-1-yl)methyl)-*N*-(naphthalen-1-ylmethyl)-1,4,5,6-tetrahydropyrrolo[3,4-*c*]pyrazole-3-carboxamide (63). Compound **63** was synthesized employing the procedure described for compound **2**, using intermediate **94** (226 mg, 0.61 mmol, 1.0 eq.), TEA (62 mg, 0.61 mmol, 1.0 eq.), 4-methoxy-1-naphthaldehyde (114 mg, 0.61 mmol, 1.0 eq.), AcOH (37 mg, 0.61 mmol, 1.0 eq.) and $NaBH(OAc)_3$ (195 mg, 0.92 mmol, 1.5 eq.) and dry THF (5 mL). Purification by FC (EtOAc/MeOH/TEA 99:0:1 to 94:5:1) gave 211 mg (68%) of the title compound **63** as a white solid. ^{1}H NMR (300 MHz, $CDCl_3$) δ 8.38 – 8.29 (m, 1H), 8.25 (dd, J = 7.6, 1.5 Hz, 1H), 8.12 – 8.02 (m, 1H), 7.92 – 7.84 (m, 1H), 7.81 (d, J = 7.8 Hz, 1H), 7.61 – 7.35 (m, 7H), 7.06 (t, J = 5.7 Hz, 1H), 6.75 (d, J = 7.8 Hz, 1H), 5.01 (d, J = 5.7 Hz, 2H), 4.30 (s, 2H), 4.12 – 4.06 (s, 2H), 4.02 (s, 3H), 3.88 (td, J = 5.5, 4.9, 2.2 Hz, 2H), 3.84 – 3.72 (m, 4H), 2.55 (bs, 1H). ^{13}C NMR (75 MHz, $CDCl_3$) δ 161.4, 155.5, 149.0, 139.1, 133.8, 133.6, 133.0, 131.5, 128.7, 128.5, 127.2, 126.8, 126.7, 126.6, 126.2, 126.0, 125.9, 125.4, 125.2, 125.0, 124.1, 123.6, 122.4, 102.8, 61.2, 58.2, 55.5, 53.1, 52.4, 50.7, 41.1. ESI HRMS (m/z): calcd. for $C_{31}H_{31}N_4O_3$ $[M+H]^+$ 507.23907, found 507.23903.

1-(2-Aminoethyl)-5-((4-methoxynaphthalen-1-yl)methyl)-*N*-(naphthalen-1-ylmethyl)-1,4,5,6-tetrahydropyrrolo[3,4-*c*]pyrazole-3-carboxamide (64). To a solution of compound **96** (64 mg, 0.12 mmol, 1.0 eq.) in THF (0.5 mL) was added PPh_3 (94 mg, 0.36 mmol, 3 eq.). The reaction mixture was stirred for further 1 h, followed by addition of water (65 mg, 3.60 mmol, 10.0 eq.). The solution was then heated to 50 °C for 4 h and concentrated *in vacuo*. Purification by FC (DCM/MeOH/7 M solution of NH_3 in MeOH 99:0:1 to 98:1:1) gave 39 mg (64%) of the title compound **64** as a white solid. ^{1}H NMR (400 MHz, DMSO-d_6) δ 8.47

(t, J = 6.1 Hz, 1H), 8.27 (d, J = 8.0 Hz, 1H), 8.22 - 8.15 (m, 2H), 7.93 (dd, J = 7.1 Hz, 1.9 Hz, 1H), 7.84 - 7.79 (m, 1H), 7.59 - 7.48 (m, 5H), 7.44 (dd, J = 5.8 Hz, 2.0 H, 3H), 6.91 (d, J = 8.0 Hz, 1H), 4.85 (d, J = 6.1 Hz, 2H), 4.24 (s, 2H), 3.97 (s, 3H), 3.94 (t, J = 6.0 Hz, 2H), 3.81 (s, 2H), 3.79 (s, 2H), 2.85 (t, J = 5.8 Hz, 2H). ^{13}C NMR (101 MHz, DMSO-d_6) δ 161.3, 154.5, 148.4, 138.4, 134.9, 133.2, 132.5, 130.8, 128.4, 127.3, 127.1, 126.6, 126.3, 126.1, 125.7, 125.4, 125.3, 125.2, 125.1, 124.6, 123.6, 123.5, 121.7, 103.4, 57.5, 55.5, 53.8, 51.9, 50.4, 41.6. 1 C-atom overlaps with DMSO-d_6 signal ESI HRMS (m/z): calcd. for $C_{31}H_{32}N_5O_2$ $[M+H]^+$ 506.25505, found 506.25515.

1-(2-((1-Hydroxy-2-methylpropan-2-yl)amino)ethyl)-5-((4-methoxynaphthalen-1-yl)methyl)-*N*-(naphthalen-1-ylmethyl)-1,4,5,6-tetrahydropyrrolo[3,4-*c*]pyrazole-3-carboxamide (65). A mixture of compound **95** (57 mg, 0.09 mmol, 1.0 eq.), 2-amino-2-methyl-1-propanol (40 mg, 0.45 mmol, 5 eq.) and K_2CO_3 (30 mg, 0.22 mmol, 2.5 eq.) in CH_3CN (0.5 mL) was stirred at reflux for 8 h. The reaction mixture was cooled to rt, and concentrated *in vacuo*. The residue was purified by FC (DCM/MeOH/7 M NH_3 in MeOH 99:0:1 to 94:5:1) to yield 40 mg (77%) of **65** as a white solid. ^{1}H NMR (400 MHz, DMSO-d_6) δ 8.45 (t, J = 6.1 Hz, 1H), 8.27 (d, J = 7.9 Hz, 1H), 8.18 (d, J = 8.3 Hz, 2H), 7.93 (dd, J = 6.8 Hz, 2.0 Hz, 1H), 7.82 (dd, J = 6.1 Hz, 3.1 Hz, 1H), 7.58 - 7.49 (m, 4H), 7.46 - 7.41 (m, 3H), 6.91 (d, J = 7.9 Hz, 1H), 4.84 (d, J = 6.1 Hz, 2H), 4.47 (bs, 1H), 4.24 (s, 2H), 4.00-3.97 (m, 5H), 3.82 (s, 2H), 3.78 (s, 2H), 3.09 (s, 2H), 2.77 (t, J = 6.2 Hz, 2H), 0.84 (s, 6H). ^{13}C NMR (101 MHz, DMSO-d_6) δ 161.3, 154.5, 148.4, 138.2, 134.8, 133.2, 132.5, 130.8, 128.4, 127.3, 127.1, 126.6, 126.2, 126.1, 125.7, 125.4, 125.3, 125.2, 125.1, 124.6, 123.6, 123.5, 121.7, 103.4, 68.0, 57.4, 55.5, 53.3, 52.3, 51.8, 50.6, 41.6, 23.6 (2xC). 1 C-atom overlaps with DMSO-d_6 signal ESI HRMS (m/z): calcd. for $C_{35}H_{40}N_5O_3$ $[M+H]^+$ 578.31257, found 578.31258.

5-(*tert*-Butyl) 3-ethyl 1,4,6,7-tetrahydro-5*H*-pyrazolo[4,3-*c*]pyridine-3,5-dicarboxylate (66). To a stirred solution of LHMDS (25.0 mL of 1 M solution in THF, 25.0 mmol, 1.0 eq.) in dry THF (50 mL) at -78 °C was added a solution of 1-boc-4-piperidinone (5.00 g, 25.0 mmol, 1.0 eq.) in dry THF (20 mL), dropwise. The reaction mixture was stirred for further 30 min at -78 °C, followed by a dropwise addition of a diethyl oxalate (3.92 g, 25.0 mmol, 1.0 eq.). The mixture was then warmed to rt and stirred for further 30 min. Subsequently, EtOH (40 mL), AcOH (10 mL) and hydrazine monohydrate (1.50 mL of 80% aqueous solution, 25 mmol, 1.0 eq.) were added. A slightly exothermic reaction was observed. The reaction mixture was then heated to reflux for 1 h, cooled to rt and concentrated *in vacuo*. The residue was partitioned between EtOAc (100 mL) and saturated aqueous solution of $NaHCO_3$ (100 mL). The aqueous phase was extracted with EtOAc (2x25 mL). The combined organic extracts were sequentially washed with water (25 mL), 1 M aqueous solution of citric acid (50 mL), water (25 mL), brine (25 mL), dried over anhydrous Na_2SO_4, filtered and concentrated *in vacuo*. The residue was purified by FC (hexane/EtOAc 2:1 to 0:1) to yield 4.35 g (59%) of the target compound **66** as a white solid. ^{1}H NMR (500 MHz, DMSO-d_6) δ 13.70 (bs, 0.3 H), 13.30 (bs, 0.7H), 4.49 (bs, 2H), 4.27 (bs, 2H), 3.59 (t, J = 5.8 Hz, 2H), 2.67 (bst, J = 5.8 Hz, 2H), 1.42 (s, 9H), 1.29 (t, J = 7.1 Hz, 3H). ^{13}C NMR (126 MHz, DMSO-d_6) δ 162.7 (bs), 159.5 (bs), 154.6, 147.6 (bs), 138.8 (bs), 128.5 (bs), 117.4 (bs), 115.9 (bs), 79.6, 61.0 (bs), 60.4 (bs), 41.6 (bs), 41.0 (bs), 28.5, 23.5 (bs), 21.4 (bs), 14.6 (bs). ESI HRMS (m/z): calcd for $C_{14}H_{22}N_3O_4$ $[M+H]^+$ 296.16048, found 296.16027.

5-(*tert*-Butyl) 3-ethyl 1-methyl-1,4,6,7-tetrahydro-5*H*-pyrazolo[4,3-*c*]pyridine-3,5-dicarboxylate (67) and 5-(*tert*-butyl) 3-ethyl 2-methyl-1,4,6,7-tetrahydro-5*H*-pyrazolo[4,3-*c*]pyridine-3,5-dicarboxylate (68). Intermediate **66** (2.30 g, 7.80 mmol, 1.0 eq.) was dissolved in dry DMF (20 mL). Cs_2CO_3 (2.54 g, 7.80 mmol, 1.0 eq.) was added followed by MeI (3.33 g, 23.4 mmol, 3.0 eq.). The mixture was stirred at rt overnight and

partitioned between water (100 mL) and EtOAc (50 mL). The layers were separated and the aqueous phase was extracted with EtOAc (2x15 mL). The combined organic extracts were washed with water (3x25 mL) saturated aqueous solution of NH_4Cl (25 mL), dried over anhydrous Na_2SO_4, filtered and concentrated *in vacuo*. The residue was purified by FC (hexane/EtOAc 3:1 to 0:1) to yield 1.38 g (57%) of slower eluting **67** as a pale-yellow solid and 0.85 g (35%) of faster eluting *N*-2 regioisomer **68** as a yellow oil that solidified upon storing in the cold. **67**: ^{1}H NMR (250 MHz, $CDCl_3$) δ 4.60 (s, 2H), 4.38 (q, J = 7.1 Hz, 2H), 3.81 (s, 3H), 3.71 (t, J = 5.7 Hz, 2H), 2.67 (t, J = 5.8 Hz, 2H), 1.47 (s, 9H), 1.38 (t, J = 7.1 Hz, 3H). ^{13}C NMR (63 MHz, $CDCl_3$) δ 159.6, 155.4, 144.9, 136.9, 116.6, 85.2, 60.0, 41.5, 40.0, 36.4, 28.4, 21.8, 14.4. ESI HRMS (m/z): calcd for $C_{15}H_{24}N_3O_4$ $[M+H]^+$ 310.17613, found 310.17650. **68** ^{1}H NMR (250 MHz, $CDCl_3$) δ 4.59 (s, 2H), 4.33 (q, J = 7.1 Hz, 2H), 4.12 (s, 3H), 3.67 (t, J = 5.8 Hz, 2H), 2.72 (t, J = 5.8 Hz, 2H), 1.47 (s, 9H), 1.37 (t, J = 7.1 Hz, 3H). ^{13}C NMR (63 MHz, $CDCl_3$) δ 159.9, 155.0, 145.7 (bs), 127.7 (bs), 119.0, 79.9, 60.9, 41.7 (bs), 40.4 (bs), 35.5, 27.4, 22.9 (bs), 14.4. ESI HRMS (m/z): calcd for $C_{15}H_{24}N_3O_4$ $[M+H]^+$ 310.17613, found 310.17625.

***tert*-Butyl 3-(benzylcarbamoyl)-2-methyl-2,4,6,7-tetrahydro-5*H*-pyrazolo[4,3-*c*]pyridine-5-carboxylate (69).** A solution of compound **68** (309 mg, 1.00 mmol, 1.0 eq.), benzylamine (128 mg, 1.00 mmol, 1.2 eq.) and TBD (44 mg, 0.30 mmol, 0.3 eq.) in dry THF (2 mL) was stirred at 60 °C for 12 h. The mixture was concentrated *in vacuo* and the residue was purified by FC (hexane/EtOAc 2:1 to 1:2) to yield 295 mg (80%) of the title compound **69** as a pale-yellow solid. ^{1}H NMR (500 MHz, $CDCl_3$) δ 7.44 - 7.30 (m, 5H), 5.96 (bs, 0.6H), 5.79 (bs, 0.4H), 4.68 - 4.46 (m, 4H), 4.12 (s, 3H), 3.67 (m, t, J = 5.5 Hz, 2H), 2.75 (t, J = 5.7 Hz, 2H), 1.48 (s, 9H). ^{13}C NMR (91 MHz, $CDCl_3$) δ 160.0, 155.0 (bs), 145.2 (bs), 137.6, 131.0, 128.9, 127.8, 127.7, 113.3, 80.4, 43.7, 41.9 (bs), 41.0 (bs), 39.2, 28.4, 23.5 (bs). ESI HRMS (m/z): calcd for $C_{20}H_{27}N_4O_3$ $[M+H]^+$ 371.20777, found 371.20809.

***tert*-Butyl 3-(benzylcarbamoyl)-1,4,6,7-tetrahydro-5*H*-pyrazolo[4,3-*c*]pyridine-5-carboxylate (70).** Compound **70** was synthesized employing the procedure described for compound **69**, using intermediate **66** (2.00 g, 6.78 mmol, 1.0 eq.), benzylamine (0.87 g, 8.14 mmol, 1.2 eq.) and TBD (0.34 g, 2.44 mmol, 0.3 eq.) and dry THF (10 mL). Purification by FC (hexane/EtOAc 1:1 to 0:1) gave 2.15 g (89%) of the title compound **70** as a white solid. ^{1}H NMR (500 MHz, DMSO-d_6) δ 13.04 (bs, 1H), 8.65 (bs, 1H), 7.35 - 7.27 (m, 4H), 7.23 (td, J = 6.0, 2.7 Hz, 1H), 4.50 (bs, 2H), 4.40 (d, J = 6.4 Hz, 2H), 3.59 (t, J = 5.7 Hz, 2H), 2.68 (t, J = 5.7 Hz, 2H), 1.42 (s, 9H). ^{13}C NMR (126 MHz, DMSO-d_6) δ 162.8 (bs), 154.6 (bs), 141.5 (bs), 140.5 (bs), 138.7 (bs), 128.7, 127.7, 127.1, 114.2 (bs), 79.5 (bs), 42.1 (bs), 41.7 (bs), 41.1 (bs), 28.5, 21.6 (bs). ESI HRMS (m/z): calcd for $C_{19}H_{25}N_3O_4$ $[M+H]^+$ 357.19212, found 357.19220.

***tert*-Butyl 3-(benzylcarbamoyl)-1-(2-ethoxy-2-oxoethyl)-1,4,6,7-tetrahydro-5*H*-pyrazolo[4,3-*c*]pyridine-5-carboxylate (71).** Compound **71** was synthesized employing the procedure described for compounds **67** and **68**, using intermediate **66** (1.50 g, 4.21 mmol, 1.0 eq.), Cs_2CO_3 (1.37 g, 4.21 mmol, 1.0 eq.), ethyl 2-bromoacetate (703 mg, 4.21 mmol, 1.0 eq.) and dry DMF (20 mL). Purification by FC (hexane/EtOAc 3:1 to 1:1) gave 1.65 g (89%) of the title **71** as a white solid. ^{1}H NMR (500 MHz, $CDCl_3$) δ 7.40 - 7.31 (m, 4H), 7.32 - 7.32 (m, 1H), 7.11 (bs, 1H), 4.78 (s, 2H), 4.74 (s, 2H), 4.60 (d, J = 6.0 Hz, 2H), 4.25 (q, J = 7.1 Hz, 2H), 3.74 (t, J = 5.8 Hz, 2H), 2.65 (t, J = 5.7 Hz, 2H), 1.50 (s, 9H), 1.30 (t, J = 7.1 Hz, 3H). ^{13}C NMR (91 MHz, $CDCl_3$) δ 167.1, 162.0 (bs), 141.4 (bs), 139.9 (bs), 138.3 (bs), 128.7, 127.9, 127.4, 116.6 (bs), 80.2 (bs), 62.2, 50.7, 42.9, 41.3 (bs), 39.7 (bs), 28.5, 21.8 (bs), 14.1. ESI HRMS (m/z): calcd for $C_{23}H_{31}N_4O_5$ $[M+H]^+$ 443.22890, found 443.22895.

5-(*tert*-Butyl) 1-ethyl 3-(benzylcarbamoyl)-6,7-dihydro-1*H*-pyrazolo[4,3-*c*]pyridine-1,5(4*H*)-dicarboxylate (72). To a stirred, cooled (ice-salt bath) solution of intermediate **66**

(1.00 g, 2.81 mmol, 1.0 eq.) and DIPEA (0.72 g, 5.62 mmol, 2.0 eq.) in dry THF (10 mL) was added ethyl chloroformate (0.31 g, 2.81 mmol, 1.0 eq), dropwise. The mixture was then warmed to rt overnight and concentrated *in vacuo*. The residue was purified by FC (hexane/EtOAc 3:1 to 2:1) to yield 1.09 g (91%) of the target compound **72** as a white solid. ^{1}H NMR (360 MHz, $CDCl_3$) δ 7.44 - 7.29 (m, 5H), 4.71 (s, 2H), 4.61 (d, J = 6.1 Hz, 2H), 4.51 (q, J = 7.2 Hz, 2H), 3.71 (t, J = 5.8 Hz, 2H), 3.06 (t, J = 5.8 Hz, 2H), 1.50 (s, 9H), 1.48 - 1.43 (m, 4H). ^{13}C NMR (91 MHz, $CDCl_3$) δ 161.2 (bs), 154.9 (bs), 149.5, 145.0 (bs), 142.9 (bs), 137.8, 128.7, 128.0, 127.6, 119.3 (bs), 80.3 (bs), 64.9, 43.1, 41.0 (bs), 39.8 (bs), 28.4, 25.2, 14.2. ESI HRMS (m/z): calcd for $C_{22}H_{29}N_4O_5$ $[M+H]^+$ 429.21325, found 429.21322.

5-(*tert*-Butyl) 3-ethyl 1-(2-hydroxyethyl)-1,4,6,7-tetrahydro-5*H*-pyrazolo[4,3-*c*]pyridine-3,5-dicarboxylate (73) and 5-(*tert*-butyl) 3-ethyl 2-(2-hydroxyethyl)-2,4,6,7-tetrahydro-5*H*-pyrazolo[4,3-*c*]pyridine-3,5-dicarboxylate (74). Compounds **73** and **74** were synthesized employing the procedure described for compound **66**, using a solution of LHMDS (37.5 mL of 1 M solution in THF, 37.5 mmol, 1.0 eq.) in dry THF (75 mL), solution of 1-boc-4-piperidinone (7.50 g, 37.5 mmol, 1.0 eq.) in dry THF (50 mL), diethyl oxalate (5.88 g, 37.5 mmol, 1.0 eq.) and 2-hydroxyethylhydrazine (2.85 g, 37.5 mmol, 1.0 eq.). Recrystallization of the reaction mixture from hexane/DCM gave 6.38 g (50%) of the title compound **73** as a white solid. The filtrate was concentrated *in vacuo* and the residue was purified by FC (hexane/EtOAc 5:1 to 0:1, then EtOAc/MeOH 95:5) to give further 1.21 g (10%) of **73** (total yield: 7.59 g, 60 %) and 2.00 g (16 %) of the *N*-2 regioisomer **74** as a yellow oil. **73** ^{1}H NMR (360 MHz, $CDCl_3$) δ 4.61 (s, 2H), 4.39 (q, J = 7.1 Hz, 2H), 4.22 - 4.13 (m, 2H), 4.02 (q, J = 5.0 Hz, 2H), 3.70 (t, J = 5.2 Hz, 2H), 2.82 - 2.62 (m, 3H), 1.49 (s, 9H), 1.37 (t, J = 7.1 Hz, 3H). ^{13}C NMR (91 MHz, $CDCl_3$) δ 162.4, 155.0 (bs), 139.4 (bs), 138.5 (bs), 117.3, 80.2, 61.4, 60.8, 51.4, 41.5 (bs), 39.8 (bs), 28.4, 22.0, 14.4. ESI HRMS (m/z): calcd. for $C_{16}H_{26}N_3O_5$ $[M+H]^+$ 340.18670, found 340.18670. **74** ^{1}H NMR (360 MHz,

$CDCl_3$) δ 4.70 (t, J = 4.7, 2H), 4.63 (bs, 2H), 4.35 (q, J = 7.1 Hz, 2H), 4.00 (t, J = 4.9 Hz, 2H), 3.70 (bs, 2H), 3.00 (bs, 1H), 2.76 (t, J = 6.2 Hz, 1H), 1.50 (s, 9H), 1.40 (t, J = 7.1 Hz, 3H). ^{13}C NMR (91 MHz, $CDCl_3$) δ 160.2, 155.0, 146.6 (bs), 127.9 (bs), 119.3, 80.0, 62.2, 61.2, 53.4, 53.1, 42.0 (bs), 28.4, 23.4 (bs), 14.3 (bs). ESI HRMS (m/z): calcd. for $C_{16}H_{26}N_3O_5$ $[M+H]^+$ 340.18670, found 340.18669.

Ethyl 5-((1*H*-indol-3-yl)methyl)-1-(2-hydroxyethyl)-4,5,6,7-tetrahydro-1*H*-pyrazolo[4,3-*c*]pyridine-3-carboxylate (75). Compound **75** was synthesized employing the procedure described for compound **2**, using intermediate **73** (1.30 g, 3.83 mmol, 1.0 eq.), 4 M solution of HCl in 1,4-dioxane (15 mL), TEA (0.39 g, 3.83 mmol, 1.0 eq.), indole-3-carboxaldehyde (0.55 g, 3.83 mmol, 1.0 eq.), AcOH (0.23 g, 3.83 mmol, 1.0 eq.) and $NaBH(OAc)_3$ (1.22 g, 5.74 mmol, 1.5 eq.) and dry THF (20 mL). Purification by FC (EtOAc/MeOH/TEA 99:0:1 to 94:5:1) gave 1.02 g (72%) of the title compound **75** as a yellow solid. ^{1}H NMR (300 MHz, $CDCl_3$) δ 8.64 (bs, 1H), 7.71 (d, J = 7.8 Hz, 1H), 7.36 (dt, J = 8.0, 1.1 Hz, 1H), 7.30 - 7.07 (m, 3H), 4.34 (q, J = 7.2 Hz, 2H), 4.12 (t, J = 5.0 Hz, 2H), 4.00 (s, 2H), 3.94 (t, J = 5.0 Hz, 2H), 3.84 (s, 2H), 3.46 (bs, 2H), 2.87 (t, J = 5.8 Hz, 2H), 2.72 (t, J = 5.9 Hz, 2H), 1.32 (t, J = 7.2 Hz, 3H). ^{13}C NMR (75 MHz, $CDCl_3$) δ 162.5, 139.4, 138.5, 136.2, 127.9, 124.4, 122.1, 119.7, 119.1, 118.3, 111.4, 111.3, 61.3, 60.7, 52.0, 51.5, 49.6, 48.7, 22.0, 14.3. ESI HRMS (m/z): calcd. for $C_{20}H_{25}N_4O_3$ $[M+H]^+$ 369.19212, found 369.19203.

***tert*-Butyl 3-(benzylcarbamoyl)-1-(2-hydroxyethyl)-1,4,6,7-tetrahydro-5*H*-pyrazolo[4,3-*c*]pyridine-5-carboxylate (76).** Compound **76** was synthesized employing the procedure described for compound **69**, using intermediate **73** (2.30 mg, 8.14 mmol, 1.2 eq.), benzylamine (0.86 g, 6.78 mmol, 1.2 eq.) and TBD (0.28 g, 2.03 mmol, 0.3 eq.) and dry THF (5 mL). Purification by FC (hexane/EtOAc 1:1 to 0:1) gave 1.94 g (72%) of the title compound **76** as a white solid. ^{1}H NMR (360 MHz, $CDCl_3$) δ 7.37 - 7.21 (m, 5H), 7.12 (bs,

1H), 4.70 (s, 2H), 4.59 (d, *J* = 6.1 Hz, 2H), 4.13 - 4.07 (m, 2H), 4.05 - 3.92 (m, 2H), 3.72 (t, *J* = 5.7 Hz, 2H), 2.81 (t, *J* = 5.8 Hz, 1H), 2.72 (t, *J* = 5.8 Hz, 2H), 1.49 (s, 9H). ^{13}C NMR (91 MHz, $CDCl_3$) δ 162.1, 155.1, 140.9, 139.6, 138.4, 128.7, 127.9, 127.4, 116.1, 80.2, 61.4, 51.1, 42.9, 41.3, 40.0, 28.5, 22.1. ESI HRMS (m/z): calcd. for $C_{21}H_{29}N_4O_4$ $[M+H]^+$ 401.21833; found 401.21830.

The free amine hydrochloride used for synthesis of derivatives **15-19** was obtained by treatment of compound **76** with 4 M solution of HCl in 1,4-dioxane at rt for 4h, followed by evaporation of the solvent *in vacuo*.

1-(2-Hydroxyethyl)-*N*-(naphthalen-1-ylmethyl)-4,5,6,7-tetrahydro-1*H*-pyrazolo[4,3-*c*]pyridine-3-carboxamide (78). To a stirred solution of compound **77** (2.10 g, 0.47 mmol) in DCM (50 mL) was added slowly 4 M solution of HCl in 1,4-dioxane (20 mL). The mixture was stirred for 3 h at rt, followed by evaporation of the solvent *in vacuo* to give 1.80 g (quantitative) of the title compound **78** as a pale-yellow solid. 1H NMR (300 MHz, DMSO-d_6) δ 9.53 (bs, 2H), 8.73 (t, *J* = 6.1 Hz, 1H), 8.22 (d, *J* = 8.7 Hz, 1H), 7.95 (d, *J* = 8.9 Hz, 1H), 7.84 (dd, *J* = 6.0, 3.4 Hz, 1H), 7.55 (p, *J* = 7.2, Hz, 2H), 7.49 - 7.40 (m, 2H), 4.89 (d, *J* = 6.1 Hz, 2H), 4.25 (bs, 2H), 4.13 (t, *J* = 5.2 Hz, 2H), 3.85 (bs, 2H), 3.73 (d, *J* = 10.4 Hz, 2H), 3.60 (bs, 1H), 3.36 (bs, 2H), 3.02 (t, *J* = 6.0 Hz, 2H). ^{13}C NMR (75 MHz, DMSO-d_6) δ 162.0, 141.2, 137.8, 135.2, 133.7, 131.3, 129.0, 127.9, 126.7, 126.2, 125.9, 125.8, 124.0, 110.7, 60.5, 52.3, 19.2. ESI HRMS (m/z): calcd. for $C_{20}H_{23}N_4O_2$ $[M+H]^+$ 351.18155, found 351.18146.

***tert*-Butyl 2-(2-hydroxyethyl)-3-((naphthalen-1-ylmethyl)carbamoyl)-2,4,6,7-tetrahydro-5*H*-pyrazolo[4,3-*c*]pyridine-5-carboxylate (79).** Compound **79** was synthesized employing the procedure described for compound **69**, using intermediate **74** (600 mg, 1.77 mmol, 1.0 eq.), 1-naphthalenemethylamine (333 mg, 2.12 mmol, 1.2 eq.) and TBD (74 mg, 0.53 mmol,

0.3 eq.) and dry THF (5 mL). Purification by FC (EtOAc) gave 670 mg (84%) of the title compound **79** as a pale-yellow solid. ^{1}H NMR (500 MHz, $CDCl_3$) δ 8.07 (d, J = 8.4 Hz, 1H), 7.91 (d, J = 8.1 Hz, 1H), 7.86 (d, J = 8.2 Hz, 1H), 7.59 (ddd, J = 8.4, 6.8, 1.4 Hz, 1H), 7.57 - 7.54 (m, 1H), 7.54 - 7.49 (m, 1H), 7.46 (dd, J = 8.2, 6.9 Hz, 1H), 6.73 (bs, 0.5H), 6.53 (bs, 0.5H), 5.07 (d, J = 5.5 Hz, 2H), 4.64 - 4.33 (m, 4H), 3.99 (t, J = 4.9 Hz, 2H), 3.65 (t, J = 5.7 Hz, 2H), 2.72 (t, J = 5.9 Hz, 2H), 1.54 - 1.29 (m, 9H). ^{13}C NMR (91 MHz, $CDCl_3$) δ 160.0, 154.8, 134.0, 132.6, 132.4, 131.2, 129.0, 126.9, 126.8, 126.1, 125.4, 123.2, 80.3, 62.3, 52.8, 42.0, 40.6, 28.3, 23.4. ESI HRMS (m/z): calcd. for $C_{25}H_{31}N_4O_4$ $[M+H]^+$ 451.23398, found 451.23398.

2-(2-Hydroxyethyl)-5-((4-methoxynaphthalen-1-yl)methyl)-*N*-(naphthalen-1-ylmethyl)-4,5,6,7-tetrahydro-2*H*-pyrazolo[4,3-*c*]pyridine-3-carboxamide (80). Compound **80** was synthesized employing the procedure described for compound **2**, using intermediate **79** (279 mg, 0.62 mmol, 1.0 eq.), 4 M solution of HCl in 1,4-dioxane (5 mL), TEA (63 mg, 0.62 mmol, 1.0 eq.), 4-methoxy-1-naphthaldehyde (115 mg, 0.62 mmol, 1.0 eq.), AcOH (37 mg, 0.62 mmol, 1.0 eq.) and $NaBH(OAc)_3$ (197 mg, 0.93 mmol, 1.5 eq.) and dry THF (5 mL). Purification by FC (EtOAc/MeOH/TEA 99:0:1 to 94:5:1) gave 131 mg (40%) of the title compound **80** as a white solid. ^{1}H NMR (300 MHz, DMSO-d_6) δ 8.74 (t, J = 5.6 Hz, 1H), 8.21 - 8.15(m, 2H), 8.13 - 8.07 (m, 1H), 7.99 - 7.92 (m, 1H), 7.86 (t, J = 4.8 Hz, 1H), 7.54 - 7.47 (m, 4H), 7.41 (d, J = 5.4 Hz, 2H), 7.28 (d, J = 7.8 Hz, 1H), 6.84 (d, J = 7.8 Hz, 1H), 5.05 (t, J = 5.1 Hz, 1H), 4.87 (d, J = 5.6 Hz, 2H), 4.28 (t, J = 5.8 Hz, 2H), 3.97 (s, 3H), 3.89 (s, 2H), 3.66 (q, J = 5.6 Hz, 2H), 3.55 (s, 2H), 2.73 (t, J = 5.6 Hz, 2H), 2.58 (t, J = 5.2 Hz, 2H). ^{13}C NMR (75 MHz, DMSO-d_6): δ 160.1, 154.5, 145.2, 134.0, 133.3, 132.8, 132.7, 130.7, 128.5, 127.6, 127.6, 126.2, 126.2, 125.8, 125.8, 125.3, 125.3, 125.2, 125.0, 124.9, 123.4, 121.7, 115.3, 103.3, 60.5, 59.5, 55.5, 52.3, 49.8, 49.0, 40.6, 23.3. ESI HRMS (m/z): calcd. for $C_{32}H_{33}N_4O_3$ $[M+H]^+$ 521.25472, found 521.25468.

***tert*-Butyl 3-((naphthalen-1-ylmethyl)carbamoyl)-1,4,6,7-tetrahydro-5*H*-pyrazolo[4,3-*c*]pyridine-5-carboxylate (81).** Compound **81** was synthesized employing the procedure described for compound **69**, using intermediate **66** (720 g, 2.44 mmol, 1.0 eq.), 1-naphthalenemethylamine (460 mg, 2.93 mmol, 1.2 eq.) and TBD (102 mg, 0.73 mmol, 0.3 eq.) and dry THF (10 mL). Purification by recrystallization from EtOAc/MeOH gave 610 mg (62%) of the title compound **81** as a white solid. ^{1}H NMR (500 MHz, DMSO-d_6) δ 13.02 (bs, 1H), 8.61 (bs, 1H), 8.23 (d, J = 8.4 Hz, 1H), 7.96 (d, J = 7.7 Hz, 1H), 7.86 - 7.82 (m, 1H), 7.62 - 7.52 (m, 2H), 7.47 (d, J = 5.5 Hz, 2H), 4.89 (d, J = 6.3 Hz, 2H), 4.52 (s, 2H), 3.60 (t, J = 5.8 Hz, 2H), 2.69 (t, J = 5.8 Hz, 2H), 1.42 (s, 9H). ^{13}C NMR (91 MHz, DMSO-d_6) δ 162.8, 154.6, 138.8, 135.4, 133.7, 131.3, 128.9, 127.8, 126.6, 126.2, 125.9, 125.6, 123.9, 114.2, 79.5, 28.55. ESI HRMS (m/z): calcd. for $C_{23}H_{27}N_4O_3$ $[M+H]^+$ 407.20777, found 407.20791.

5-((4-Methoxynaphthalen-1-yl)methyl)-*N*-(naphthalen-1-ylmethyl)-4,5,6,7-tetrahydro-1*H*-pyrazolo[4,3-*c*]pyridine-3-carboxamide (82). Compound **82** was synthesized employing the procedure described for compound **2**, using intermediate **81** (379 mg, 0.93 mmol, 1.0 eq.), 4 M solution of HCl in 1,4-dioxane (5 mL), TEA (94 mg, 0.93 mmol, 1.0 eq.), 4-methoxy-1-naphthaldehyde (172 mg, 0.93 mmol, 1.0 eq.), AcOH (56 mg, 0.62 mmol, 1.0 eq.) and $NaBH(OAc)_3$ (296 mg, 1.40 mmol, 1.5 eq.) and dry THF (7 mL). Purification by recrystallization from EtOAc/MeOH gave 245 mg (55%) of the title compound **82** as a white solid. ^{1}H NMR (400 MHz, DMSO-d_6) δ 12.90 (s, 1H), 8.51 (t, J = 6.1 Hz, 1H), 8.25 (d, J = 7.7 Hz, 1H), 8.21 - 8.14 (m, 2H), 7.93 (dd, J = 6.2, 3.0 Hz, 1H), 7.81 (d, J = 6.6 Hz, 1H), 7.58 - 7.35 (m, 7H), 6.91 (d, J = 7.9 Hz, 1H), 4.82 (d, J = 6.0, 2H), 4.00 (s, 2H), 3.97 (s, 3H), 3.59 (s, 2H), 2.77 (t, J = 5.8 Hz, 2H), 2.68 (s, J = 5.8 Hz, 2H). ^{13}C NMR (101 MHz, DMSO-d_6) δ 162.9, 155.0, 141.5, 139.0, 135.4, 133.7, 133.3, 131.2, 128.9, 128.2, 127.7, 126.7, 126.6, 126.5, 126.1, 125.8, 125.7, 125.6, 125.5, 125.4, 123.9, 122.1, 115.6, 103.9, 60.0, 56.0, 49.8, 46.0, 22.0. ESI HRMS (m/z): calcd. for $C_{30}H_{29}N_4O_2$ $[M+H]^+$ 477.22850, found 477.22853.

1-(5-((4-Methoxynaphthalen-1-yl)methyl)-4,5,6,7-tetrahydro-1*H*-pyrazolo[4,3-*c*]pyridin-3-yl)-*N*-(naphthalen-1-ylmethyl)methanamine (83). To a stirred, cooled (ice-salt bath) solution of compound **82** (600 mg, 1.26 mmol, 1.0 eq.) in dry THF (15 mL) was added $LiAlH_4$ (3.15 mL of a 2 M solution in THF, 6.30 mmol, 5.0 eq.). The reaction mixture was allowed to reach rt followed by refluxing overnight. The solution was cooled (ice-salt bath) and water (0.5 mL) was added slowly. The mixture was treated with 15% aqueous solution of NaOH (0.5 mL) and water (1.5 mL), followed by $MgSO_4$. Next, DCM (5 mL) and MeOH (5 mL) were added, followed by filtration of the mixture and evaporation *in vacuo*. Purification by FC (DCM/MeOH/7 M solution of NH_3 in MeOH 94:5:1) gave 380 mg (65%) of the title compound **83** as a white solid. ^{1}H NMR (400 MHz, DMSO-d_6) δ 12.21 (bs, 0.5H), 12.13 (bs, 0.5H), 8.23 (d, J = 7.8 Hz, 1H), 8.18 (dd, J = 8.2, 1.7 Hz, 1H), 8.10 d, J = 8.0 Hz, 1H), 7.97 - 7.86 (m, 1H), 7.80 (d, J = 8.0 Hz, 1H), 7.58 - 7.40 (m, 4H), 7.39 (t, J = 7.5 Hz, 1H), 7.34 (d, J = 8.0 Hz, 1H), 6.87 (d, J = 7.8 Hz, 1H), 4.07 (s, 2H), 3.96 (s, 3H), 3.93 (s, 2H), 3.66 (s, 2H), 3.44 (s, 2H),2.73 (t, J = 5.8 Hz, 2H), 2.59 (t, J = 5.7 Hz, 2H), 2.37 (bs, 1H). ^{13}C NMR (126 MHz, DMSO-d_6) δ 154.9, 146.4 (bs), 136.5 (bs), 133.8, 133.3, 131.9, 128.8, 128.2, 127.6, 126.6, 126.6, 126.2, 126.1, 126.0, 125.8, 125.7, 125.5, 125.4, 124.6, 122.1, 112.1 (bs), 103.8, 61.2, 60.3 (bs), 56.0, 50.5, 49.4, 45.9 (bs), 43.0 (bs), 29.7. ESI HRMS (m/z): calcd. for $C_{30}H_{31}N_4O$ $[M+H]^+$ 463.24924; found 463.25043.

***tert*-Butyl 3-carbamoyl-1-(2-hydroxyethyl)-1,4,6,7-tetrahydro-5*H*-pyrazolo[4,3-*c*]pyridine-5-carboxylate (84).** The solution of compound **73** (1.50 g, 4.42 mmol) in 7 M methanolic solution of NH_3 (20 mL) was refluxed in a sealed pressure tube for 2 days. The mixture was cooled and evaporated *in vacuo*. The residue was heated with diethyl ether and the resulting solid was filtered and dried *in vacuo* to give 1.36 g (quantitative) of the title compound **84** as a white solid. ^{1}H NMR (400 MHz, DMSO-d_6) δ 7.34 (s, 1H), 7.16 (s, 1H), 4.91 (t, J = 5.4 Hz, 1H), 4.48 (s, 2H), 4.06 (t, J = 5.4 Hz, 2H), 3.72 (q, J = 5.4 Hz, 2H), 3.59

(t, *J* = 5.7 Hz, 2H), 2.72 (t, *J* = 5.7 Hz, 2H), 1.42 (s, 9H). ^{13}C NMR (101 MHz, DMSO-d_6) δ 164.4, 154.6, 140.8, 139.7, 115.0, 79.5, 60.6, 52.0, 41.7, 41.1, 28.6, 22.0.

1-(2-Hydroxyethyl)-5-((4-methoxynaphthalen-1-yl)methyl)-4,5,6,7-tetrahydro-1*H*-pyrazolo[4,3-*c*]pyridine-3-carboxamide (85). Compound **85** was synthesized employing the procedure described for compound **2**, using intermediate **84** (728 mg, 2.35 mmol, 1.0 eq.), 4 M solution of HCl in 1,4-dioxane (5 mL), TEA (237 mg, 2.35 mmol, 1.0 eq.), 4-methoxy-1-naphthtaldehyde (437 mg, 2.35 mmol, 1.0 eq.), AcOH (141 mg, 2.35 mmol, 1.0 eq.), $NaBH(OAc)_3$ (747 mg, 3.52 mmol, 1.5 eq.) and dry THF (15 mL). Purification by FC (DCM/MeOH 99:1 to 95:5) gave 557 mg (62%) of the title compound **85** as a white solid. ^{1}H NMR (400 MHz, $CDCl_3$) *δ* 8.30 (dd, *J* = 8.2, 1.6 Hz, 1H), 8.23 (dd, *J* = 7.8, 2.0 Hz, 1H), 7.56 - 7.42 (m, 2H), 7.37 (d, *J* = 7.8 Hz, 1H), 6.76 (d, *J* = 7.8 Hz, 1H), 6.62 (bs, 1H), 5.45 (bs, 1H), 4.09 - 4.02 (m, 4H), 4.02 (s, 3H), 3.95 (dd, *J* = 5.7, 4.0 Hz, 2H), 3.88 (s, 2H), 2.91 (bs, 1H), 2.78 (t, *J* = 5.7 Hz, 2H), 2.63 (t, *J* = 5.8 Hz, 2H). ^{13}C NMR (101 MHz, $CDCl_3$) δ 164.5, 155.3, 140.2, 139. 9, 133.4, 127.7, 126.4, 126.0, 125.0, 124.6, 122.3, 117.8, 102. 9, 76.7, 61.3, 59.8, 55.5, 51.0, 50.1, 48.5, 22.3. ESI HRMS (m/z): calcd. for $C_{21}H_{25}N_4O_3$ $[M+H]^+$ 381.19212, found 381.19212.

2-(3-(Aminomethyl)-5-((4-methoxynaphthalen-1-yl)methyl)-4,5,6,7-tetrahydro-1*H*-pyrazolo[4,3-*c*]pyridin-1-yl)ethan-1-ol (86). To a stirred, cooled (ice-salt bath) solution of compound **85** (545 mg, 1.43 mmol, 1.0 eq.) in dry THF (10 mL) was added $LiAlH_4$ (2.89 mL of a 2 M solution in THF, 5.74 mmol, 4.0 eq.). The reaction mixture was allowed to reach rt followed by refluxing overnight. The solution was cooled (ice-salt bath) and water (0.5 mL) was added slowly. The mixture was treated with 15% aqueous solution of NaOH (0.5 mL) and water (1.5 mL), followed by $MgSO_4$. The solids were filtered off and the resulting solution was evaporation *in vacuo*. Purification by automated preparative chromatography

(RP-C18, linear gradient from water/MeOH 90:10 to 15:85) gave 220 mg (42%) of the title compound **86** as a white solid. ^{1}H NMR (400 MHz, DMSO-d_6) δ 8.24 (d, J = 8.1 Hz, 1H), 8.18 (d, J = 7.9 Hz, 1H), 7.61 - 7.43 (m, 2H), 7.38 (d, J = 7.8 Hz, 1H), 6.91 (d, J = 7.8 Hz, 1H), 4.77 (bs, 1H), 3.97 (s, 3H), 3.96 - 3.93 (m, 2H), 3.89 (t, J = 5.8 Hz, 2H), 3.63 (t, J = 5.8 Hz, 2H), 3.52 (s, 2H), 3.46 (s, 2H), 2.71 (t, J = 5.8 Hz, 2H), 2.60 (t, J = 5.8 Hz, 2H), 1.86 (bs, 2H). ^{13}C NMR (101 MHz, DMSO-d_6) δ 155.0, 148.2, 138.0, 133.4, 128.2, 126.7, 126.6, 125.7, 125.5, 125.4, 122.1, 112.0, 103.9, 60.8, 60.0, 56.0, 51.1, 49.8, 49.3, 39.0, 22.2. ESI HRMS (m/z): calcd. for $C_{21}H_{27}N_4O_2$ $[M+H]^+$ 367.21285, found 367.21289.

***tert*-Butyl 3-(5-((4-methoxynaphthalen-1-yl)methyl)-3-((naphthalen-1-ylmethyl)carbamoyl)-4,5,6,7-tetrahydro-1*H*-pyrazolo[4,3-*c*]pyridin-1-yl)azetidine-1-carboxylate (88).** A mixture of compound **82** (270 mg, 0.57 mmol, 1.0 eq), *tert*-butyl 3-((methylsulfonyl)oxy)azetidine-1-carboxylate (231 mg, 0.86 mmol, 1.5 eq.) and Cs_2CO_3 (336 mg, 1.14 mmol, 2.0 eq.) in dry DMF (4 mL) was stirred at 95 °C overnight. The mixture was cooled and partitioned between water (30 mL) and EtOAc (5 mL). The aqueous layer was extracted with EtOAc (3x5 mL) and the combined organic phase was washed with water (3x 5 mL), brine (3x5 mL), dried over anhydrous Na_2SO_4, filtered and evaporated *in vacuo*. Purification by FC (hexane/EtOAc 2:1 to 0:1) gave 300 mg (83%) of the title compound **88** as a colorless oil. ^{1}H NMR (400 MHz, $CDCl_3$) δ 8.31 (dd, J = 7.7, 2.1 Hz, 1H), 8.28 – 8.23 (m, 1H), 8.18 – 8.11 (m, 1H), 7.91 (dd, J = 7.6, 2.0 Hz, 1H), 7.85 (d, J = 8.2 Hz, 1H), 7.61 – 7.44 (m, 6H), 7.38 (d, J = 7.8 Hz, 1H), 7.18 (t, J = 5.7 Hz, 1H), 6.77 (d, J = 7.9 Hz, 1H), 5.09 (d, J = 5.7 Hz, 2H), 4.82 (tt, J = 8.0, 5.6 Hz, 1H), 4.36 – 4.28 (m, 2H), 4.23 (t, J = 8.5 Hz, 2H), 4.09 (s, 2H), 4.03 (s, 3H), 3.98 (s, 2H), 2.79 (t, J = 5.7 Hz, 2H), 2.57 (t, J = 5.7 Hz, 2H), 1.41 (s, 9H). ^{13}C NMR (101 MHz, $CDCl_3$) δ 162.2, 156.1, 155.4, 141.2, 139.2, 133. 9, 133.8, 133.4, 131.6, 128.7, 128.5, 127.7, 126.7, 126.6, 126.4, 126.1, 126.03, 125.9, 125.5, 125.0,

124.7, 123.7, 122.3, 118.2, 102.9, 80.0, 60.1, 55.9 (bs), 55.5, 50.2, 48.5, 46.8, 40.9, 28.3, 22.3. ESI HRMS (m/z): calcd. for $C_{38}H_{42}N_5O_4$ $[M+H]^+$ 632.32313, found 632.32395.

Ethyl 1-(2-acetoxyethyl)-5-benzyl-1,4,5,6-tetrahydropyrrolo[3,4-*c*]pyrazole-3-carboxylate (89), ethyl 2-(2-acetoxyethyl)-5-benzyl-2,4,5,6-tetrahydropyrrolo[3,4-*c*]pyrazole-3-carboxylate (90) and 2-benzyl-2,3,6,7-tetrahydropyrrolo[3',4':3,4]pyrazolo[5,1-*c*][1,4]oxazin-9(1*H*)-one (91). To a stirred solution of DIPA (8.84 g, 68.5 mmol, 1.2 eq.) in dry THF (100 mL) at -78 °C was added *n*-BuLi (25.1 mL of 2.5 M solution in hexane, 62.8 mmol, 1.1 eq.). After stirring at -78 °C for 45 min, a solution of 1-benzylpyrrolidin-3-one (10.0 g, 57.1 mmol, 1.0 eq.) in dry THF (50 mL) was added dropwise. The reaction mixture was stirred for further 30 min at -78 °C, followed by a dropwise addition of a solution of diethyl oxalate (8.34 mL, 57.1 mmol, 1.0 eq.) in dry THF (50 mL). The mixture was then warmed to rt and stirred for further 30 min. Subsequently, EtOH (40 mL), AcOH (40 mL) and hydroxyethylhydrazine (3.87 mL, 57.1 mmol, 1.0 eq.) were added. The reaction mixture was then heated to reflux for 1 h, cooled to rt and concentrated *in vacuo*. The residue was dissolved in AcOH (40 mL) and refluxed for further 4h after which TLC (EtOAc) showed a formation of a predominant spot ($R_f \approx 0.2$). The solution was evaporated *in vacuo* and the resulting oil was partitioned between EtOAc (100 mL) and saturated aqueous solution of $NaHCO_3$ (70 mL). The aqueous phase was extracted with EtOAc (2x25 mL). The combined organic extracts were washed with water (25 mL), brine (25 mL), dried over anhydrous Na_2SO_4, filtered and concentrated *in vacuo*. The residue was purified by FC (hexane/EtOAc 1:1 to 0:1, then EtOAc/MeOH 99:1 to 95:5) gave 5.82 g of an oil. LC/MS (ESI+) analysis of this material showed the presence of both tetrahydropyrrolo[3,4-*c*]pyrazole (m/z = 316 $[M+H]^+$) and the corresponding acyclic hydrazone species (m/z = 334 $[M+H]^+$). To achieve a full cyclization, the oil was again dissolved in AcOH (50 mL) and refluxed for 14 h. The solution was evaporated *in vacuo* and

the resulting oil was partitioned between EtOAc (100 mL) and saturated aqueous solution of $NaHCO_3$ (70 mL). The aqueous phase was extracted with EtOAc (2x25 mL). The combined organic extracts were washed with water (25 mL), brine (25 mL), dried over anhydrous Na_2SO_4, filtered and concentrated *in vacuo*. Purification of the residue by FC (hexane/EtOAc 3:1 to 0:1) gave the title acetylated derivatives **89** (3.51 g, 17%, brown oil) and **90** (0.84 g, 4%, yellow oil) along with the cyclic lactone **91** (0.60 g, 4%, brown solid). **89**: ^{1}H NMR (400 MHz, $CDCl_3$) δ 7.45 - 7.34 (m, 4H), 7.34 - 7.29 (m, 1H), 4.43 - 4.34 (m, 4H), 4.34 - 4.29 (m, 2H), 4.04 - 3.98 (m, 4H), 3.87 (bs, 2H), 2.01 (s, 3H), 1.37 (t, J = 7.1 Hz, 3H). ^{13}C NMR (101 MHz, $CDCl_3$) δ 170.3, 162.0, 148.1, 138.2, 136.7, 128.7, 128.6, 127.5, 126.8, 62.8, 60.9, 60.3, 52.6, 51.1, 50.6, 20.7, 14.4. ESI HRMS (m/z): calcd. for $C_{19}H_{24}N_3O_4$ $[M+H]^+$ 358.17613, found 358.17639. **90**: ^{1}H NMR (400 MHz, $CDCl_3$) δ 7.46 - 7.41 (m, 2H), 7.38 (ddd, J = 7.8, 6.8, 0.9 Hz, 2H), 7.34 - 7.29 (m, 1H), 4.79 (t, J = 5.4 Hz, 2H), 4.47 - 4.38 (m, 2H), 4.31 (q, J = 7.1 Hz, 2H), 4.01 (s, 2H), 3.95 (s, 2H), 3.87 (s, 2H), 2.02 (s, 3H), 1.33 (t, J = 7.1 Hz, 3H). ^{13}C NMR (101 MHz, $CDCl_3$) δ 170.7, 159.6, 156.1 (bs), 138.4 (bs), 128.7, 128.5, 127.4, 126.0, 63.3, 61.0, 60.3, 52.5, 51.9, 50.4, 20.8, 14.3. ESI HRMS (m/z): calcd. for $C_{19}H_{24}N_3O_4$ $[M+H]^+$ 358.17613, found 358.17630. **91**: ^{1}H NMR (500 MHz, $CDCl_3$) δ 7.41 (d, J = 7.2 Hz, 2H), 7.37 (t, J = 7.6 Hz, 2H), 7.34 - 7.27 (m, 1H), 4.74 - 4.65 (m, 2H), 4.47 - 4.41 (m, 2H), 4.01 (s, 2H), 3.99 (s, 2H), 3.89 (s, 2H). ^{13}C NMR (101 MHz, $CDCl_3$) δ 158.1, 157.1, 138.2, 128.7, 128.6, 127.4, 127.2, 123.1, 66.3, 60.2, 51.7, 51.5, 46.0. ESI HRMS (m/z): calcd. for $C_{15}H_{16}N_3O_2$ $[M+H]^+$ 270.12370, found 270.12378.

Ethyl 5-benzyl-1-(2-hydroxyethyl)-1,4,5,6-tetrahydropyrrolo[3,4-*c*]pyrazole-3-carboxylate (92). A mixture of compound **90** (3.46, 9.69 mmol, 1.0 eq.), K_2CO_3 (1.34 g, 9.69 mmol, 1.0 eq.) and EtOH (15 mL) was stirred for 0.5 h at 60 °C. The reaction mixture was cooled, filtered and evaporated *in vacuo*. Purification of the residue by FC (EtOAc/MeOH 99:1 to 95:5) gave 2.93 g (96%) of the title compound **92** as a brown oil. ^{1}H NMR (400 MHz,

$CDCl_3$) δ 7.43 - 7.34 (m, 4H), 7.34 - 7.30 (m, 1H), 4.36 (q, J = 7.2 Hz, 2H), 4.20 - 4.14 (m, 2H), 4.04 - 3.96 (m, 6H), 3.93 (t, J = 2.2 Hz, 2H), 2.88 (bs, 1H), 1.36 (t, J = 7.2 Hz, 3H). ^{13}C NMR (101 MHz, $CDCl_3$) δ 162.0, 148.2, 137.9, 136.4, 128.8, 128.6, 127.6, 126.2, 76.7, 61.4, 60.9, 60.3, 53.7, 52.6, 51.2, 14.4. ESI HRMS (m/z): calcd. for $C_{17}H_{22}N_3O_3$ $[M+H]+$ 316.16557, found 316.16540.

5-Benzyl-1-(2-hydroxyethyl)-*N*-(naphthalen-1-ylmethyl)-1,4,5,6-tetrahydropyrrolo[3,4-*c*]pyrazole-3-carboxamide (93). Compound **93** was synthesized employing the procedure described for compound **69**, using intermediate **92** (1.97 g, 5.68 mmol, 1.0 eq.), 1-naphthalenemethylamine (1.34 g, 8.52 mmol, 1.5 eq.) and TBD (0.24 g, 1.70 mmol, 0.3 eq.) and dry THF (5 mL). Purification by FC (EtOAc) gave 1.14 mg (47%) of the title compound **93** as a beige solid. ^{1}H NMR (500 MHz, DMSO-d_6) δ 8.49 (t, J = 6.2 Hz, 1H), 8.21 (dd, J = 8.1, 1.7 Hz, 1H), 7.95 (dd, J = 7.6, 1.9 Hz, 1H), 7.84 (dt, J = 6.2, 3.5 Hz, 1H), 7.60 - 7.50 (m, 2H), 7.50 - 7.42 (m, 2H), 7.42 - 7.32 (m, 4H), 7.30 - 7.24 (m, 1H), 4.92 (t, J = 5.4 Hz, 1H), 4.86 (d, J = 6.2 Hz, 2H), 4.06 (t, J = 5.2 Hz, 2H), 3.92 (s, 2H), 3.85 - 3.76 (m, 4H), 3.68 (q, J = 5.3 Hz, 2H). ^{13}C NMR (126 MHz, DMSO-d_6) δ 161. 8, 149.2, 139.6, 138.8, 135.4, 133.7, 131.3, 129.0, 128.9, 128.8, 127.8, 127.4, 126.6, 126.2, 125.9, 125.8, 124.1, 124.0, 60.4, 59.90, 54.2, 52.5, 51.2. ESI HRMS (m/z): calcd. for $C_{26}H_{27}N_4O_2$ $[M+H]^+$ 427.21285, found 427.21280.

1-(2-Hydroxyethyl)-*N*-(naphthalen-1-ylmethyl)-1,4,5,6-tetrahydropyrrolo[3,4-*c*]pyrazole-3-carboxamide hydrochloride (94). The mixture of compound **94** (1.10 g, 2.58 mmol, 1.0 eq.), 1,4-cyclohexadiene (2.07 g, 25.80 mmol, 10.0 eq.), 10% Pd/C (0.11 g) and MeOH (15 mL, degassed by bubbling argon through for 1 h) was stirred for 4 h at 70 °C, in a sealed pressure tube. The mixture was then cooled, filtered through a pad of celite and evaporated *in vacuo*. The residue was dissolved in DCM (10 mL), cooled (ice-salt bath),

followed by treatment with 1 M solution of hydrochloric acid in Et_2O (5 mL). The solvents were evaporated *in vacuo* to give 0.91 g (quantitative) of the title compound **94** as a white solid. ^{1}H NMR (500 MHz, DMSO-d_6) δ 10.59 (s, 2H), 8.78 (t, J = 6.1 Hz, 1H), 8.22 (d, J = 8.2 Hz, 1H), 7.95 (d, J = 7.9 Hz, 1H), 7.84 (dd, J = 6.5, 3.1 Hz, 1H), 7.62 - 7.51 (m, 2H), 7.51 - 7.43 (m, 2H), 5.15 (t, J = 5.2 Hz, 1H), 4.88 (d, J = 6.1 Hz, 2H), 4.45 (s, 2H), 4.35 (s, 2H), 4.18 (t, J = 4.9 Hz, 2H), 3.72 (q, J = 5.0 Hz, 2H). ^{13}C NMR (101 MHz, DMSO-d_6) δ 161.0, 145.9, 139.3, 135.1, 133.7, 131.3, 129.0, 127.9, 126.7, 126.2, 125.9, 124.0, 121.4, 60.3, 54.6, 44.9, 43.7. ESI HRMS (m/z): calcd. for $C_{19}H_{21}N_4O_2$ $[M+H]^+$ 337.16590, found 337.16568.

2-(5-((4-Methoxynaphthalen-1-yl)methyl)-3-((naphthalen-1-ylmethyl)carbamoyl)-5,6-dihydropyrrolo[3,4-*c*]pyrazol-1(4*H*)-yl)ethyl 4-methylbenzenesulfonate (95). To a stirred, cooled (ice-salt bath) solution of **63** (193 mg, 0.38 mmol, 1 eq.) and DMAP (2 mg, 0.02 mmol, 5 mol%) in dry DCM (5 mL) was added 4-toluenesulfonyl chloride (80 mg, 0.42 mmol, 1.1 eq) and TEA (58 mg, 0.57 mmol, 1.5 eq.). The solution was allowed to warm up to rt then stirred overnight. The reaction mixture was washed with water (20 mL), brine (20 mL), dried over anhydrous Na_2SO_4, filtered and concentrated *in vacuo*.). Purification by FC (EtOAc/MeOH/TEA 99:0:1 to 94:5:1) gave 191 mg (76%) of the title compound **95** as a white solid. ^{1}H NMR (500 MHz, $CDCl_3$) δ 8.34 (dd, J = 8.4, 1.4 Hz, 1H), 8.28 (d, J = 8.3 Hz, 1H), 8.10 (d, J = 8.3 Hz, 1H), 7.90 (dd, J = 8.0, 1.6 Hz, 1H), 7.84 (d, J = 8.1 Hz, 1H), 7.63 - 7.49 (m, 7H), 7.46 (dd, J = 8.1, 7.0 Hz, 1H), 7.40 (d, J = 7.8 Hz, 1H), 7.12 (d, J = 8.0 Hz, 2H), 6.89 (t, J = 5.8 Hz, 1H), 6.79 (d, J = 7.8 Hz, 1H), 5.02 (d, J = 5.8 Hz, 2H), 4.33 - 4.24 (m, 4H), 4.06 (t, J = 5.0 Hz, 2H), 4.05 (s, 3H), 3.99 (t, J = 2.4 Hz, 2H), 3.76 (s, 2H), 2.34 (s, 3H). ^{13}C NMR (75 MHz, $CDCl_3$) δ 162.5, 161.2, 155.5, 149.2, 145.3, 139.4, 133.9, 133.7, 133.02, 132.04, 131.51, 129.83, 128.76, 128.58, 127.64, 127.14, 126.76, 126.65, 126.02, 126.0, 125.4, 125.2, 124.2, 123.6, 122.4, 102.9, 67.8, 58.3, 55.6, 52.2, 50.6, 50.0, 41.1, 21.6. ESI HRMS (m/z): calcd. for $C_{38}H_{37}N_4O_5S$ $[M+H]^+$ 661.24792, found 661.24811.

1-(2-Azidoethyl)-5-((4-methoxynaphthalen-1-yl)methyl)-*N*-(naphthalen-1-ylmethyl)-1,4,5,6-tetrahydropyrrolo[3,4-*c*]pyrazole-3-carboxamide (96). A mixture of compound **95** (114 mg, 0.17 mmol) and NaN_3 (56 mg, 0.86 mmol, 5.0 eq.) in dry DMF (2 mL) was vigorously stirred at 70 °C for 4 h. The reaction mixture was partitioned between EtOAc (5 mL) and water (10 mL) and the aqueous layer was extracted with EtOAc (2x2 mL). The combined organic extracts were washed with water (2x2 mL), brine (2x2 mL), dried over anhydrous Na_2SO_4, filtered and concentrated *in vacuo*. Purification by FC (hexane/EtOAc 1:1 to 0:1) gave 81 mg (78%) of the title compound **96** as a white solid. ^{1}H NMR (400 MHz, $CDCl_3$) δ 8.36 - 8.29 (m, 1H), 8.27 (d, J = 8.3 Hz, 1H), 8.11 (ddd, J = 7.8, 0.8 Hz, 1H), 7.90 (dd, J = 8.0, 1.5 Hz, 1H), 7.84 (dt, J = 8.2, 1.1 Hz, 1H), 7.60 - 7.49 (m, 5H), 7.48 - 7.41 (m, 2H), 7.01 (t, J = 5.7 Hz, 1H), 6.78 (d, J = 7.8 Hz, 1H), 5.05 (d, J = 5.6 Hz, 2H), 4.36 (s, 2H), 4.15 (s, 2H), 4.04 (s, 3H), 3.98 (dd, J = 6.2, 5.1 Hz, 2H), 3.85 (s, 2H), 3.63 (dd, J = 6.2, 5.1 Hz, 2H). ^{13}C NMR (101 MHz, $CDCl_3$) δ 161.4, 155.5, 149.0, 139.5, 133.9, 133.7, 133.0, 131.6, 128.7, 128.5, 127.1, 126.7, 126.7, 126.6, 126.5, 126.0, 126.0, 125.4, 125.2, 124.2, 123.7, 122.4, 102.9, 58.4, 55.5, 52.4, 50.6, 50.4, 50.2, 41.1. ESI HRMS (m/z): calcd. for $C_{31}H_{30}N_7O_2$ $[M+H]^+$ 532.24555, found 532.24615.

Protein expression and purification. Human, *T. cruzi* and *T. brucei N*-His-PEX14 (19-84) proteins were cloned into pETM-11 (EMBL) vector and expressed in standard *E. coli* BL21 system using autoinduction medium.[49] The proteins were initially purified by affinity chromatography using NiNTA column. Following dialysis to TEV cleavage buffer (50 mM Tris pH 8.0, 1mM EDTA, 5 mM β-mercaptoethanol) the TEV protease was added and the reaction was allowed to proceed overnight at room temperature. This step was omitted when the proteins were prepared for AlphaScreen assay that requires presence of a His-tag. Next, the proteins were purified by size exclusion chromatography into either PBS buffer or crystallization buffer (5 mM Tris pH 8.0, 50 mM NaCl, 5 mM β-mercaptoethanol).

AlphaScreen – based competition assays. To determine the compounds' effective concentration (EC_{50}) values against PEX14-PEX5 PPI, an AlphaScreen-based assay was developed according to a PerkinElmer manual. The assay mixture was composed of 3 nM *N*-His-PEX14 (21-84) and 10 nM of biotinylated PEX5-derived peptide (ALSENWAQEFLA) in a PBS buffer supplemented with 5 mg/mL of BSA and 0.01 % (v/v) Tween-80. The assay employed 5 μg/mL of streptavidin donor beads and 5 μg/mL of nickel chelate acceptor beads (PerkinElmer). Compound was added to the assay mixture as a DMSO solution. DMSO concentration was kept constant at 5% (v/v). This concentration was shown to have no effect on the assay readout. The competition curves were measured using a serial dilution of the inhibitor (12 points) while keeping the concentrations of all other assay components constant. The inhibitor EC_{50} was calculated from the Hill sigmoidal fit of the experimental data with asymptotes fixed at maximal assay signal (no inhibitor added) and 0, respectively, using OriginLab OriginPro 9.0[50].

Crystallization and X-ray structure solution. The purified protein was mixed with 10-fold molar excess of ligand (50 mM solution in DMSO) in storage buffer (10 mM Tris pH 8.0, 100 mM NaCl and 5 mM β-mercaptoethanol) with 3% DMSO and the mixture was incubated for 1h at room temperature. The excess ligand and DMSO were removed by washing the complex at 4 °C on a 10 kDa-cutoff Centricon concentrator with storage buffer. Prior to crystallization the complex was concentrated to about 30 mg/mL. Initial crystallization trials were set up using commercial kits and TTP LabTech Mosquito automated crystallization workstation. Crystals suitable for diffraction testing appeared in different condition, after few days. They were transferred into a cryo-protectant solution containing the harvesting solution and 25% (v/v) glycerol and cryo-cooled in liquid nitrogen. Diffraction data were collected at European Synchrotron Radiation Facility (ESRF, Grenoble, France) beamline ID29. The best diffracting crystal was obtained at room temperature in 0.2 M $MgCl_2$, 0.1 M Tris pH 8.0,

20% (w/v) PEG 6000. The experimental data were processed using XDS and XSCALE software.[51] Crystals of *Tb*PEX14-ligand complex diffracted up to 1.2 Å resolution and belonged to the orthorhombic $P3_221$ space group. The Matthews coefficient analysis suggested the presence of one molecule in the asymmetric unit.[52] The structure was solved by molecular replacement using Phaser[53] with *Tb*PEX14 structure (PDB code: 5AON[54]) as a search model. The analysis of the electron density calculated with (Fo – Fc) and (2Fo – Fc) coefficients allowed to build the initial model and to unambiguously place the ligand using COOT.[55] The starting model was refined by iterations of manual and automated refinement using Refmac5.[56] Throughout the refinement 5% of the reflections were used for the cross-validation analysis,[57] and the behavior of R_{free} was employed to monitor the refinement strategy. Water molecules were added using Arp/Warp[58] and subsequently manually inspected. Hydrogens were generated and refined using Refmac5. Detailed information on data collection and refinement statistics are reported in Table S2 - see *Supporting Information*.

Molecular dynamics simulations. The PDB files of the three different ligand-protein complexes (*Tb*PEX14-**50**: 5N8V[35] and *Tb*PEX14-**61**: 6SPT, *Tb*PEX14-**29** complex structure was generated in Maestro v11.1[59] by replacing the nitrogen of the pendant amine of **50** in 5N8V with the oxygen, assuming the same consensus-binding mode) were prepared adding missing sidechains and hydrogens using YASARA Biosciences YASARA Structure's[60] *clean* built-in command. Structures were then imported into Schrödinger Maestro version 2018.3[59] and further refined using the Maestro v11.1 'Protein Preparation Wizard'[61]. Protonation states were calculated using PROPKA[62, 63] at pH 7.0 ± 2.0 and minimization of hydrogen positions with restrained backbone was performed using OPLS_2005 FF[64] in order to optimize the hydrogen bonding network. All the systems were then prepared for simulation using Maestro v11.1 'System Builder' GUI using TIP4P solvent model[65, 66] (crystallographic water

molecules were deleted) in an automatically generated cubic cell with periodic boundary conditions. In addition to the solvated complex, Na^+ and Cl^- ions corresponding to a 150 mM buffer were placed in the cell in order to set the total net charge to zero. Molecular Dynamics simulations were run using Schrödinger Maestro Desmond Molecular Dynamics Package version 2018.3[67] on a NVIDIA 1060 graphics processing unit using Desmond graphical user interface for a total simulation time of 50 ns to ensure system convergence, with xyz coordinates recording interval every 50 ps (1000 snapshots in total) and 1.2 ps for potential energy calculations of the ensemble. Ensemble class was set to NPT at a temperature of 300 K and pressure of 1.01 bar, force cut-off radius was set to 9.0 Å and each solvated model was relaxed with Desmond default relaxation protocol before starting the actual simulation.

In vitro* trypanocidal activity of compounds against *T. brucei brucei. *T. brucei brucei* bloodstream form (Lister 427, MITat 1.2) parasites were grown in a HMI-11 medium[68] containing 10% fetal bovine serum (FBS) at 37 ºC with 5% CO_2. Anti-trypanosomal activities of the compounds were tested using resazurin-based 96-well plate assay. Two-fold serial dilutions of each compound (10 wells in each row) were prepared in 96-well plates in HMI-11 medium (100 µL/well, quadruplicates). As controls, each row included a well without compound and a well with medium alone. 100 µL of parasite cultures ($4x10^3$/mL) were inoculated in all wells, except in the well with media alone. Final concentration of parasites was $2x10^3$/mL. The plates were incubated for 66 h. Resazurin (25 µL of 0.1 mg/mL in Hanks Balanced Salt Solution) was added to all wells and the plates were further incubated untill 72 h time-point. Reduction of resazurin by living cells was quantified by measuring the fluorescence with Synergy H1 microplate reader (excitation 530 nm, emission 585 nm). After subtracting the background fluorescence of the well with media alone, percent survival values were calculated by setting the fluorescence of the wells without compound to "100% survival". Non-linear regression graphs were plotted in GraphPad Software GraphPad Prism

6.04[69] to yield sigmoidal dose-response curves and half-maximal effective concentration (EC_{50}) values were determined.

Cytotoxicity of compounds against HepG2 cells. HepG2 (Hepatocyte) cells were seeded in 96 well plates (5000 cells/well in rows B-H) and grown overnight at 37 °C in humidified incubator with 5% CO_2. Compounds were tested in triplicate from 100 μM to 3.125 μM (2-fold serial dilutions, from row H to row C). Row A contained medium alone and served as a negative control. Row B contained cells alone without inhibitors and served as positive control. Hygromycin B (InvivoGen) was used as positive control for cytotoxicity. After incubation for 66 h, 25 μl of 0.1 mg/mL resazurin (dissolved in Hanks Balanced Salt Solution HBSS, Sigma) was added to all wells. Plates were further incubated for 6 hours. Fluorescence was measured and data processed as described above for the *T. brucei brucei* cytotoxicity assay.

In vitro* trypanocidal activity of compounds against *T. brucei rhodesiense STIB900. This stock was isolated in 1982 from a human patient in Tanzania and after several mouse passages cloned and adapted to axenic culture conditions.[70] Minimum Essential Medium (50 μL) supplemented with 25 mM HEPES, 1g/L additional glucose, 1% MEM non-essential amino acids (100x), 0.2 mM β-mercaptoethanol, 1mM Na-pyruvate and 15% heat-inactivated horse serum was added to each well of a 96-well microtiter plate. Serial drug dilutions of eleven 3-fold dilution steps covering a range from 100 to 0.002 μg/mL were prepared. Next, $4x10^3$ bloodstream forms of *T. b. rhodesiense* STIB 900 in 50 μL was added to each well and the plate incubated at 37 °C under a 5% CO_2 atmosphere for 70 h. Alamar Blue (resazurin, 10 μL of 12.5 mg solution in 100 mL double-distilled water) was then added to each well and incubation was continued for a further 2–4 h[71]. Subsequently, the plates were read with a Molecular Devices Spectramax Gemini XS microplate fluorometer, using an excitation wave

length of 536 nm and an emission wave length of 588 nm. The IC_{50} values were calculated by linear regression[72] from the sigmoidal dose inhibition curves using Molecular Devices SoftmaxPro software.

In vitro* trypanocidal activity of compounds against *T. cruzi. Rat skeletal myoblasts (L-6 cells) were seeded in 96-well microtitre plates at 2000 cells/well in 100 μL RPMI 1640 medium with 10% FBS and 2 mM L-glutamine. After 24 h the medium was removed and replaced with 100 μL per well containing 5000 trypomastigote forms of *T. cruzi* Tulahuen strain C2C4 expressing the β-galactosidase (Lac Z) gene.[73] After 48 h, the medium was removed from the wells and replaced by 100 μL fresh medium with or without a serial drug dilution of eleven 3-fold dilution steps covering a range from 100 to 0.002 μg/mL. After 96 h of incubation the plates were inspected under an inverted microscope to assure growth of the controls and sterility. Then the substrate CPRG/Nonidet (50 μL) was added to all wells. A color reaction developed within 2–6 h and was read photometrically at 540 nm. Data were analyzed with Molecular Devices Softmax Pro software, which calculated the IC_{50} values by linear regression[72] from the sigmoidal dose inhibition curves.

ANCILLARY INFORMATION

Supporting information. Crystal structure data collection and refinement statistics for *Tb*PEX14-**61** complex structure; Details on molecular dynamics simulations performed for *Tb*PEX14-**50**, *Tb*PEX14-**61** and *Tb*PEX14-**20** complexes; ^{1}H and ^{13}C NMR spectra (PDF);

PDB File of *Tb*PEX14 model used for docking (PDB);

Molecular formula strings (CSV).

Accession Codes. The coordinates of the crystal structures have been deposited to the RCSB Protein Data Bank under the following accession codes: 6SPT (*Tb*PEX14-**61**).

Corresponding Authors

* E-mail: grzegorz.popowicz@helmholtz-muenchen.de (G.M.P.)

* E-mail: sattler@helmholtz-muenchen.de (M.S)

* E-mail: maciej.dawidowski@wum.edu.pl (M.D.)

Present Addresses

† Department of Biology, Institute of Molecular Biology and Biophysics, ETH Zürich, Hönggerbergring 64, 8093 Zürich, Switzerland (L.E.)

ORCID

Grzegorz Popowicz 0000-0003-2818-7498

Michael Sattler: 0000-0002-1594-0527

Maciej Dawidowski: 0000-0002-7262-5718

Grzegorz Dubin: 0000-0002-5535-5760

Oliver Plettenburg: 0000-0001-9671-278X

Kamyar Hadian: 0000-0001-8727-2575

Igor V. Tetko: 0000-0002-6855-0012

Vishal C. Kalel: 0000-0001-6023-7454

Author Contributions. The manuscript was written through contributions of all authors. All authors have given approval to the final version of the manuscript.

Notes. The authors declare the following competing financial interest(s): No competing financial interests are reported.

Acknowledgements. The authors acknowledge financial support from grant UMO-2018/31/B/NZ7/02089 (to MD) and 2017/26/M/NZ1/00797 (to GD) from the National Science Center, Poland. This project has received funding from the European Union's Framework Programme for Research and Innovation Horizon 2020 (2014-2020) under the Marie Skłodowska-Curie Grant Agreement No. 675555, Accelerated Early staGe drug discovery (AEGIS). MCB Structural Biology Core Facility (supported by the TEAM TECH CORE FACILITY/2017-4/6 grant from the Foundation for Polish Science) is acknowledged for valuable support. The work was supported by the Deutsche Forschungsgemeinschaft (DFG) grant FOR1905 to RE and MS; FoRUM grants of the Ruhr-University Bochum F883-2016 and F913-2017 to RE, WS and VCK. MK was supported by Wrocław Centre of Biotechnology program, The Leading National Research Centre (KNOW) for years 2014–2018. The funders had no role in study design, data collection and analysis, decision to publish, or preparation of the manuscript.

Abbreviations used

PPI, protein-protein interaction; HAT, human african trypanosomiasis; NTD, neglected tropical disease; NECT, nifurtimox-eflornithine combination therapy; DNDi, Drugs for Neglected Diseases initiative; PEX, peroxin; PTS, peroxisome targeting sequences; CSP, chemical shift perturbation; TBD, 1,5,7-Triazabicyclo[4.4.0]dec-5-ene; TEA, triethylamine; DIPEA, *N*,*N*-diisopropyl-*N*-ethylamine; CDI, 1,1'-Carbonyldiimidazole; FC, flash column chromatography; dd, doublet of doublets; dt, doubet of triplets; bs, broad signal; SI, selectivity index; FBS, fetal bovine serum; *Tb*PEX14, *T. brucei* PEX14 *N*-terminal domain; *Hs*PEX14, human PEX14 *N*-terminal domain; *Tc*PEX14, *T. cruzi* PEX14 *N*-terminal domain.

REFERENCES

1. Molyneux, D. H.; Savioli, L.; Engels, D. Neglected tropical diseases: progress towards addressing the chronic pandemic. *Lancet* **2017***, 389* (10066), 312-325.
2. Research Priorities for Chagas Disease, Human African Trypanosomiasis and Leishmaniasis. *World Health Organization Technical Report Series* **2012,** (975), v-xii, 1-100.
3. Trypanosomiasis, Human African Trypanosomiasis (Sleeping Sickness), Fact Sheet http://www.who.int/mediacentre/factsheets/fs259/en/ (accessed April 10, 2018).
4. Chagas Disease (American Trypanosomiasis), Fact Sheet. http://www.who.int/mediacentre/factsheets/fs340/en/ (accessed April 10, 2018).
5. Giordani, F.; Morrison, L. J.; Rowan, T. G.; De Koning, H. P.; Barrett, M. P. The animal trypanosomiases and their chemotherapy: a review. *Parasitology* **2016***, 143* (14), 1862-1889.
6. Büscher, P.; Cecchi, G.; Jamonneau, V.; Priotto, G. Human African trypanosomiasis. *Lancet* **2017***, 390* (10110), 2397-2409.
7. Magez, S.; Caljon, G.; Tran, T.; Stijlemans, B.; Radwanska, M. Current status of vaccination against African trypanosomiasis. Parasitology **2010***, 137* (14), 2017-2027.
8. Stijlemans, B.; Radwanska, M.; De Trez, C.; Magez, S. African trypanosomes undermine humoral responses and vaccine development: link with inflammatory responses? *Front. Immunol.* **2017,** *8* (582), 1-14.
9. Kennedy, P. G. E. Clinical features, diagnosis, and treatment of human African trypanosomiasis (sleeping sickness). *Lancet Neurol.* **2013***, 12* (2), 186-194.
10. Mesu, V. K. B. K.; Kalonji, W. M.; Bardonneau, C.; Mordt, O. V.; Blesson, S.; Simon, F.; Delhomme, S.; Bernhard, S.; Kuziena, W.; Lubaki, J.-P. F.; Vuvu, S. L.; Ngima, P. N.; Mbembo, H. M.; Ilunga, M.; Bonama, A. K.; Heradi, J. A.; Solomo, J. L. L.; Mandula, G.; Badibabi, L. K.; Dama, F. R.; Lukula, P. K.; Tete, D. N.; Lumbala, C.; Scherrer, B.; Strub-Wourgaft, N.; Tarral, A. Oral fexinidazole for late-stage African Trypanosoma brucei gambiense trypanosomiasis: a pivotal multicentre, randomised, non-inferiority trial. *Lancet* **2018***, 391* (10116), 144-154.
11. Pollastri, M. P. Fexinidazole: a new drug for African sleeping sickness on the horizon. *Trends Parasitol*. **2018***, 34* (3), 178-179.
12. Patterson, S.; Wyllie, S. Nitro drugs for the treatment of trypanosomatid diseases: past, present, and future prospects. *Trends Parasitol*. **2014***, 30* (6), 289-298.
13. Deeks, E. D. Fexinidazole: first global approval. *Drugs* **2019***, 79* (2), 215-220.
14. Wyllie, S.; Foth, B. J.; Kelner, A.; Sokolova, A. Y.; Berriman, M.; Fairlamb, A. H. Nitroheterocyclic drug resistance mechanisms in Trypanosoma brucei. *J. Antimicrob. Chemotherap.* **2016***, 71* (3), 625-634.
15. Sokolova, A. Y.; Wyllie, S.; Patterson, S.; Oza, S. L.; Read, K. D.; Fairlamb, A. H. Cross-resistance to nitro drugs and implications for treatment of human African trypanosomiasis. *Antimicrob. Agents Chemotherap.* **2010***, 54* (7), 2893-2900.
16. Field, M. C.; Horn, D.; Fairlamb, A. H.; Ferguson, M. A.; Gray, D. W.; Read, K. D.; De Rycker, M.; Torrie, L. S.; Wyatt, P. G.; Wyllie, S.; Gilbert, I. H. Anti-trypanosomatid drug discovery: an ongoing challenge and a continuing need. *Nat. Rev. Microb.* **2017***, 15* (4), 217-231.
17. DNDi Announces Successful Completion of SCYX-7158 Phase I Study for Treatment of Sleeping Sickness. https://www.news-medical.net/news/20150909/DNDi-announces-successful-completion-of-SCYX-7158-Phase-I-study-for-treatment-of-sleeping-sickness.aspx (accessed April 10, 2018).
18. Alarcón de Noya, B.; Díaz-Bello, Z.; Colmenares, C.; Ruiz-Guevara, R.; Mauriello, L.; Zavala-Jaspe, R.; Suarez, J. A.; Abate, T.; Naranjo, L.; Paiva, M.; Rivas, L.; Castro, J.;

Márques, J.; Mendoza, I.; Acquatella, H.; Torres, J.; Noya, O. Large urban outbreak of orally acquired acute Chagas disease at a school in Caracas, Venezuela. *J. Infect. Dis.* **2010**, *201* (9), 1308-1315.
19. Pérez-Molina, J. A.; Molina, I. Chagas disease. *Lancet* **2018**, *391* (10115), 82-94.
20. Barros-Alvarez, X.; Gualdron-Lopez, M.; Acosta, H.; Caceres, A. J.; Graminha, M. A. S.; Michels, P. A. M.; Concepcion, J. L.; Quinones, W. Glycosomal targets for anti-trypanosomatid drug discovery. *Curr. Med. Chem.* **2014,** *21* (15), 1679-1706.
21. Smirlis, D.; Soares, M. B. P. Selection of Molecular Targets for Drug Development Against Trypanosomatids. In *Proteins and Proteomics of Leishmania and Trypanosoma*, Santos, A. L. S.; Branquinha, M. H.; d'Avila-Levy, C. M.; Kneipp, L. F.; Sodré, C. L., Eds. Springer Netherlands: Dordrecht, 2014; pp 43-76.
22. El-Sayed, N. M.; Myler, P. J.; Blandin, G.; Berriman, M.; Crabtree, J.; Aggarwal, G.; Caler, E.; Renauld, H.; Worthey, E. A.; Hertz-Fowler, C.; Ghedin, E.; Peacock, C.; Bartholomeu, D. C.; Haas, B. J.; Tran, A. N.; Wortman, J. R.; Alsmark, U. C.; Angiuoli, S.; Anupama, A.; Badger, J.; Bringaud, F.; Cadag, E.; Carlton, J. M.; Cerqueira, G. C.; Creasy, T.; Delcher, A. L.; Djikeng, A.; Embley, T. M.; Hauser, C.; Ivens, A. C.; Kummerfeld, S. K.; Pereira-Leal, J. B.; Nilsson, D.; Peterson, J.; Salzberg, S. L.; Shallom, J.; Silva, J. C.; Sundaram, J.; Westenberger, S.; White, O.; Melville, S. E.; Donelson, J. E.; Andersson, B.; Stuart, K. D.; Hall, N. Comparative genomics of trypanosomatid parasitic protozoa. *Science* **2005**, *309* (5733), 404-409.
23. Stuart, K.; Brun, R.; Croft, S.; Fairlamb, A.; Gürtler, R. E.; McKerrow, J.; Reed, S.; Tarleton, R. Kinetoplastids: related protozoan pathogens, different diseases. *J. Clin. Invest.* **2008**, *118* (4), 1301-1310.
24. Khare, S.; Nagle, A. S.; Biggart, A.; Lai, Y. H.; Liang, F.; Davis, L. C.; Barnes, S. W.; Mathison, C. J. N.; Myburgh, E.; Gao, M.-Y.; Gillespie, J. R.; Liu, X.; Tan, J. L.; Stinson, M.; Rivera, I. C.; Ballard, J.; Yeh, V.; Groessl, T.; Federe, G.; Koh, H. X. Y.; Venable, J. D.; Bursulaya, B.; Shapiro, M.; Mishra, P. K.; Spraggon, G.; Brock, A.; Mottram, J. C.; Buckner, F. S.; Rao, S. P. S.; Wen, B. G.; Walker, J. R.; Tuntland, T.; Molteni, V.; Glynne, R. J.; Supek, F. Proteasome inhibition for treatment of leishmaniasis, Chagas disease and sleeping sickness. *Nature* **2016**, *537*, (7619), 229-233.
25. Russell, S.; Rahmani, R.; Jones, A. J.; Newson, H. L.; Neilde, K.; Cotillo, I.; Rahmani Khajouei, M.; Ferrins, L.; Qureishi, S.; Nguyen, N.; Martinez-Martinez, M. S.; Weaver, D. F.; Kaiser, M.; Riley, J.; Thomas, J.; De Rycker, M.; Read, K. D.; Flematti, G. R.; Ryan, E.; Tanghe, S.; Rodriguez, A.; Charman, S. A.; Kessler, A.; Avery, V. M.; Baell, J. B.; Piggott, M. J. Hit-to-lead optimization of a novel class of potent, broad-spectrum trypanosomacides. *J. Med. Chem.* **2016**, *59* (21), 9686-9720.
26. Fraser, A. L.; Menzies, S. K.; King, E. F. B.; Tulloch, L. B.; Gould, E. R.; Zacharova, M. K.; Smith, T. K.; Florence, G. J. Design and synthesis of broad spectrum trypanosomatid selective inhibitors. *ACS Infect. Dis.* **2018,** *4* (4), 560-567.
27. Di Pietro, O.; Vicente-Garcia, E.; Taylor, M. C.; Berenguer, D.; Viayna, E.; Lanzoni, A.; Sola, I.; Sayago, H.; Riera, C.; Fisa, R.; Clos, M. V.; Perez, B.; Kelly, J. M.; Lavilla, R.; Munoz-Torrero, D. Multicomponent reaction-based synthesis and biological evaluation of tricyclic heterofused quinolines with multi-trypanosomatid activity. *Eur. J Med. Chem.* **2015**, *105*, 120-137.
28. Haanstra, J. R.; Gonzalez-Marcano, E. B.; Gualdrón-López, M.; Michels, P. A. Biogenesis, maintenance and dynamics of glycosomes in trypanosomatid parasites. *Biochim. Biophys. Acta.* **2016**, *1863* (5), 1038-1048.
29. Gualdrón-López, M.; Brennand, A. N. A.; Avilán, L.; Michels, P. A. M. Translocation of solutes and proteins across the glycosomal membrane of trypanosomes; possibilities and limitations for targeting with trypanocidal drugs. *Parasitology* **2013**, *140* (1), 1-20.

30. Schliebs, W. Sleeping sickness: PEX and drugs. *Biochim. Biophys. Acta.* **2006**, *1763* (1), 4-5.
31. Moyersoen, J.; Choe, J.; Kumar, A.; Voncken, F. G.; Hol, W. G.; Michels, P. A. Characterization of Trypanosoma brucei PEX14 and its role in the import of glycosomal matrix proteins. *European journal of biochemistry* **2003**, *270* (9), 2059-2067.
32. Haanstra, J. R.; Van Tuijl, A.; Kessler, P.; Reijnders, W.; Michels, P. A. M.; Westerhoff, H. V.; Parsons, M.; Bakker, B. M. Compartmentation prevents a lethal turbo-explosion of glycolysis in trypanosomes. *Proc. Natl. Acad. Sci. U. S. A.* **2008**, *105* (46), 17718-17723.
33. Kessler, P. S.; Parsons, M. Probing the role of compartmentation of glycolysis in procyclic form Trypanosoma brucei: RNA interference studies of PEX14, hexokinase, and phosphofructokinase. *J. Biol. Chem.* **2005**, *280* (10), 9030-9036.
34. Furuya, T.; Kessler, P.; Jardim, A.; Schnaufer, A.; Crudder, C.; Parsons, M. Glucose is toxic to glycosome-deficient trypanosomes. *Proc. Natl. Acad. Sci. U. S. A.* **2002**, *99* (22), 14177-14182.
35. Dawidowski, M.; Emmanouilidis, L.; Kalel, V. C.; Tripsianes, K.; Schorpp, K.; Hadian, K.; Kaiser, M.; Mäser, P.; Kolonko, M.; Tanghe, S.; Rodriguez, A.; Schliebs, W.; Erdmann, R.; Sattler, M.; Popowicz, G. M. Inhibitors of PEX14 disrupt protein import into glycosomes and kill Trypanosoma parasites. *Science* **2017**, *355* (6332), 1416-1420.
36. Neufeld, C.; Filipp, F. V.; Simon, B.; Neuhaus, A.; Schuller, N.; David, C.; Kooshapur, H.; Madl, T.; Erdmann, R.; Schliebs, W.; Wilmanns, M.; Sattler, M. Structural basis for competitive interactions of Pex14 with the import receptors Pex5 and Pex19. *EMBO J.* **2009**, *28* (6), 745-754.
37. Su, J. R.; Takeda, K.; Tamura, S.; Fujiki, Y.; Miki, K. Crystal structure of the conserved N-terminal domain of the peroxisomal matrix protein import receptor, Pex14p. *Proc. Natl. Acad. Sci. U. S. A.* **2009**, *106* (2), 417-421.
38. Neuhaus, A.; Kooshapur, H.; Wolf, J.; Meyer, N. H.; Madl, T.; Saidowsky, J.; Hambruch, E.; Lazam, A.; Jung, M.; Sattler, M.; Schliebs, W.; Erdmann, R. A novel Pex14 protein-interacting site of human Pex5 is critical for matrix protein import into peroxisomes. *J. Biol.Chem.* **2014**, *289* (1), 437-448.
39. Scott, D. E.; Bayly, A. R.; Abell, C.; Skidmore, J. Small molecules, big targets: drug discovery faces the protein–protein interaction challenge. *Nat. Rev. Drug Discov.* **2016**, *15*, 533.
40. Rew, Y.; Sun, D. Discovery of a small molecule MDM2 inhibitor (AMG 232) for treating cancer. *J. Med. Chem.* **2014**, *57* (15), 6332-6341.
41. Zhao, Y.; Aguilar, A.; Bernard, D.; Wang, S. Small-molecule inhibitors of the MDM2–p53 protein–protein interaction (MDM2 inhibitors) in clinical trials for cancer treatment. *J. Med. Chem.* **2015**, *58* (3), 1038-1052.
42. Jennings, L. E.; Schiedel, M.; Hewings, D. S.; Picaud, S.; Laurin, C. M. C.; Bruno, P. A.; Bluck, J. P.; Scorah, A. R.; See, L.; Reynolds, J. K.; Moroglu, M.; Mistry, I. N.; Hicks, A.; Guzanov, P.; Clayton, J.; Evans, C. N. G.; Stazi, G.; Biggin, P. C.; Mapp, A. K.; Hammond, E. M.; Humphreys, P. G.; Filippakopoulos, P.; Conway, S. J. BET bromodomain ligands: probing the WPF shelf to improve BRD4 bromodomain affinity and metabolic stability. *Bioorg. Med. Chem.* **2018**, *26* (11), 2937-2957.
43. Yasgar, A.; Jadhav, A.; Simeonov, A.; Coussens, N. P. AlphaScreen-based assays: ultra-high-throughput screening for small-molecule inhibitors of challenging enzymes and protein-protein interactions. *Methods Mol. Biol.* **2016**, *1439*, 77-98.
44. Cramer, J.; Krimmer, S. G.; Heine, A.; Klebe, G. Paying the price of desolvation in solvent-exposed protein pockets: impact of distal solubilizing groups on affinity and binding thermodynamics in a series of thermolysin inhibitors. *J. Med. Chem.* **2017**, *60* (13), 5791-5799.

45. Hartman, G. D. K., Kuduk, S. Derivatives and methods of treating Hepatitis B infections. US2016/185777/A1, 2016.
46. Sabot, C.; Kumar, K. A.; Meunier, S.; Mioskowski, C. A convenient aminolysis of esters catalyzed by 1,5,7-triazabicyclo[4.4.0]dec-5-ene (TBD) under solvent-free conditions. *Tetrahedron Lett.* **2007***, 48* (22), 3863-3866.
47. Dai, H. G.; Li, J. T.; Li, T. S. Efficient and practical synthesis of mannich bases related to gramine mediated by zinc chloride. *Synthetic Commun.* **2006***, 36* (13), 1829-1835.
48. DeGoey, D. A.; Chen, H.-J.; Cox, P. B.; Wendt, M. D. Beyond the rule of 5: lessons learned from AbbVie's drugs and compound collection. *J. Med. Chem.* **2018***, 61* (7), 2636-2651.
49. Studier, F. W. Protein production by auto-induction in high density shaking cultures. *Protein Expr. Purif.* **2005***, 41* (1), 207-234.
50. *OriginPro*, 9.0; OriginLab Corporation: Northampton, MA, USA.
51. Kabsch, W., XDS. *Acta Crystallogr. D Biol. Crystallogr.* **2010***, 66* (Pt 2), 125-132.
52. Kantardjieff, K. A.; Rupp, B. Matthews coefficient probabilities: improved estimates for unit cell contents of proteins, DNA, and protein-nucleic acid complex crystals. *Protein Sci.* **2003***, 12* (9), 1865-1871.
53. McCoy, A. J.; Grosse-Kunstleve, R. W.; Adams, P. D.; Winn, M. D.; Storoni, L. C.; Read, R. J. Phaser crystallographic software. *J. Appl. Cryst.* **2007***, 40* (Pt 4), 658-674.
54. Watanabe, Y.; Kawaguchi, K.; Okuyama, N.; Sugawara, Y.; Obita, T.; Mizuguchi, M.; Morita, M.; Imanaka, T. Characterization of the interaction between Trypanosoma brucei Pex5p and its receptor Pex14p. *FEBS Lett.* **2016***, 590* (2), 242-250.
55. Emsley, P.; Lohkamp, B.; Scott, W. G.; Cowtan, K. Features and development of Coot. *Acta Crystallogr. D Biol. Crystallogr.* **2010***, 66* (Pt 4), 486-501.
56. Murshudov, G. N.; Skubak, P.; Lebedev, A. A.; Pannu, N. S.; Steiner, R. A.; Nicholls, R. A.; Winn, M. D.; Long, F.; Vagin, A. A. REFMAC5 for the refinement of macromolecular crystal structures. *Acta Crystallogr. D Biol. Crystallogr.* **2011***, 67* (Pt 4), 355-367.
57. Brünger, A. T. Free R value: a novel statistical quantity for assessing the accuracy of crystal structures. *Nature* **1992***, 355* (6359), 472-475.
58. Morris, R. J.; Perrakis, A.; Lamzin, V. S. ARP/wARP and automatic interpretation of protein electron density maps. *Methods Enzymol.* **2003***, 374*, 229-244.
59. *Schrödinger Release 2018.3: Maestro* Schrödinger, LLC, New York, NY, 2019: 2018.
60. Krieger, E.; Vriend, G. YASARA View—molecular graphics for all devices—from smartphones to workstations. *Bioinformatics* **2014***, 30* (20), 2981-2982.
61. Madhavi Sastry, G.; Adzhigirey, M.; Day, T.; Annabhimoju, R.; Sherman, W. Protein and ligand preparation: parameters, protocols, and influence on virtual screening enrichments. *J. Comput. Aided Mol. Des.* **2013***, 27* (3), 221-234.
62. Søndergaard, C. R.; Olsson, M. H. M.; Rostkowski, M.; Jensen, J. H. Improved treatment of ligands and coupling effects in empirical calculation and rationalization of pKa values. *J. Chem. Theory Comput.* **2011***, 7* (7), 2284-2295.
63. Olsson, M. H. M.; Søndergaard, C. R.; Rostkowski, M.; Jensen, J. H. PROPKA3: consistent treatment of internal and surface residues in empirical pKa predictions. *J. Chem. Theory Comput.* **2011,** *7* (2), 525-537.
64. Jorgensen, W. L.; Tirado-Rives, J. The OPLS [optimized potentials for liquid simulations] potential functions for proteins, energy minimizations for crystals of cyclic peptides and crambin. *J. Am. Chem. Soc.* **1988***, 110* (6), 1657-1666.
65. Jorgensen, W. L.; Chandrasekhar, J.; Madura, J. D.; Impey, R. W.; Klein, M. L. Comparison of simple potential functions for simulating liquid water. *J. Chem. Phys.* **1983***, 79* (2), 926-935.

66. Jorgensen, W. L.; Madura, J. D. Temperature and size dependence for Monte Carlo simulations of TIP4P water. *Mol. Phys.* **1985**, *56* (6), 1381-1392.
67. Bowers, K. J.; Chow, E.; Xu, H.; Dror, R. O.; Eastwood, M. P.; Gregersen, B. A.; Klepeis, J. L.; Kolossvary, I.; Moraes, M. A.; Sacerdoti, F. D.; Salmon, J. K.; Shan, Y.; Shaw, D. E. Scalable Algorithms for Molecular Dynamics Simulations on Commodity Clusters. In *Proceedings of the 2006 ACM/IEEE Conference on Supercomputing*, Tampa, Florida, ACM: Tampa, Florida, 2006; DOI: 10.1145/1188455.1188544
68. Hirumi, H.; Hirumi, K. Continuous cultivation of Trypanosoma brucei blood stream forms in a medium containing a low concentration of serum protein without feeder cell layers. *J. Parasitol.* **1989**, *75* (6), 985-989.
69. *GraphPad Prism*, 6.04; GraphPad Software, Inc: San Diego, CA, USA.
70. Baltz, T.; Baltz, D.; Giroud, C.; Crockett, J. Cultivation in a semi-defined medium of animal infective forms of Trypanosoma brucei, T. equiperdum, T. evansi, T. rhodesiense and T. gambiense. *EMBO J.* **1985**, *4* (5), 1273-1277.
71. Raz, B.; Iten, M.; Grether-Buhler, Y.; Kaminsky, R.; Brun, R. The Alamar Blue assay to determine drug sensitivity of African trypanosomes (T.b. rhodesiense and T.b. gambiense) in vitro. *Acta Trop.* **1997**, *68* (2), 139-147.
72. Huber, W.; Koella, J. C. A comparison of three methods of estimating EC50 in studies of drug resistance of malaria parasites. *Acta Trop.* **1993**, *55* (4), 257-261.
73. Buckner, F. S.; Verlinde, C. L.; La Flamme, A. C.; Van Voorhis, W. C. Efficient technique for screening drugs for activity against Trypanosoma cruzi using parasites expressing beta-galactosidase. *Antimicrob. Agents Chemother.* **1996**, *40* (11), 2592-2597.

TOC GRAPHIC

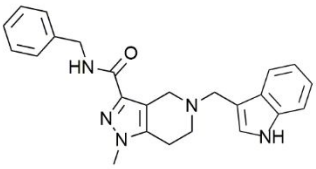

1

EC_{50} = 267 μM (*Tb*PEX14-PEX5 PPI)
IC_{50} = 18 μM (*T. b. brucei*)

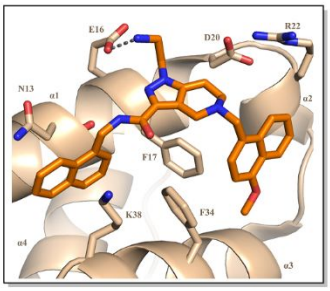

SBDD optimization

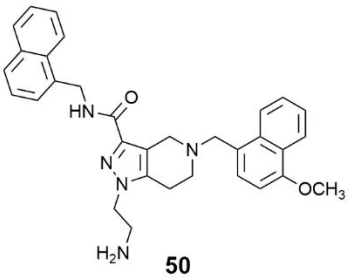

50

EC_{50} = 3.94 μM (*Tb*PEX14-PEX5 PPI)
IC_{50} = 81 nM (*T. b. brucei*)
IC_{50} = 320 nM (*T. cruzi*)

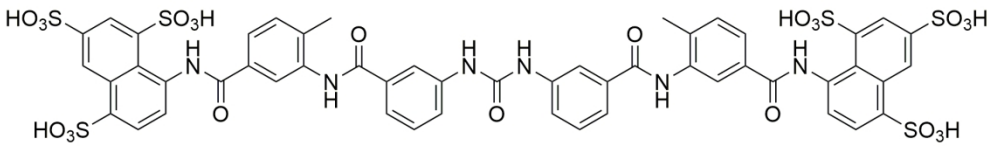

suramin

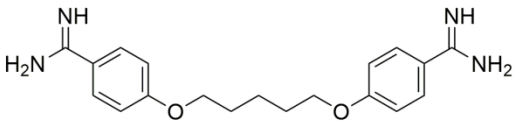

pentamidine

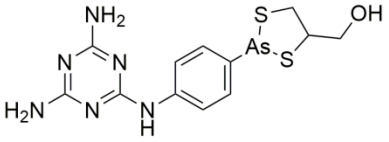

melarsoprol

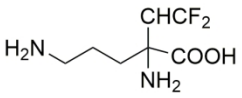

eflornithine

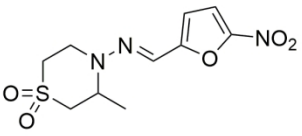

nifurtimox

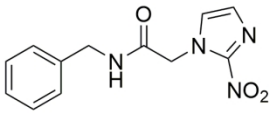

benznidazole

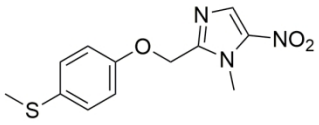

fexinidazole

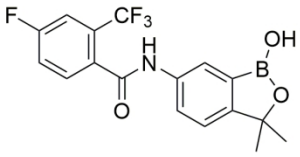

SCYX-7158

84x84mm (600 x 600 DPI)

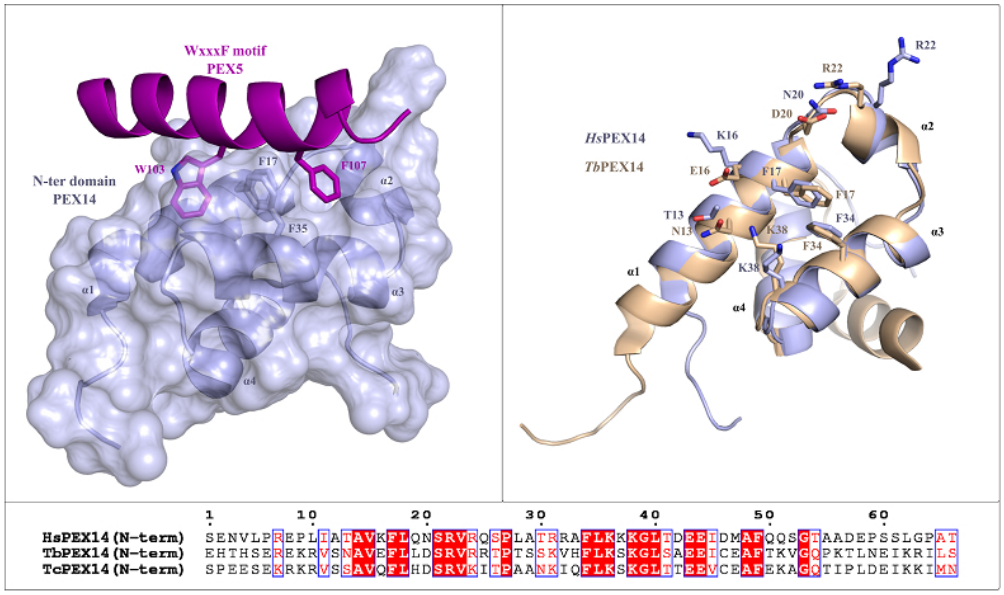
WxxxF motif
PEX5
N-ter domain
PEX14
W103
F17
F107
α2
F35
α1
α3
α4
HsPEX14
TbPEX14
R22
N20
D20
K16
E16
F17
T13
N13
K38
F34
α1
α2
α3
α4
HsPEX14 (N-term) SENVLPREPLIATAVKFLQNSRVRQSPLATRRAFLKKGLIDEEIDMAFQQSGTAADEPSSLGPAT
TbPEX14 (N-term) EHTHSERERKRVSNAVEFLLDSRVRRTPTSSKVHFLKSKGLSAEEICEAFTKVGQPKTLNEIKRILS
TcPEX14 (N-term) SPEESEKRKRVSSAVQFLHDSRVKITPAANKIQFLKSKGLITEEVCEAFEKAGQTIPLDEIKKIMN

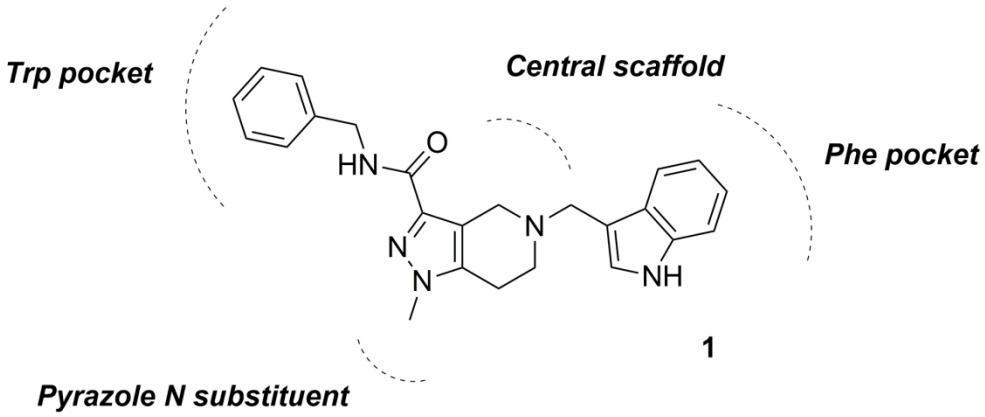

*Tb*PEX14, Kd ~ 50 μM
*Tb*PEX14-PEX5, EC_{50} = 265 μM
*Tc*PEX14-PEX5, EC_{50} = 539 μM

cLogP = 2.8
MW = 399
nON = 6
nOHNH = 2

83x50mm (600 x 600 DPI)

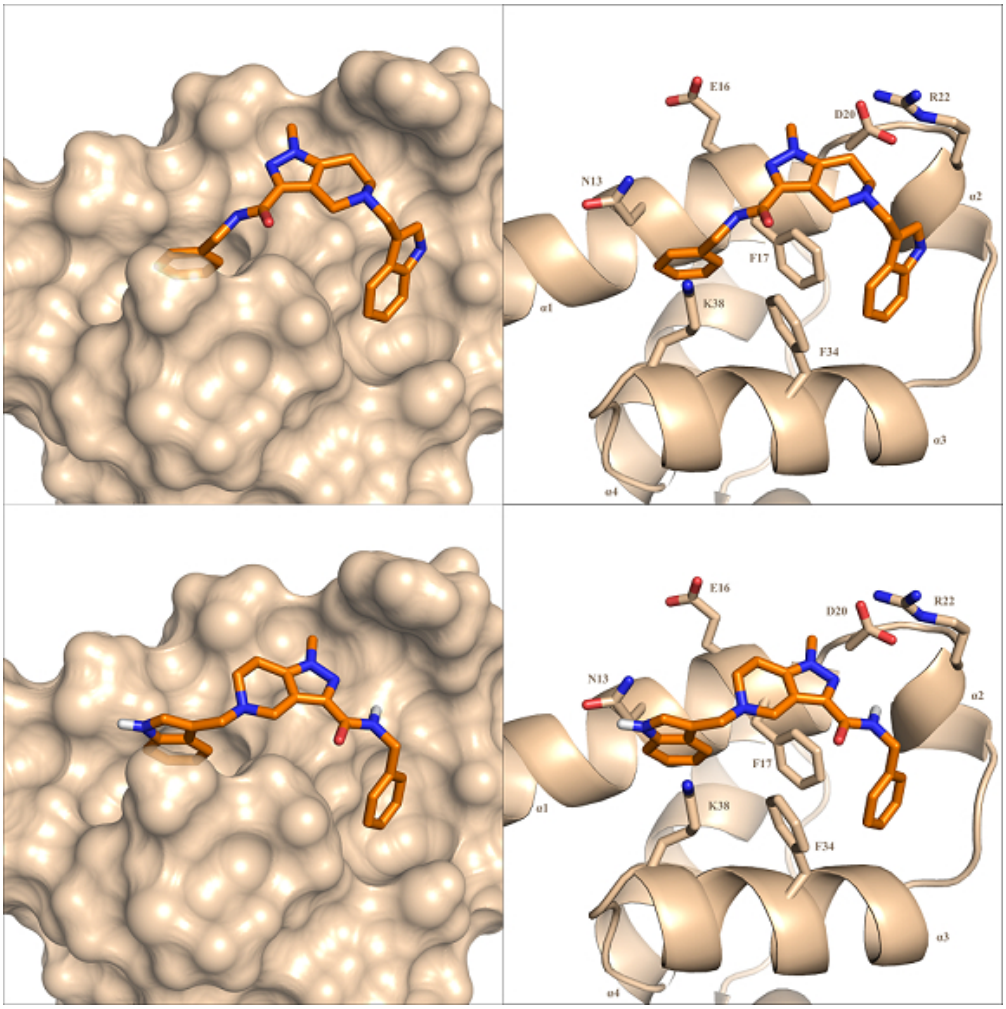
E16
D20
R22
N13
α2
F17
α1
K38
F34
α3
α4
E16
D20
R22
N13
α2
F17
α1
K38
F34
α3
α4

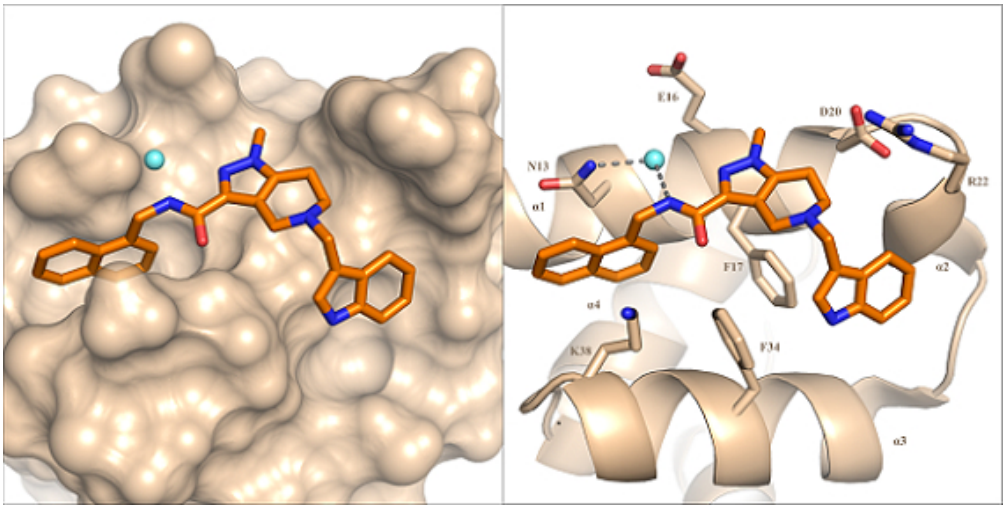
E16
D20
N13
α1
R22
F17
α2
α4
K38
F34
α3

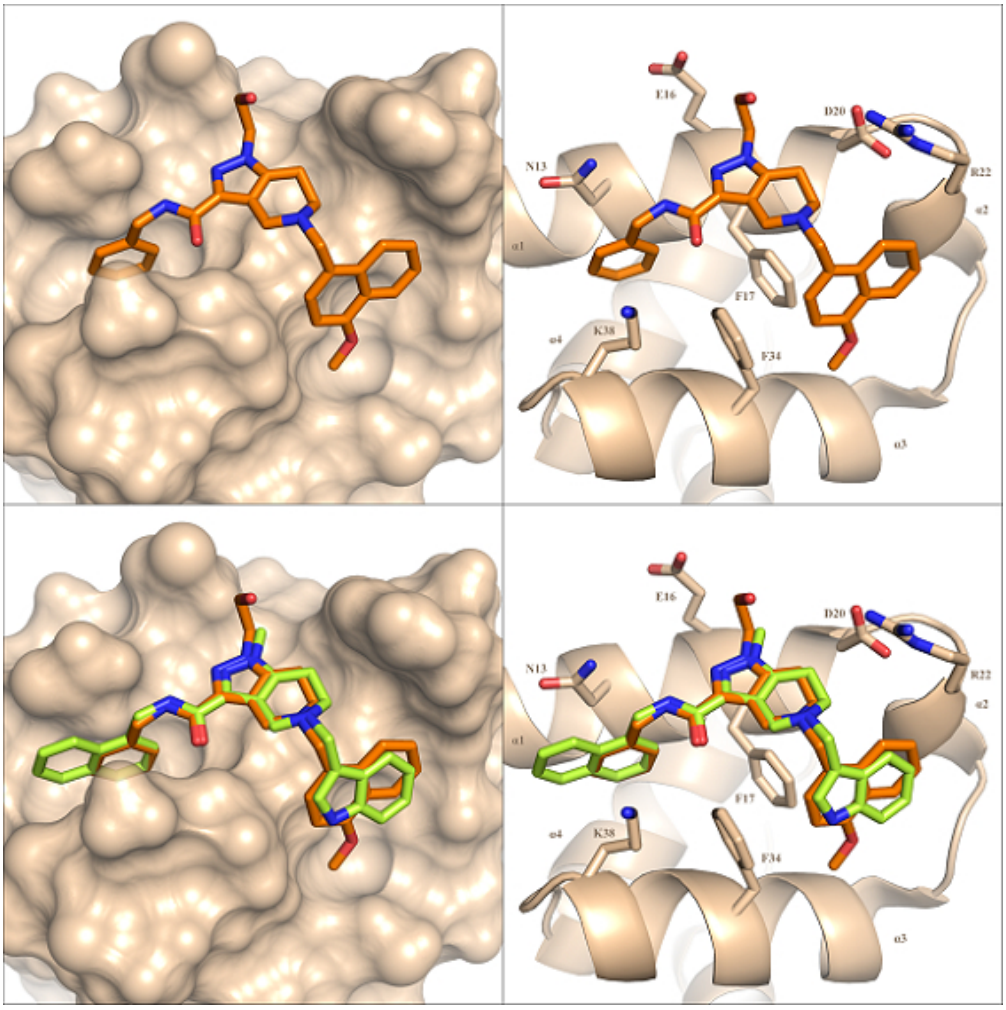
E16
D20
N13
R22
α2
α1
F17
α4
K38
F34
α3
E16
D20
N13
R22
α2
α1
F17
α4
K38
F34
α3

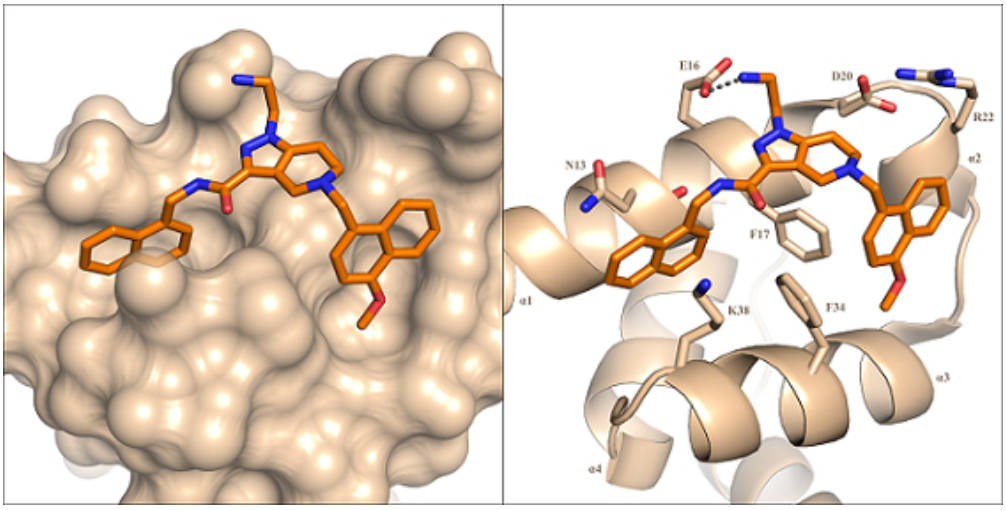
E16
D20
R22
N13
α2
F17
α1
K38
F34
α3
α4

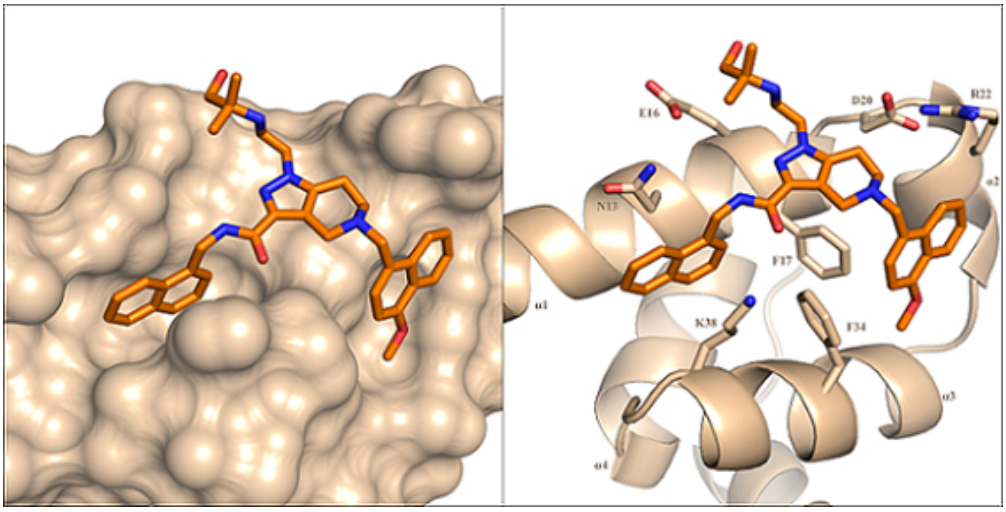
E16
D20
R22
α2
N13
F17
α1
K38
F34
α3
α4

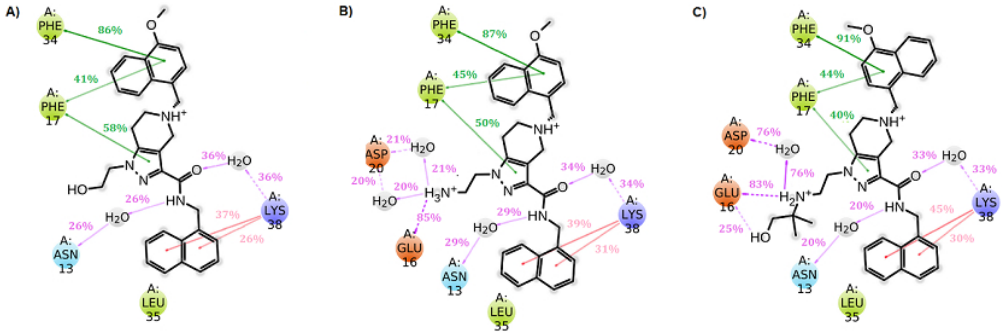
A)
A: PHE 34
86%
41%
A: PHE 17
58%
NH+
N
N
HO
O
HN
36%
H2O
36%
A: LYS 38
26%
H2O
37%
26%
26%
A: ASN 13
A: LEU 35
B)
A: PHE 34
87%
45%
A: PHE 17
50%
NH+
A: ASP 20
21%
H2O
21%
20%
20%
H2O
H3N+
85%
A: GLU 16
N
N
O
HN
34%
H2O
34%
A: LYS 38
29%
H2O
39%
31%
A: ASN 13
A: LEU 35
C)
A: PHE 34
91%
44%
A: PHE 17
40%
NH+
A: ASP 20
76%
H2O
76%
A: GLU 16
83%
H2N+
25%
HO
N
N
O
HN
33%
H2O
33%
A: LYS 38
20%
H2O
20%
45%
30%
A: ASN 13
A: LEU 35

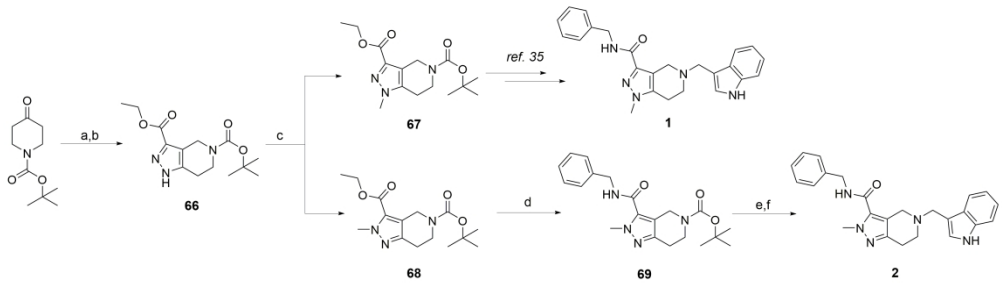

158x45mm (600 x 600 DPI)

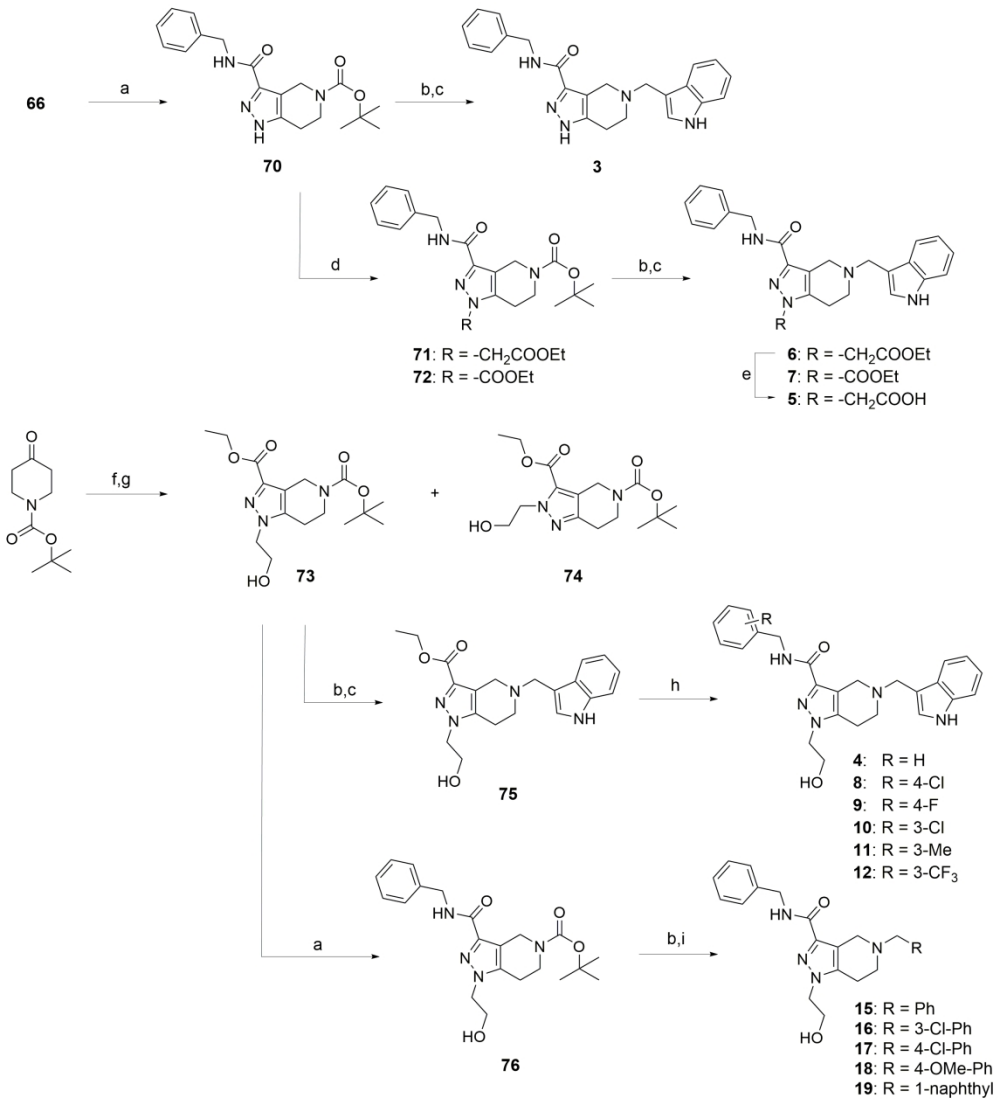

121x134mm (600 x 600 DPI)

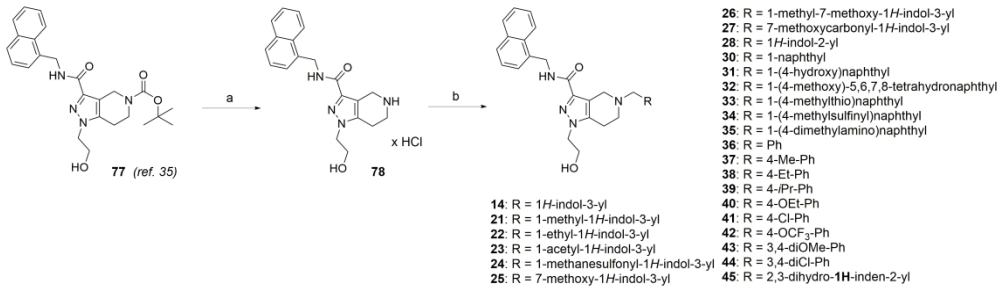

164x47mm (600 x 600 DPI)

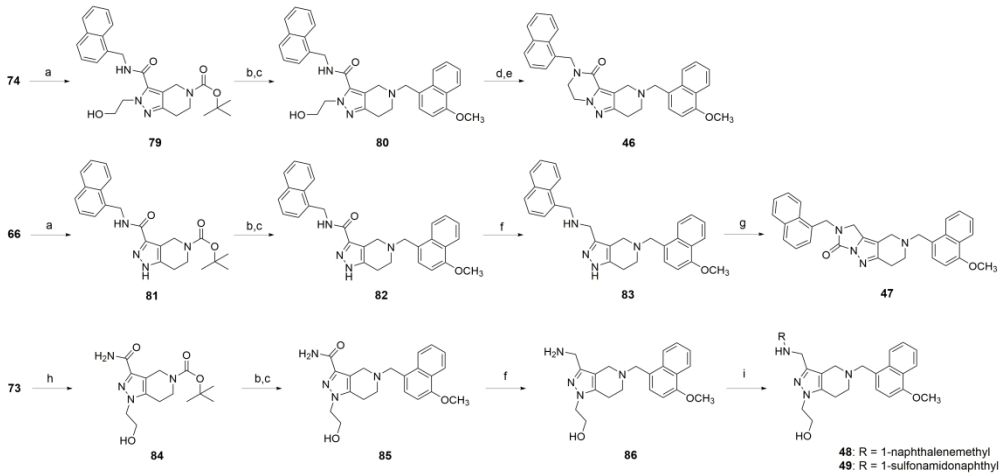

176x84mm (600 x 600 DPI)

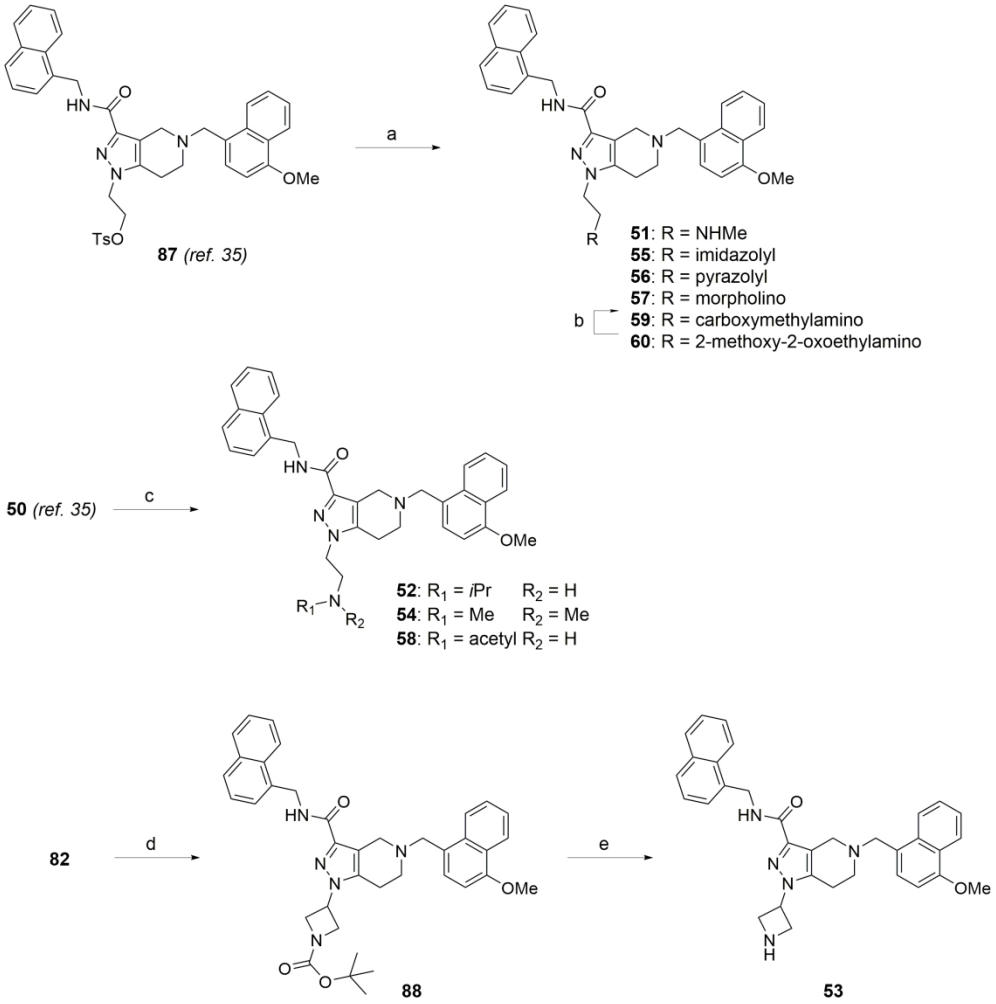

112x113mm (600 x 600 DPI)

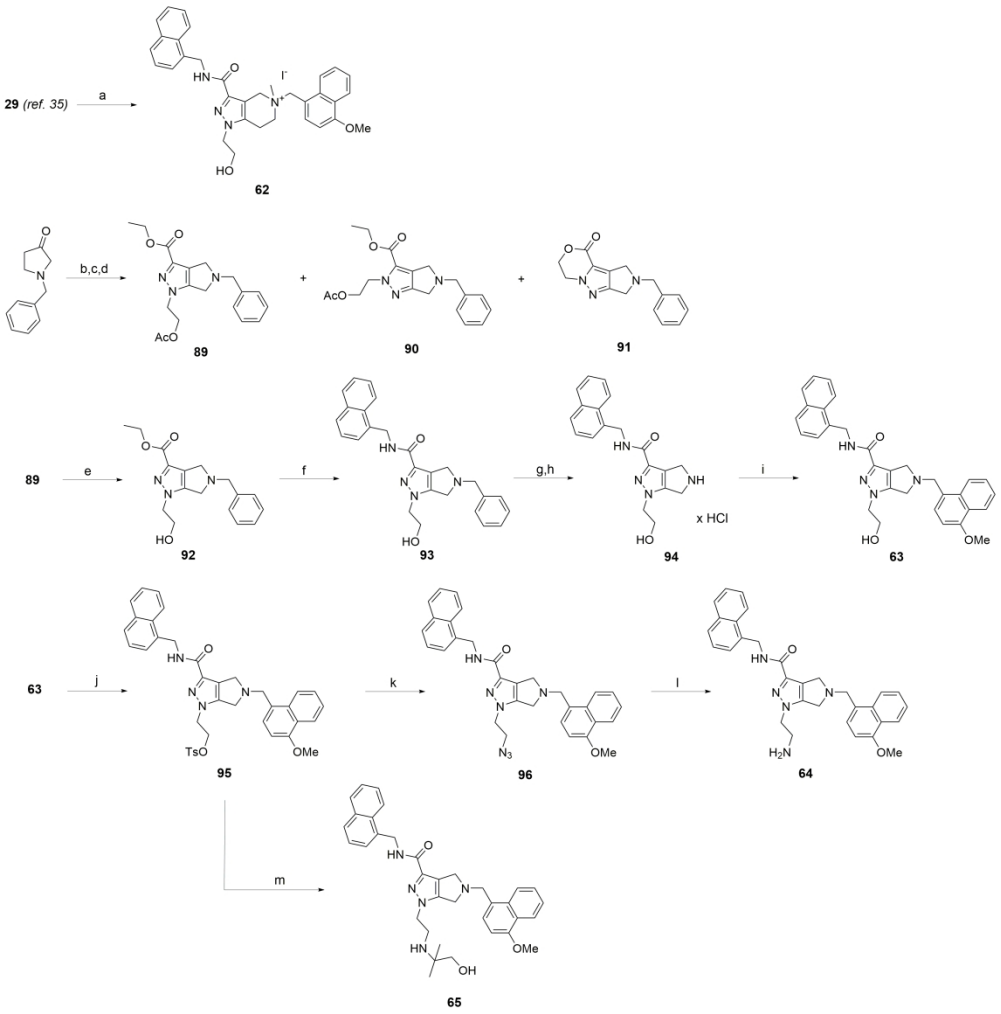

160x162mm (600 x 600 DPI)

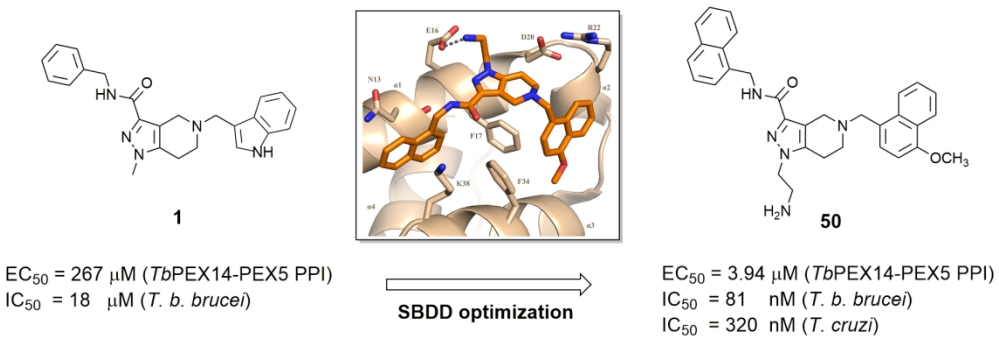

404x147mm (120 x 120 DPI)